Establishment and optimization of the LC-MS-based strategy for screening of passively absorbed açaí and maca constituents for CYP3A4 inhibition

by

Thankhoe Abram Rants'o

A thesis submitted to the Graduate Faculty of
Auburn University
in partial fulfillment of the
requirements for the Degree of
Master of Science

Auburn, Alabama
August 5, 2017

Keywords: liquid chromatography-mass spectrometry, açaí, maca, intestinal absorption,
CYP3A4 inhibition, metabolism

Copyright 2017 by Thankhoe Abram Rants'o

Approved by

Angela I. Calderón, Chair, Associate Professor of Drug Discovery and Development
Randall Clark, Professor of Drug Discovery and Development
Jack DeRuiter, Professor of Drug Discovery and Development
Forrest Smith, Associate Professor of Drug Discovery and Development

Abstract

The escalation of cancer morbidity and mortality has increased the use of botanical dietary supplements among cancer patients undergoing chemotherapy. *Euterpe oleracea* Mart. (açaí) berry and *Lepidium meyenii* Walpers (maca) root are some of the most common botanical dietary supplements used concomitantly with anticancer agents. CYP3A4 is an important enzyme in the metabolism and clearance of anticancer agents. While often used for their scientific claims against cancer, the supplements may also cause botanical-drug pharmacokinetic interactions of which one is through CYP3A4 inhibition. Consideration of bioavailable constituents of botanical dietary supplements has been identified as a route to counteract the discrepancy between preclinical and clinical botanical-drug interaction data. Passive absorption is the most common mechanism of absorption for medicines in the market. The goal of this study is to screen passively absorbable açaí berry and maca root constituents and their Phase I and Phase II metabolites for CYP3A4 inhibition.

Chapter one is an overview of cancer prevalence, treatment, botanical dietary supplements use and the herbal-drug interactions. The chapter also goes into the chemical characterization of açaí berry and maca root extracts.

Chapter two describes in detail, the methods used in açaí and maca plant extracts fingerprinting, establishment of intestinal passive absorption model, metabolism and CYP3A4 inhibition assays. The experimental work used LC-MS and other orthogonal confirmatory assays.

Chapter three presents the results, discussion and conclusions. The findings of this study, after identifying the extracts with moderate to strong CYP3A4 inhibition, suggest that açaí and maca

botanical dietary supplements have a potential to cause significant botanical-drug interactions in the clinical setting.

Acknowledgements

Above all, I thank God for the everlasting protection, love and perfect guidance He gave to me throughout this journey. I am more than thankful to my family that had faith to let me leave my country and follow my passion but never ceased to support me every second. I therefore dedicate this work to my father, Mr. Motlatsi Rants'o, my mother, Mrs 'Majane Rants'o, my brother Jane Rants'o and my sister 'Majapi Rants'o. Their love and care kept me going even through the tough times.

My hearty acknowledgements go to the Fulbright Scholarship that generously sponsored all my tuition and living costs. I believe that without Fulbright I wouldn't have set my foot on the land of destiny, United States of America. I want to thank the US Embassy in Lesotho that helped me with all preparations to come to the US and constantly supported me during my stay. I am grateful of my Fulbright advisors, Ms. Megan Ames and Ms. 'Mathabang Fanyane who always ensured that I had all I needed to reach the completion of my study.

I want to take this opportunity to thank my academic advisor, Dr. Angela Calderón for giving me an opportunity to join her great lab and for her constant guidance, support, encouragement and for making me realize my potential. I here observe my committee members who tirelessly helped me not only through my research but also in the academic courses. I highly thank Dr. Jack Deruiter who stimulated my passion into the career of drug discovery through his Advanced Medicinal Chemistry courses that also happened to be the major part of my research. I greatly thank Dr. Randall Clark who has helped me understand my research better and been always most welcoming supportive. In the same way, my sincere regards go to Dr. Forrest Smith for his valuable input that always gave me a direction in analyzing my research data.

I would like to also extend my gratitude to our collaborators, Dr. Richard Hansen and Dr. Jingjing Qian who are tirelessly complementing this project by searching for population-based statistical reports of the findings of this research. I would also like to thank Dr. Richard van

Table of Contents

List of Figures

List of Tables

List of abbreviations

μL   Microliter

μg   Microgram

mL   Milliliter

μM   Micromolar

°C   Degree Celsius

UDPGA Uridine 5'-diphospho-glucuronic acid

UGT   5'-diphospho-glucuronosyltransferases

NADPH Nicotinamide adenine dinucleotide phosphate-oxidase

PAMPA Parallel artificial membrane permeability assay

CYP Cytochrome P450

DMSO Dimethyl sulfoxide

TIC   Total ion chromatogram

EIC   Extracted ion chromatogram

ESI   Electrospray ionization

CID   Collision-induced dissociation

Da   Dalton

HPLC   High performance liquid chromatography

RRLC   Rapid resolution liquid chromatography

LC-MS Liquid chromatography-mass spectrometry

NMR   Nuclear magnetic resonance

HPLC-UV High performance liquid chromatography-ultra-violet visible spectroscopy

MS   Mass spectrometry

MS/MS Tandem mass spectrometry

EMA   European Medicines Agency

FDA   Food and Drug Administration

CAM   Complementary and alternative medicine

NCCIH National Center for Complementary and Integrative Health

DSHEA Dietary Supplements Health Education Act

cGMP   Current good manufacturing practices

DPPH   2,2-diphenyl-1-picrylhydrazyl

TOSC   Total oxidant scavenging capacity

TEAC   Trolox equivalent antioxidant capacity

ORAC   Oxygen radial absorbance capacity

SEAP   Embryonic alkaline phosphatase

DNA   Deoxyribonucleic acid

CAP-e   Cell-based antioxidant protection

ROS   Reactive oxygen species

BP   Benzo[α]pyrene

SJW   St. John's Wort

P_e Effective permeability

HLMs   Human liver microsomes

DCM   Dichloromethane

MeOH   Methanol

ACN   Acetonitrile

NIH   National Institutes of Health

IS   Internal standard

RT   Retention time

DBE   Double-bond equivalence

GIT   Gastrointestinal tract

NAT Na^+-coupled amino acid transporters

HMF   5-hydroxymethylfurfural

PCA   Protocatechuic acid

IC_{50} Half maximal inhibitory concentration

EGFR   Epidermal growth factor receptor

Chapter 1: Literature review

1.1 Introduction

Cancer is the second leading cause of death globally and reported to have claimed 8.8 million deaths in 2015 whereby nearly 1 in 6 deaths was due to cancer in global context [1]. Furthermore, it is stated that every year, cancer is responsible for death of more than half a million Americans making it a second leading cause of death in the United States, exceeded only by heart disease [2]. Prevalence of cancer in 2016 in the United States (U.S.) was estimated to more than 15.5 million people [3]. The most prevalent cancer types in the U.S. in 2016 as reported from statistical data were breast (3,560,570), uterine corpus (757,190), and colon and rectum (727,350) among females. For males, the 3 common cancers were prostate (3,306,760), colon and rectum (724,690), and melanoma (614,460) [3]. American Cancer Society projected that there will be 1,688,780 new cancer cases diagnosed and 600,920 cancer deaths in the US in 2017 with common cancer types being breast cancer, prostate cancer, colorectal cancer and lung cancer among others [4]. The current standard kinds of cancer treatment include surgery, radiation therapy, chemotherapy, immunotherapy, hormone therapy, targeted therapy, precision cancer medicine and stem cell transplant [5]. Chemotherapy, the common strategy of cancer treatment, is the use of medicines to kill cancer cells by arresting their growth [3]. Although an ideal situation would be to have anticancer agents affecting only rapidly dividing cancerous cells, they also affect normal cells especially those possessing high cell turnover such as bone marrow [6]. Cancer treatment is therefore often accompanied by serious side effects such as anemia, thrombocytopenia [7], peripheral neuropathy, central neurotoxicity [8] and loss of memory [9]. Chemotherapy-induced liver injury (hepatotoxicity) has been identified as a significant cause of morbidity and mortality in cancer [10]. Due to life-threatening toxic effects of chemotherapy [11] and narrow therapeutic window [12], chemotherapeutic agents are often dose-limited and their detoxification by metabolism is of utmost importance. Metabolism is a process by which a chemical structure of a drug or xenobiotic is modified by cytochrome P450 (CYP) enzymes present in human tissues mainly predominant in the intestinal barrier and liver [13]. Generally, metabolism occurs through

two phases consisting of Phase I responsible for functionalization and Phase II that executes conjugation reactions on a molecule [6]. Most common Phase I reactions are oxidation, reduction and hydrolysis catalyzed by oxidoreductases, reductases and hydrolases respectively [14, 15]. Glucuronidation is the major Phase II conjugation in adults catalyzed by uridine 5'-diphospho-glucuronosyltransferases (UGTs) and sulfate conjugation mainly important for neonates and children is carried out by sulfotransferases. Other conjugation reactions include glutathione (GSH) conjugation, amino acid conjugation, acetylation and methylation [16]. While Phase I reactions introduce a polar functional group such as a hydroxyl (-OH), Phase II adds a conjugative group like D-glucuronic acid to the Phase I metabolites or parent molecule. This produces a very polar molecule and in most cases, favors excretion of such a metabolite from the body (Figure 1.1) [17].

Given the deleterious consequences of cancer, patients affected tend to try alternatives to allopathic medicine that could relief them from their illness [18]. In these cases, most cancer patients use complementary and alternative medicine (CAM) together with their prescribed chemotherapeutic agents [19]. According to National Center for Complementary and Integrative Health (NCCIH), CAM can be defined as wide medical and health care systems, practices, and products that are not presently considered to be part of conventional medicine. In details, complementary medicine is used together with conventional medicine while alternative medicine replaces a conventional medicine [20]. The most popular forms of CAM are herbal preparations and botanical dietary supplements [21]. Herbal supplements (also called botanicals or phytomedicines) are botanical products that contain herbs, either as single entities or in mixtures and used to maintain or improve health. This can be a plant or part of a plant used for its scent, flavor, and/or therapeutic properties [22]. As xenobiotics, dietary supplements containing a myriad of compounds are also metabolized in the same way as conventional medicines and have potential to cause botanical-drug interactions with anticancer agents in concomitant use [23].
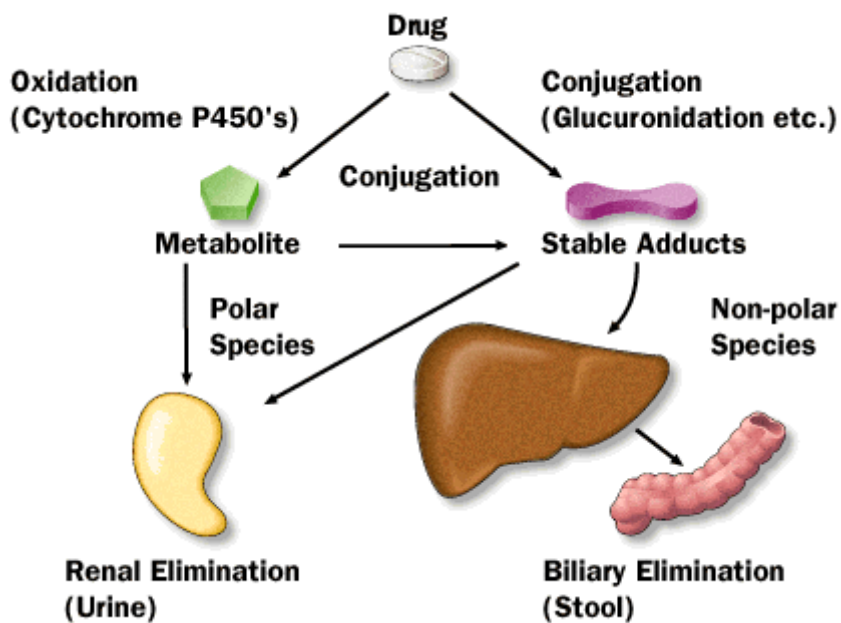
Fig. 1.1 Drug metabolism pathway [24].

1.2 Botanical dietary supplement use in the United States

According to 2008 CAM survey by the National Center for Complementary and Integrative Health (NCCIH) and the National Center for Health Statistics, approximately 38% of adults and 12% of children in the US use herbal preparations or other natural supplements [25], however, only one-third disclose this to their medical practitioner [26]. The recent CAM survey conducted in 2012 reports 34% adults and about 12% of children using any kind of complementary health approach. This study acknowledged that its CAM prevalence results are not fully informative and may be misleading because the study did not take into consideration which complementary health approaches are included in the definition of "any complementary health approach" [27]. Interestingly, Dima *et al* reported that the use of botanical dietary supplements specifically, increased from 51.8% in 2005 to 63.7% in 2011 [28] while Christine *et al* stated that about 50% of US adults use dietary supplements and 33% use multivitamin/multimineral supplements [29].

3

Studies report that generally people use CAM for treating cancer symptoms and side-effects of cancer treatment, preventing recurrence or spread of cancer [30], increasing the body's immunity to fight the disease, improving physical and emotional well-being [31] while others considered a certain CAM therapy because it has been used in the past with success or they heard that it worked for someone else, or they believed it was less harmful/more natural than conventional therapy. For those with terminal diseases such as cancer also reported using CAM because they wanted to try every option available [32]. The use of CAM is most common in patients with chronic diseases (46.4% - 59.6%) than in other patients [33, 34] and nonvitamin, botanical dietary supplements have always been the most popular form of CAM [35]. Current market status and projection to 2019 states that the herbal products manufacturing is increasingly becoming a multibillion dollar industry [36].

Regulation of botanical dietary supplements in the US is not as strict as one for conventional medicines [37]. While drugs are regulated by Food and Drug Administration (FDA) requiring their well-documented and detailed safety and efficacy data from clinical trials, dietary supplements, considered as "foods", are instead regulated by 1994 Dietary Supplements Health Education Act (DSHEA). In this act, manufacturers can distribute their products without proven safety and efficacy although they should not link their product to a certain disease as such a claim would then classify it as a drug. Due to complicated legal definition of what constitutes "specific disease-linking to a particular product", manufactures may, and of course they still make structure/function claims without any safety and efficacy evidence [37]. This loose regulation of botanical dietary supplements means their safety and efficacy may be compromised. In addition, the chemical composition of these products in the market may vary significantly from one supplier to another. Also, differences in content and potency may be obtained in different batches of the same product from the same manufacturer [38]. However, the U.S. FDA released the current good manufacturing practices (cGMP) for the dietary supplement industry in June 2007 requiring that the proper controls be in place during manufacturing, packaging, labeling, and holding operations of botanical dietary supplements [39].

1.2.1 Use of botanical dietary supplements among cancer patients

Cancer patients get much interest into the botanical dietary supplements as a measure to help ease their illness [19]. While about 50% of the general population are presumed to be consuming botanical dietary supplements, prevalence of these products ranges from 64% to 84% in cancer patients [29, 40]. Specific cancer-related motivations behind using the dietary supplements include relief of chemotherapy side effects and symptoms such anxiety and fatigue not addressed by their conventional cancer therapy [41]. Substantial studies have reported use of dietary supplements presumed to be alternative anticancer agents [42, 43]. Cancer patients use dietary supplements more than the general US population. Cancer patients tend to use botanical dietary supplements more frequently than patients with benign acute or chronic diseases [44]. Breast cancer followed by colorectal cancer patients become the most predominant users of dietary supplements than patients with other cancer types. The general perceptions of cancer recurrence and death have been spotted as the main reasons due to vast reports of recurrence and high mortality rates in breast and colorectal cancer incidences [45, 46]. Despite the lack of scientific evidence on safety and effectiveness, significant use of botanical dietary supplements has been reported at all cancer treatment phases comprising initial, continuing and end-stage phases [47]. The use of botanical dietary supplements has also been reported in clinical trials resulting into inconsistent therapeutic efficacy and safety of new investigational anticancer agents [48]. While 84% use of botanical dietary supplements has been reported for breast cancer patients [40], 46% has been reported in pediatric cancer [49], 43% in prostate cancer [50] and 35% in head and neck cancer [51]. Recent studies report that generally 95% of cancer patients use botanical dietary supplements and 77% of these do not disclose their use of botanical dietary supplements to the physicians [52].

1.2.2 *Euterpe oleracea* Mart. (açaí)

Euterpe oleracea Mart. (açaí) is a tropical palm tree originally from the Amazon belonging to the Arecaceae family and species of *Euterpe* genus [53]. It has originally been found growing in the lowland and in the flooded forest land of the Amazon River estuary, in the Brazilian estates of

Pará, Maranhão, Tocantins, Amapá. It is also found growing in Guyana South America and in Venezuela [54, 55]. Açaí berry is one of the most popular "super foods" and highly used globally. Highest use of açaí dietary supplements has been observed in the US, Europe, Japan, China and Brazil [53] where attention to açaí has been given to its potential health benefits, particularly chemopreventive effects [56]. Found in different formulations, açaí is widely sold in the nutraceutical, cosmetic and pharmaceutical industries [53]. Açaí fruits have mainly been prepared as beverages and exported all over the world as an energy drink. Alarming increase in the use of açaí energy drink has been fueled by scientific studies reporting its anti-aging properties and the presence of bioactive constituents [53, 57]. Due to high sales of açaí supplements in both Brazil and the international markets, it has been named a product of great economic importance [57].

Reports of chemical profiling of açaí extracts using high performance liquid chromatography coupled to ultra-violet visible spectroscopy (HPLC-UV) or mass spectrometry (HPLC-MS) and nuclear magnetic resonance (NMR) have suggested approximately 31% of flavonoids, 23% of phenolic constituents, 11% lignoids and 9% anthocyanins content. Other minor constituents reported include fatty acids and quinones. The predominant polyphenolic components orientin, isoorientin, vanillic acid and anthocyanins cyanidin-3-glucoside and cyanidin-3-rutinoside have also been reported [53, 58]. Moreover, the predominant phenolic acids have been reported by Del Pozo-Insfran *et al.* as ferulic acid, *p*-hydroxybenzoic acid, gallic acid, protocatechuic acid, ellagic acid and its glycoside, vanillic acid and *p*-coumaric acid [59]. Studies have also reported predominantly anthocyanins in açaí berry which are glycosides of anthocyanidins responsible for the purple açaí color [60, 61].

Documented *in vitro* pharmacological screening assays of açaí berry extracts have reported antioxidant, anti-inflammatory and anti-proliferative activities [62, 63]. The antioxidant activity of the açaí berry has shown positive results from different biological assays reported in the literature including the 2,2-diphenyl-1-picrylhydrazyl (DPPH) radical scavenging assay, total oxidant scavenging capacity (TOSC) assay, peroxyl and hydroxyl radical scavenging, trolox equivalent antioxidant capacity (TEAC) and inhibition of oxidation of liposomes [56, 63-65]. The

antioxidant activity has been linked to seven flavonoids (orientin, homoorientin, vitexin, luteolin, chrysoeriol, quercetin, and dihydrokaempferol) [64, 66] and anthocyanins [58]. Dihydroconiferyl alcohol, protocatechuic methyl ester, chrysoeriol, and dihydrokaempferol have also been stated to have the antioxidant effects from the hydroxyl radical-scavenging assay [67]. Velutin has also been reported to have displayed antioxidant activity in oxygen radial absorbance capacity (ORAC) assay and anti-inflammatory effects in embryonic alkaline phosphatase (SEAP) reporter assay designed to measure NF-κB activation [68]. The NF-κB family of transcription factors, essential for inflammation and innate immunity, plays a crucial role in many steps of cancer initiation and progression interferons [69].

Cytoprotection and responsible constituents from açaí extracts have also been reported [67]. Cytoprotective agents that have been reported from identification by bioactivity-guided fractionation of açaí extracts include dihydroconiferyl alcohol, (+)-lariciresinol, (+)-pinoresinol, (+)-syringaresinol, and protocatechuic acid methyl ester. After isolation, these constituents are reported to have displayed significant cytoprotective activity in cultured MCF-7 breast cancer cells exposed to H_2O_2. In the same study, protocatechuic acid methyl ester was identified as the most cytoprotective agent [67]. Hu *et al* recently isolated 3 new glucosides; (–)-7R8S-7′,8′-dihydroxy-dihydrodehydroconiferyl alcohol-9-O-β-D-glucopyranoside, (+)-7S8R-7′,8′-dihydroxy-dihydrodehydroconiferyl alcohol-9-O-β-D-glucopyranoside and 4-hydroxy-2-methoxyphenyl 1-O-[6-(hydrogen 3-hydroxy-3-methylpentanedioate)]-β-D-glucopyranoside and demonstrated their antioxidant and cytoprotective activities on myelomonocytic HL-60 cells suggesting activity against blood cancer (leukemia) [70]. In the animal models Romualdo *et al* discovered the cytoprotective effects of açaí berry in mice injected with colorectal carcinogen azoxymethane suggesting potential activity in colorectal cancer [71]. The literature also states that the açaí berry has shown relief of chemotherapy side effects in the case of antitumoral agent doxorubicin-induced genototoxicity in the study conducted on wistar rats. In that study, açaí berry exhibited inhibition of genotoxicity when given together with doxorubicin and when given for 14 days before doxorubicin administration in mice [72]. Other scientific studies report the antitumor effects

exhibited by açaí berry by inhibiting the transitional cell carcinoma development as seen in a study with male Swiss mice [71].

In cell culture assays, açaí berry was reported to have shown promising activity against age-related neurodegenerative diseases by demonstrating antioxidant and anti-inflammatory activities in the cerebral cortex, hippocampus and cerebellum of rats exposed to the oxidant hydrogen peroxide (H_2O_2) [73]. In other studies, inflammation was shown to increase oxidative deoxyribonucleic acid (DNA) damage in brain cancer [74]. Further activity against brain cancer has been found from anthocyanin-rich extract of açaí berry in C-6 rat brain glioma cells. This extract also showed antiproliferative effects against MDA-468 human breast cancer cells according to Hogan et al. [75]. The antitumorigenic potential of the açaí berry hydroalcoholic extracts was also demonstrated in human breast cancer MCF-7 cell line [76]. Kang et al also states that the cell-based antioxidant protection (CAP-e) assay confirmed that luteolin, quercetin and dihydrokaempferol could efficiently enter the cytosol and inhibit reactive oxygen species (ROS) formation within the cell [68].

In clinical studies, 6 weeks' consumption of açaí berry-based juice blend was reported to increase the total antioxidant capacity of plasma and attenuation of the exercise-induced muscle damage [77]. In a randomized, double-blind, placebo-controlled, crossover study with human healthy subjects by Jensen et al., administered an anthocyanin-rich açaí berry juice led to significant and rapid increase in antioxidant activity of serum and increased cellular protection from reactive oxygen species was confirmed by using the cell-based antioxidant protection in erythrocytes (CAP-e) assay as reported [78]. Another study demonstrated the absorption and increased plasma antioxidant activity of açaí berry and its juice in human healthy volunteers [79]. In general, while the preclinical studies and animal models reported cytoprotective [67, 71], antitumor [71], antioxidant [64, 70] and anti-inflammatory activities [63, 73] for açaí berry, only antioxidant activity has been proven in humans [78, 79] so far based on the extensive literature search done in this study.

These various scientific claims of açaí's potential clinical benefit for cancer patients and the observed antioxidant activity from clinical studies [77-79] most likely contribute to the increased use of açaí dietary supplements by cancer patients to complement their conventional chemotherapeutic medicines.

1.2.3 *Lepidium meyenii* Walpers (maca)

Lepidium meyenii Walpers (maca) is a cruciferous plant that belongs to the Brassicaceae family and *Lepidium* genus [80]. Maca is a biennial herbaceous vegetable native to the Andes of Peru [81]. Maca, cultivated as a starch crop, was traditionally grown for food by the Pumpush, Yaros, and Ayarmaca Indians. In Huancayo, Peru, maca jam and pudding are popular, and maca is often made into a sweet, fragrant, fermented drink called maca chichi [82]. Wide formulations of commercial maca products including juices, soft drinks, pills, capsules, cocktails, alcoholic beverages and maca coffee have gained popularity as dietary supplements across the world and used for medicinal and nutritional purposes [82, 83]. Maca dietary supplements are sold in web markets and drug stores and their highest consumption has been reported in South America, including Peru. These dietary supplements are derived from the processed tuberous root of *L. meyenii* and are rich in protein, starches, sugars, and essential minerals, mainly iodine and iron [84]. Maca is reported to have been used in traditional medicine for various medical conditions such as to cure or relieve cancer, as well as to combat leukemia and anemia [80].

In general, from reported chemical fingerprinting studies, maca is composed of sterols [85], glucosinolates [86], fatty acids, amino acids and several secondary metabolites [87]. Dry maca hypocotyls are reported to be composed of primary metabolites of approximately 10-16% protein, 59% carbohydrates, 8.5% fiber, 2.2% lipids and free fatty acids of which saturated fatty acids constitutes 40.1% and unsaturated fatty acids account for 52.7% [85, 88, 89]. Reports also show that maca is rich in essential amino acids of which major are phenylalanine, tyrosine, and tryptophan. Important minerals reported in maca include iron, calcium, potassium, copper, and zinc [88].

The major secondary metabolites of maca can be classified into glucosinolates, alkaloids and macamides as reported in the literature [89]. The secondary metabolites macaridine, macaene, macamides, and maca alkaloids have only been reported from *L. meyenii* [87, 89]. Furthermore, the two main glucosinolates, glucotropeolin and *m*-methoxybenzylglucosinolate are considered chemotaxonomic markers in maca due to their absence in other members of the Brassicaceae family [90]. Three marker alkaloids have also been isolated from maca tuber extracts. These are the two imidazole derivatives (lepidiline A and lepidiline B) [91] and one benzylated derivative of 1,2-dihydro-*N*-hydroxypyridine named macaridine [82]. The main macamides in maca have been identified in numerous studies as *n*-benzylhexadecanamide, *n*-benzyl-(9Z)-octadecenamide, *n*-benzyl-(9Z, 12Z)-octadecadienamide, *n*-benzyl-(9Z, 12Z, 15Z) octadecatrienamide and *n*-benzyloctadecanamide [92, 93]. Macamides and macaenes are typical markers of *L. meyenii* being the novel polyunsaturated fatty acids and their amides which are not found in other plants [93].

Maca has reported anti-proliferative activities linked to its potential anticancer effects [86] through the proposed mechanisms from pharmacological studies that include scavenging of free radicals resulting in cytoprotection under oxidative stress conditions [94]. This has been demonstrated in several studies by maca extracts scavenging reactive oxygen and nitrogen species (ROS/RNS) (superoxide, hydroxyl, peroxyl, hydrogen peroxide (H_2O_2) and peroxynitrite) [81, 94]. The antioxidant activities of maca have also been demonstrated in the *in vitro* 1,1-diphenyl-2-picrylhydrazyl (DPPH) radical inhibition by maca methanolic extract [94] and its cytoprotection was obtained using macrophages (RAW 264.7) treated with peroxynitrite or H_2O_2 in a study by another Sandoval *et al* [81]. Maca polysaccharides isolated from aqueous extract have also been reported with high antioxidant activity shown by free radical scavenging [95].

Most phytosterols extracted from maca [85, 89] have been reported to exhibit anticancer, antioxidant and anti-inflammatory activities. For instance, literature states that the 1,3-dibenzylimidazolium chloride derivatives of lepidiline A and lepidiline B have been patented for treatment of cancer [96]. Isothiocyanates and their precursors, glucosinolates have shown

significant chemopreventive effects according to the documented data [97]. Benzyl isocyanate, a known maca glucosinolate metabolite [87], is said to have exhibited cancer chemopreventive activity by inhibiting major microsome-mediated benzo[α]pyrene (BP)-DNA adducts [98]. Furthermore, reports show that a known flavonolignan with anticancer properties, tricin [99], and its derivative, tricin 4′-O-[threo-β-guaiacyl-(7″-O-methyl)-glyceryl] ether were isolated and identified in maca root extract and exhibited cytotoxicity specific to human promyelocytic leukemia (HL-60) cell lines with the half maximal (50%) inhibitory concentration (IC_{50}) values of 40.4 and 52.1 μM, respectively.   This tricin derivative and lepidiline B also showed anti-inflammatory activities in LPS-treated RAW 264.7 macrophages by inhibiting nitrite production [100]. Studies show that inflammation plays a critical role in oncogenesis enhancing tumor initiation and promoting tumor progression due to its ability to release a variety of cytokines, chemokines, and cytotoxic mediators such as reactive oxygen species (ROS), metalloproteinases, interleukins, and interferons [69, 101]. Animal studies with the hydroalcoholic or aqueous extract of red maca containing 0.1 mg of benzylglucosinolate report reduction of a prostate size in male rats where prostatic hyperplasia had been induced by testosterone enanthate [86].

Maca is probably getting more attention in the society among the cancer patients due to these vast biological activities related to cancer in the literature [81, 102]. However, the cytotoxic, antioxidant and anti-inflammatory effects reported from the *in vitro* and animal studies have not yet been confirmed in humans.

1.3 Botanical-drug pharmacokinetic interactions

Since most cancer patients combine their conventional therapy with botanical dietary supplements [40], these are capable of interfering with the metabolism of concurrently used drugs, leading to unpredictable therapeutic outcome [19]. As the main metabolizing enzyme, CYP3A4 is a key enzyme in biotransformation of most chemotherapeutics [12]. Botanical constituents can interact with medicines either through CYP3A4 inhibition or induction [103]. Pharmacokinetic

interactions result mainly from changes in metabolism since most chemotherapeutics are administered intravenously making interactions at the intestinal absorption site infrequent [12]. Changes in metabolism directly affects excretion of the affected drug, resulting in subtherapeutic or toxic levels of the chemotherapeutic agent [38]. In the case of anticancer drugs, with their usually narrow therapeutic window, the metabolic interactions are more critical and may cause clinically unacceptable toxicities or decreased therapeutic effects [12, 19]. It is also worth noting that generally chemotherapeutics are dose-limited due to high off-site toxicity [11] and of course a decrease in their metabolic clearance may be lethal since this would increase their tissue concentrations [104].

In observation of the increasing risk of drug-botanical interactions, NCCIH presently stresses the importance of evaluating the safety and efficacy of widely used botanical dietary supplements [37]. Interactions between botanical dietary supplements and anticancer agents are currently underexplored and less well documented. Açaí and maca are among the most common botanical dietary supplements but with no reported drug interaction studies [105]. St. John's Wort (SJW) (*Hypericum perforatum* L.) is one of the few reported clinically interacting botanical dietary supplement. Having demonstrated a mild antidepressant activity, SJW however showed CYP3A4 inhibition after short-term exposure and induction after long-term exposure. Furthermore, clinical studies revealed that SJW interacts with anticancer agents which are CYP3A4 substrates, notably irinotecan, imatinib, and docetaxel. Due to CYP3A4 induction, subtherapeutic low blood levels of these agents were reported in concomitant administration with SJW [103, 106]. Aesculetin and aescin have also been identified as CYP3A4 inhibitors from horse chestnut (*Aesculus hippocastanum* L.) seed extract with reported IC_{50} values of 12.1 μM and 6.18 μM, respectively [107]. Black cohosh (*Actaea racemosa* L.) has been reported as the strong inhibitor of both CYP450 and carboxyesterase mediated biotransformation of tamoxifen and irinotecan, respectively, to their active metabolites posing a risk of cancer treatment failure [108]. Ginger (*Zingiber officinale*) root extract has also inhibited both tamoxifen CYP-mediated pathway and the irinotecan carboxyesterase-mediated pathway in the same study [108]. Other botanical dietary supplements with potential pharmacokinetic interactions with anticancer drugs by modulation of

CYP 450 metabolic enzymes according to the literature are garlic (*Allium sativum* L.), ginkgo (*Ginkgo biloba* L.), green tea (*Camellia sinensis* (L.) Kuntze), echinacea (*Echinacea purpurea* (L.) Moench), and kava (*Piper methysticum* G. Forst.) [109, 110].

1.3.1 Importance of determination of intestinal absorption of botanical constituents

It has been reported that more than 100,000 deaths per year in the United States may be caused by botanical-drug interactions [111]. While many studies have been conducted to predict botanical-drug interactions, omission of absorption determination of botanicals in the preclinical studies has been spotted as the main cause of discrepancy between preclinical interaction data and clinical details [105]. One of the prominent examples is with milk thistle (*Silybum marianum* (L.) Gaertn.) and ginseng (*Panax ginseng* C.A. Mey.) that showed predominant CYP3A4 inhibition *in vitro*. These botanical dietary supplements, however, did not cause significant pharmacokinetic interactions in clinical studies these CAM with midazolam, irinotecan, docetaxel or imatinib. A crucial factor attributed to this discrepancy was lack of bioavailability studies [103]. Determination of the intestinal permeability properties of drug candidates is recently becoming key in characterization studies performed during the lead selection and lead optimization [112] and this strategy can be effectively utilized in early stage prediction of drug-botanical interactions. The European Medicines Agency (EMA) recommends that clinically relevant interaction can only be claimed after factors and mechanisms related to a test compound's absorption are cleared [113].

Parallel artificial membrane permeability assay (PAMPA) and Caco-2 cells are the most frequently used *in vitro* models to assess intestinal permeability of constituents in the botanical dietary supplements [112]. The major absorption mechanism for medicines in the market is passive diffusion. Passive absorption occurs most commonly through the cell membrane of enterocytes (transcellular route) or via the tight junctions between the enterocytes (paracellular route) for the very small compounds often less than 200 Da [112]. PAMPA is a robust method to predict the transcellular passive absorption through a biological membrane that mimics gastrointestinal tract [114]. Effective permeability values calculated from PAMPA results have been reported to

correlate well with the *in vivo* absorption data. Having been validated with known medicines in the market, 30% fraction absorbable calculated by using effective permeability (P_e) equation is considered an acceptable starting point for predicting absorption in many drug discovery studies and it is also used to rank absorption extent of plant constituents in PAMPA [115]. PAMPA serves as a very useful tool for primary permeability screening during early bioavailability screening of natural products because of its high throughput capability [114].

Identification of bioavailable components of dietary supplements in the preclinical studies will most likely predict botanical dietary supplements and constituents that have a potential to cause pharmacokinetic interactions in the clinical studies.

1.3.2 Relevance of Phase I and Phase II metabolism of botanical constituents

For an *in vitro* system to have the best potential to predict *in vivo* botanical-drug interactions, the system should achieve *in vivo*-relevant intracellular concentrations of both the botanical constituents and their metabolites [116]. This is because the botanical-drug interactions may not only be caused by the original molecule but also by a metabolite of such a molecule [117]. Metabolism of a botanical constituent may generate metabolites with physicochemical and pharmacological properties that differ from those of the original constituent and therefore having impact on safety and efficacy [118]. Phase I biotransformations are mainly carried out by CYP enzymes and most common reactions are oxidation, reduction and hydrolysis [119]. Oxidation is the major Phase I reaction achieved by utilization of a cofactor nicotinamide adenine dinucleotide phosphate (NADPH) [14, 120]. Types of Phase I oxidation transformations may include aliphatic hydroxylation, aromatic hydroxylation, *N*-dealkylation, O-dealkylation, epoxidation, S-oxidation and *N*-oxidation [13]. Phase II reactions which are generally conjugations, are conducted by uridine 5'-diphospho-glucuronosyltransferases (UGTs). Main Phase II conjugation is glucuronidation via the cofactor uridine 5'-diphospho-glucuronic acid (UDPGA) [121]. Glucuronidation involves the transfer of glucuronic acid from UDPGA to wide structurally unrelated substrates possessing hydroxyl, carboxyl, amino or sulfhydryl groups, converting them

to water-soluble glucuronides [122]. Since metabolism generally results in the production of a more polar derivative that favours excretion, enterohepatic circulation plays a key role in its continued effects on CYP enzymes and extended exposure of the patient to such a toxic metabolite [11, 117]. Also, if a toxic botanical constituent is modified by Phase I and/or Phase II metabolism especially at absorption site, the bioavailability and effects on CYP enzymes may be significantly decreased [105].

1.3.3 CYP3A4 metabolic enzyme and significance in botanical-drug interactions

CYP3A4 is the most abundantly expressed cytochrome P450 isoform in the human liver and intestinal mucosa [123]. It comprises about 60% of total CYP enzymes [120, 124]. Due to its feature of structurally diverse substrates, CYP3A4 is responsible for the metabolism of approximately 70% of all drugs in the market [125] and it therefore plays a key role in both drug-drug and botanical-drug interactions because it can also be inhibited and induced by a wide range of structurally different compounds [13]. As the main metabolizing enzyme, CYP3A4 is a key enzyme in biotransformation of most chemotherapeutics. Drug interaction can occur through CYP3A4 inhibition resulting into increased systemic availability of the anticancer drug or CYP3A4 induction leading to decreased blood concentration of the anticancer drug [12]. The logarithmic concentrations are said to be of immense importance for evaluation of safety and efficacy. These include IC_{50} determination that should be done at different concentrations of the inhibiting agent in the case of CYP3A4 inhibition [126]. Due to narrow therapeutic window of most chemotherapeutic agents and inherent toxicity [12], any disturbance on their metabolism poses a danger of significant metabolic interaction. Studies have shown that botanical dietary supplements consist of multiple constituents which can alter drug disposition by multiple mechanisms [103] and indeed clinically relevant pharmacokinetic interactions have been reported between several botanical dietary supplements and anticancer agents [103, 106, 108].

1.7 Project rationale

The concomitant use of botanical dietary supplements and anticancer drugs is significantly high in cancer patients. Açaí berry and maca root are some of the most common botanical dietary supplements among cancer patients in the US due to scientific claims indicating their biological activity against cancer. CYP3A4 is the main metabolizing enzyme for chemotherapeutics. However, with its wide substrate spectrum, CYP3A4 can also be inhibited and induced by structurally diverse compounds. The botanical dietary supplements, having a complex mixture of different classes of natural constituents, contain CYP3A4 substrates, inhibitors and inducers. The inhibition or induction of CYP3A4 in the presence of an anticancer agent causes a deep concern due to their narrow therapeutic window and inherent off-site toxicity. The inhibition of CYP3A4 therefore increases anticancer drug blood concentration and half-life exposing a patient to toxic levels of the anticancer drug for longer times. Chemotherapy-induced toxicity is a significant cause of mortality and morbidity in cancer. Preclinical studies are therefore required to predict pharmacokinetic interactions. However, the *in vitro* studies omitting bioavailability of botanical constituents have shown poorer prediction of pharmacokinetic interactions seen by lack of correlation with the *in vivo* data.

In this work, incorporation of intestinal absorption studies in the prediction of pharmacokinetic interactions by CYP3A4 inhibition has been established. This is achieved by screening açaí berry and maca root constituents for intestinal passive absorption and then evaluating only absorbed constituents in the CYP3A4 inhibition studies. Thus, the rationale of this study is to establish a reliable clinically-relevant strategy for better prediction of botanical-drug pharmacokinetic interactions by CYP3A4 inhibition. As a result, by reducing the discrepancy between preclinical and clinical drug-botanical dietary supplements interaction data, this strategy sets a way to avoid unnecessary clinical trials.

1.8 Research objectives

The aim of this research is to establish an LC-MS-based strategy for clinically-relevant prediction of botanical-drug pharmacokinetic interactions by CYP3A4 inhibition using açaí berry and maca plant extracts. The specific goals of this research are:

1. Evaluation of açaí berry and maca root extracts in parallel artificial membrane permeability assay (PAMPA) to determine intestinal transcellular passive absorption profile of the chemical constituents.

2. Evaluation of bioavailable açaí berry and maca root constituents in CYP3A4 interference studies to determine potential for CYP3A4 inhibition.

3. Evaluation of açaí berry and maca root extracts in Phase I & II metabolism bioassays to determine metabolites and further evaluation of metabolites for CYP3A4 inhibition.

4. Structural elucidation of Phase I & II metabolites from açaí berry and maca root extracts.

Chapter 2: Establishment and optimization of the LC-MS-based strategy for screening of passively absorbed plant extract constituents for CYP3A4 inhibition

2.1 Introduction

As EMA recommends that clinically relevant interaction can only be claimed after factors and mechanisms related to a bioactive plant constituent or compound's absorption are cleared [113], botanical-drug interactions in concomitant use of anticancer drugs and açaí and maca dietary supplements can be reliably predicted after identifying bioavailable constituents from the extracts of these plants. LC-MS has proved great usefulness in prediction of botanical-drug pharmacokinetic interactions especially in CYP3A4 inhibition studies [127-129]. The well-established metabolic interaction studies through CYP3A4 activity modification have shown that a probe substrate should be used as a "victim" drug [130]. In these studies, mass spectrometry was used to measure the extent of inhibition displayed by the plant extracts or pure natural product compounds by monitoring a metabolite of a probe substrate specific to CYP3A4 enzyme [125, 131]. The use of a probe substrate at the concentration around its Km (substrate concentration at half the maximum velocity) has been demonstrated a standard method for drug-interaction studies practiced in the pharmaceutical industry [131-133]. Further, metabolic inhibition studies resemble the *in vivo* pharmacokinetic interactions more closely if human liver microsomes (HLMs), expressing a mixture of different metabolizing enzymes are used. More precisely, HLMs are not only preferred for CYP inhibition studies over hepatocytes but also accepted for regulatory *in vitro* drug interaction studies used by pharmaceutical companies [134].

In the current research, LC-MS-based PAMPA studies are used to identify açaí berry and maca root constituents that are absorbable via transcellular passive absorption across the lipid membrane mimicking the human gastrointestinal barrier. The absorbed sample is then screened for CYP3A4 inhibition utilizing HLMs.

2.2 Materials and methods

2.2.1 Chemicals

All solvents used were HPLC and LC-MS grade and were purchase from Thermo Fisher Scientific (Atlanta, GA). LC-MS grade formic acid, KH_2PO_4, Na_2HPO_4, $MgCl_2$, EDTA, midazolam, ketoconazole, β-estradiol, zidovudine, 1-naphthol, testosterone, D-saccharolactone, alamethicin, sulfasalazine, amiloride, caffeine, NADPH and UDPGA were purchased from Sigma-Aldrich (Allentown, PA). A standard 1'-hydroxymidazolam and the internal standard $[^{13}C_3]$ 1'-hydroxymidazolam were bought from Sigma-Aldrich (Allentown, PA) and Corning Life Sciences (Tewksbury MA) respectively. All standards purchased from Sigma-Aldrich and and Corning Life Sciences had no less than 98% purity, as analyzed by HPLC. Deionized water was purified by a Milli-Q reagent water system (Millipore, MA). All buffers and media used for the assays were prepared using LC-MS grade water (Thermo Fisher Scientific, Atlanta, GA). PAMPA plates were bought from Corning® Gentest™ (Tewksbury MA). Human liver microsomes for CYP3A4 inhibition and Phase I assays (HMMC-PL) were sourced from Thermo Fischer Scientific (Atlanta, GA) while those for Phase II metabolism assays were purchased from Sekisui XenoTech, LLC (H0610) (Kansas City, KS).

2.2.1.1 Identity of the plant materials

The samples of açaí (lot 20569) and maca (lot 21780) plant materials were supplied by Mountain Rose Herbs (Eugene, OR). These plant materials were authenticated as follows:

1. Açaí

Title	Açaí Berry powder
Plant part	Fruit
Sample description	~78g in a zip locked bag
Form of botanical	Crude plant powder
Appearance	Brown fine powder
Lot	(20569) $\longrightarrow$ Lanes 4(3µl), 5(3µl)
Sample	AAV16113MRH1_1
Latin name	*Euterpe oleracea*
Supplier	Mountain Rose Herbs
Reference sample	Lane 2(3µl) (AAV7509MRH) (Fruit); Lane 3(3µl) (AAV33808AÇAÍ) (Fruit); Lanes 6(4µl), 7(2µl) (AAV22609NOW) (Skin and pulp) *Euterpe oleracea*; authenticated by macroscopic, microscopic &/or TLC studies according to the reference source cited below, held at Alkemist Labs, Costa Mesa, CA
Reference source	Method developed by Alkemists Laboratories SOP-700-0001-R3
Analyst	JN, ML, RT 35724
Sample prep:	0.3g+3mL CH_3OH sonicate/heat @ ~50 ˚C ~1/2 hr.
Stationary phase:	Silica gel 60, F_{254}, 10 x 10 cm HPTLC plates
Mobile phase:	Acetone: toluene: HCOOH [5/4/1]

Detection:	(1) UV 365 nm (2) 10% Ethanolic H_2SO_4 $\longrightarrow$ 115 ˚C 15 min $\longrightarrow$ UV 365 nm
Reference standard	Lanes 1(3µl) and 8(3µl) L-ascorbic acid (10930EE, Sigma-Aldrich, ~0.1% in CH_3OH
Comments and conclusions	Yellow line = sample origin @ 10 mm, red line = solvent front @ 70 mm. Lanes 4, 5 are test sample Açaí Berry Powder (20569). Lanes 2, 3, 6, 7 are the authenticated reference samples used for comparison. This test sample, Açaí Berry Powder (20569), is consistent with the chromatographic profile of the reference samples of *Euterpe oleracea*, used above. This test sample, Açaí Berry Powder (20569) has characteristics of *Euterpe oleracea* fruit.
Note:	The above conclusion may be a function of the natural variance found in botanicals. The growing and drying conditions, age, seasonal variations etc. all play a role in the phytochemical fingerprint of botanicals and variations are expected.
Examined, reviewed & authorized by:	Elan Sudberg, CEO, Alkemist Labs
Work performed at:	Alkemist Labs 1260 Logan Ave B2 Costa Mesa, CA 92626 714-754-4372 714-668-9972 (Fax) Email: sales@alkemist.com

	Web Site: www.alkemist.com
Report date	06/14/13

2. Maca

Title	Maca powder
Plant part	Root
Sample description	Clear reclosable plastic bag
Form of botanical	Crude plant powder
Appearance	Sand-colored powder
Lot	21780
Sample	GC35614MRH1_1
Latin name	*Lepidium meyenii* Walp. [Brassicaceae]
Supplier	Mountain Rose Herbs
Reference sample	GC33208NI1; GC3803MP *Lepidium meyenii* Walp. [Brassicaceae] authenticated by macroscopic, microscopic &/or TLC studies held at Alkemist Labs, Costa Mesa, CA
Reference source	Internal reference sample SOP-1000-0001-R1 USP-PF, Vol. 27(2) (Mar.-Apr. 2001); Official methods of analysis of AOAC. 16th Ed.
Analyst	E. Sudberg
Magnification	400X
Chemical reagents	Acidified chloral hydrate glycerol solution
Sample findings	(2) oval and irregular starch granules (3) long narrow scalariform treachery vessels

Comments and conclusions	The sample is representative of *Lepidium meyenii* Walp. [Brassicaceae] root based on reference samples and the consistent characteristic cellular structure of a root. The characteristic cellular structures identified in this sample are the oval and irregular starch granules seen in monograph (2) and long narrow scalariform treachery vessels seen in monograph (3). The test sample, maca powder (21780), is consistent with the microscopic characteristics of the reference samples of *Lepidium meyenii* Walp. [Brassicaceae] used above & is characteristic of *Lepidium meyenii* Walp. [Brassicaceae] root.
Note:	The presence of soluble excipients and other plant species material was not detected in this test sample.
Analyzed by:	Élan M Sudberg
Examined, reviewed & authorized by:	Sidney Sudberg, Director, Alkemist Labs
Work performed at:	Alkemist Labs 1260 Logan Ave B2 Costa Mesa, CA 92626 714-754-4372 714-668-9972 (Fax) Email: sales@alkemist.com Web Site: www.alkemist.com
Report date	01/12/15

2.2.1.2 Açaí and maca plant standard compounds

The well HPLC-analyzed açaí standard anthocyanins, cyanidin-3-O-glucoside ($\geq$ 96%), cyanidin-3-O-rutinoside ($>$ 96%), cyanidin-3-O-sambubioside ($\geq$ 95%), pelargonidin-3-O-glucoside ($\geq$ 95%) and pelargonidin-3-O-rutinoside ($\geq$ 90%), were purchased from Indofine Chemical Company, Inc. (Hillsborough, NJ). Other açaí standard compounds, quercetin-3-O-rutinoside ($\geq$ 95%, HPLC), quercetin-3-glucoside ($>$ 98%, HPLC) and isovitexin ($>$ 98%, HPLC) were sourced from Sigma-Aldrich (St. Louis, MO) while orientin (neat, HPLC), homoorientin (95.7%, HPLC), quercetin (93.4%, HPLC), protocatechuic acid (neat, HPLC), catechin (99.6, HPLC), chrysoeriol (neat, HPLC), vitexin (99.3%, HPLC), gallic acid (96%, HPLC), syringic acid, (93.9%), taxifolin (99.9%), vanillic acid (neat, HPLC), ferulic acid (96.8%, HPLC) were purchased from ChromaDex, Inc. (Irvine, CA) and catechol ($\geq$ 95%, HPLC) from Extrasynthese (Genay, France).

Maca standard macamides, N-benzylhexadecanamide ($\geq$ 98%, HPLC), and N-(8Z-Heptadecen-1-yl)-O-(3-pyridylmethyl) carbamate ($\geq$ 98%, HPLC) were purchased from Cayman Chemical Company (Ann Arbor, MI 48108, USA) and amino acids L-phenylalanine ($>$ 99%, HPLC), L-tryptophan ($>$ 98%, HPLC) and L-tyrosine ($>$ 98%, HPLC) from Sigma-Aldrich (St. Louis, MO).

2.2.2 Plant extracts preparation

Dichloromethane (DCM), methanol and acidic-methanol extracts were prepared for açaí and maca plant materials. To enhance efficient extraction, the extract: solvent ratio of 1:5 was selected.

2.2.2.1 Açaí plant extracts

2.2.2.1.1 Dichloromethane and methanol extracts

To analyze the fatty acids, a sample of açaí plant material powder (50.0 g average dry wt.) was weighed and sonicated in a Bransonic Model 2510 ultrasonic bath (VWR International, Atlanta, GA) with DCM (250 mL) at 25 °C for 40 min with temperature monitoring at 0, 10, 20, 30 and 40 min to avoid overheating where water in the ultrasonic bath was replaced with fresh deionized water if temperatures reached about 40 °C. The sample was put into different 50 mL polypropylene centrifuge tubes in volumes of 30 mL and centrifuged at 4000 rpm for 20 min in Beckmann Coulter Allegra® 6 Series centrifuge (Beckman Coulter, Inc., Brea CA) at 4 °C. The produced supernatant was decanted into one 250 mL Erlenmeyer flask and the DCM soluble portion filtered through 0.2 μm PTFE membrane filters (VWR International, Atlanta, GA). The filtrate was transferred into a 1 L round bottom flask (Yamato Scientific America Inc, Orangeburg, NY) and dried under monitored high vacuum (850 mbar) at 40 °C using a Büchi rotavapor R-210 equipped with Büchi recirculating chiller B-740 and Büchi vacuum pump V-700 (VWR International, Atlanta, GA). Three times extraction with DCM was done.

The generated residue was further extracted by sonication with methanol for three times (250 mL x 3) under similar experimental conditions listed above to extract polyphenols. The methanol soluble portions were then filtered and dried under high vacuum (295 mbar) at 40 °C.

2.2.2.1.2 Acidic methanol extracts

Following the same procedure as above, to extract anthocyanins, a sample of açaí plant material powder (30.0 g average dry wt.) was accurately weighed and extracted with 150 mL of acidic methanol: water (70:30, 0.1% hydrochloric acid v/v). The acidic methanol portions were dried under monitored high vacuum (300 mbar down to 72 mbar as methanol evaporates and leaves only the water content) at 40°C.

2.2.2.2 Maca plant extracts

2.2.2.2.1 Dichloromethane and methanol extracts

To extract macamides, the maca plant material powder (50 g average wt.) was accurately weighed and extracted with 250 mL of DCM following the procedure used for açaí. The DCM soluble portions were dried under high vacuum (850 mbar) at 40 °C. In extraction of maca phenolic constituents, the generated residue was further extracted by sonication with methanol for three times (250 mL x 3) under similar experimental conditions. The methanol soluble portions were dried under high vacuum (245 mbar) at 40 °C.

2.2.2.1.2 Acidic methanol extracts

To extract glucosinolates, maca plant material powder (30.0 g average dry wt) was weighed accurately and extracted with 150 mL of acidic methanol: water (70:30, 0.1% hydrochloric acid v/v) following the similar described procedure. The acidic methanol portions were dried under monitored high vacuum (300 mbar down to 72 mbar as methanol evaporates and leaves only the water content) at 40°C.

All açaí and maca samples from the rotavapor, enclosed with the supremium aluminum foil (VWR International, Atlanta, GA) were transferred to 20 mL disposable scintillation vials and subjected to the nitrogen evaporator (Organomation Associates, Inc., Berlin, MA) at 25 psi. Samples from the nitrogen evaporator were further treated under a lyophilizer (DOTmed, New York, NY) to produce sufficiently dried final extracts. `

2.2.3 Chemical fingerprinting and profiling of açaí and maca plant extracts

An Agilent 6520 Q-TOF mass spectrometer equipped with a 1220 rapid resolution liquid chromatography (RRLC) system (Agilent Technologies, Little Falls, DE) and electrospray ion

(ESI) source was used for fingerprinting and mass profiling of açaí and maca plant samples. To prepare samples for LC-MS analyses, dried DCM and methanol açaí extracts were both weighed separately to 10 mg and reconstituted in 1 mL of methanol–water (80:20 v/v) while acidic-methanol extract was reconstituted in methanol and water (70:30, 0.1% formic acid v/v) to the same concentration. Similarly, dried DCM and methanol maca extracts were both reconstituted in methanol–water (80:20 v/v) to 10 mg/ml. The dried acidic-methanol maca extract was instead reconstituted in acetonitrile: water (75:35, 0.1% formic acid v/v) to the same concentration. All samples were filtered through 0.2 μm PTFE membrane filters (VWR International, Atlanta, GA) into the autosampler vials prior to LC-MS analyses.

All extracts except for acidic methanol of maca were analyzed on a 4.6 x 100 mm, 3.5 μm ZORBAX Eclipse Plus C18 column (Agilent Technologies, New Castle, DE). Acidic methanol maca extract, on the other hand, was analyzed on a Waters Xbridge Amide 3.5 μm, 3.0 mm x 100 mm column (Waters Corporation, Milford, MA). The flow rate was set at 0.4 mL/min and the sample injection volume at 5 μL while the acquisition rate was 1.41 scan/s with the complete mass scanning range from m/z 100–1000. The MS conditions were optimized with a negative and positive ion ESI-MS analysis performed with a capillary voltage of 3200 V; drying gas temperature 350°C; fragmentor voltage 175 V and skimmer 65 V. Nitrogen was supplied as a nebulizing gas at the pressure of 25 psig and as a drying gas at flow rate 10 L/min.

LC separation for anthocyanins from acidic methanol açaí extract was carried out using a gradient mobile phase containing (A) 0.1% formic acid (FA) in water and (B) 0.1% FA in methanol and acetonitrile (50:50, v/v) with an initial condition of 1% B for 2 min. The mobile phase was then linearly increased to 99% B at 25 min and maintained same until 27 min. The conditions were then taken back to 1% B at 30 min and equilibrated further for 5 min. The analysis was carried out at 25 °C column temperature. MS experiments were carried out in positive electrospray ionization mode.

Chromatographic analyses of açaí fatty acids and non-anthocyanin polyphenols in DCM and methanol extracts of açaí samples respectively, were both conducted with a gradient mobile phase consisting of (A) 0.1% formic acid in water and (B) 0.1% formic acid in methanol (MeOH) at 40

27

°C. A linear gradient was run as follows: 0-2 min, 30% B; 25-29 min, 99% B; 30-35 min, 30% B followed by 5 min post time. Negative electrospray ionization mode was used.

For maca LC-MS analysis, qualitative analysis of macamides and phenolics from DCM and methanol maca extracts, respectively, was performed using a mobile phase consisting of solvent (A) water and solvent (B) acetonitrile (ACN). A mobile phase gradient was run as follows: 0 min, 5% B; 4 min, 25% B; 8 min, 45% B; 12 min, 65% B; 16 min, 85% B; 20 min, 100% B, 26-30 min, 5% B followed by 4 min post time. MS experiments were carried out in positive electrospray ionization mode.

Qualitative analysis of maca glucosinolates was performed using a mobile phase consisting of solvent (A) water, 0.1% formic acid (FA) and solvent (B) ACN, 0.1% FA from acidic methanol maca extracts. A mobile phase gradient was run as follows: 0 min, 95% B; 4 min, 75% B; 8 min, 55% B; 12 min, 35% B; 16 min, 15% B; 20 min, 0% B, 26-30 min, 95% B followed by 4 min post time. Negative electrospray ionization mode was used.

Selected available plant standard compounds listed in the section 2.2.1.2 at 50 µg/mL were analyzed under the same LC-MS conditions as their corresponding plant extracts and used to confirm their presence in the plant extracts.

2.2.4 Determination of intestinal absorption via transcellular passive diffusion for plant extracts and plant standard compounds

2.2.4.1 Development and optimization of PAMPA intestinal absorption assay

Plant extracts selected for this study and further screenings were methanol and acidic methanol açaí extracts and DCM, methanol and acidic methanol maca extracts. DCM açaí extract was left out because it contained mainly well-known fatty acids [135] whose absorption and metabolism properties are well studied [136-138]. The testing concentrations were chosen based on the concentrations of açaí and maca botanical dietary supplements in the market and on the *in vitro*

biologically active (cytotoxic and antioxidant) concentrations. The biologically active concentrations for extracts from both plants ranged from 5-10 µg/µL [76, 139] while the doses of their commercial dietary supplements (i.e. 100% açaí juice and natural maca pure dietary supplements) found from an online National Health Institute (NIH) dietary supplement label database generally ranged from 1400 mg – 30000 mg daily (https://dsld.nlm.nih.gov/dsld/). This means that in the human plasma total volume of 4 L, concentration of the botanical dietary supplement in that case is approximately 0.25 – 7.5 µg/µL if absorption is not the rate-limiting step. However, it is known that intestinal absorption is a major barrier which will surely result into blood concentrations lower than those from theoretical calculation. Nevertheless, these concentrations from *in vitro* and commercial dietary supplements directed a better choice of testing concentrations. General schematic representation of the PAMPA intestinal absorption assay followed by Phase I and Phase II metabolism is shown below (Fig. 2.1).

PAMPA plates were kept in -20 °C upon receipt and were warmed to the room temperature for 30 min prior to use. All plant extract stock solutions were prepared in 1:5 DMSO: buffer at a concentration of 50 µg/µL. The stock solutions were then diluted to 5, 7.5, 10 and 15 µg/µL with buffer composed of 0.014 M KH_2PO_4 and 0.054 M Na_2HPO_4 (final pH 7.4) making a total of 300 µL in each well of the PAMPA donor site. Similarly, these concentrations were expected to be much lower in PAMPA acceptor site upon the completion of the experiment and indeed the PAMPA plate supplier, Corning® Gentest™, states that the concentration in the acceptor site will be approximately 50x lower than the initial PAMPA donor concentration [140]. Two hundred (200) µL per well of buffer was then added in the PAMPA acceptor plate. The acceptor plate was then slowly placed on the donor plate and the system incubated at room temperature for 5 hours protected with its lid to prevent evaporation under constant light shaking (75 rpm) using Inheco Single TEC Controller (INHECO Industrial Heating & Cooling GmbH, Fraunhoferstrasse, Germany). After incubation, the plates were separated and sample from each well in both the donor and acceptor plates transferred to corresponding wells in different 96-well plates denoting donor and acceptor sites. Sample transfer to 96-well plates was done immediately after completion of incubation time to prevent constituents from diffusing back to the donor site. Also, this transfer was carried out carefully using good pipetting technique to avoid breaking the lipid membrane

which would compromise a barrier between two sites thereby exaggerating the absorption results. To confirm the integrity of the PAMPA lipid membrane, three standards sulfasalazine (log P_e -5.52, non-permeable [114]), amiloride HCl (log P_e -4.4, mid-permeable [141] and caffeine (log P_e -4.2, high permeable [142]) were used. These standards were dissolved in 1:5 DMSO: buffer at a concentration of 10 mM stcok solutions and 50 μM used in PAMPA tests. DMSO concentration used in all these studies was 0.996%. This was pertinent since DMSO concentration above 1% exerts its penetration enhancing effects resulting into exaggerated absorption data [143]. Control wells were included in the PAMPA plate in which 1% DMSO or only buffer was tested for effects on membrane permeability. Another control experiment was carried out in parallel with the actual PAMPA experiment. This control experiment was carried out only to generate sample donor concentrations at the beginning of PAMPA, $C_D(0)$, that would later be compared to donor concentration at the end of the assay, $C_D(t)$, and acceptor concentration, $C_A(t)$, to assess the extent of absorption. All experiments were done in triplicate.

After extensive optimization, this study also established a sample cleaning method to increase MS detection of passively absorbable constituents since individual constituents are usually found in lower concentrations in the plant extracts [114] making their concentration in the PAMPA acceptor site even lower because passive absorption is concentration dependent [144]. This problem was exacerbated by the used PAMPA assay buffer since it is known that non-volatile phosphate buffers cause signal suppression and ionization interferences during the LC-MS analysis [145]. The use of a solid-phase extraction (SPE) resource TARGA C18 macroSpin^{TM} SMM column that can be used for salt removal from small molecules [146] was established. In this procedure, 50 μL from each well was desalted through TARGA-C18 MacroSpin^{TM} SMM columns. Desalting procedures with TARGA-C18 MacroSpin^{TM} SMM columns were completely specific to each extract (Table 2.1-2.2).

Table 2.1 Desalting steps of açaí plant extracts

Desalting steps	Acidic MeOH extract	MeOH extract
1. Conditioning	100 µL ACN	100 µL MeOH
2. Equilibration	100 µL LC-MS grade H_2O	100 µL LC-MS grade H_2O
3. Sample loading	50 µL sample	50 µL sample
4. Rinsing	No rinse	50 µL LC-MS grade H_2O
5. Elution	50 µL 80% MeOH, 0.2% FA	50 µL 80% MeOH, 0.2% FA

Table 2.2 Desalting steps of maca plant extracts

Desalting steps	Acidic MeOH extract	MeOH extract	DCM extract
1. Conditioning	100 µL ACN	100 µL ACN	100 µL MeOH
2. Equilibration	100 µL LC-MS grade H_2O	100 µL LC-MS grade H_2O	100 µL LC-MS grade H_2O
3. Sample loading	50 µL sample	50 µL sample	50 µL sample
4. Rinsing	No rinse	50 µL LC-MS grade H_2O	50 µL LC-MS grade H_2O
5. Elution	50 µL 70% ACN, 0.1% FA	50 µL 70% ACN, 0.1% FA	50 µL 100% ACN

All the steps were separated by centrifuging at 8000 rpm for 1 min at 4 °C on Beckman Coulter Microfuge® 22R centrifuge (Beckman Coulter, Inc., Brea CA) and the final eluates injected into LC-MS.

The same plant standard compounds used for chemical fingerprinting were also studied for passive absorption in PAMPA to accurately identify absorbable constituents. These standard compounds were made into a stock solution of 1 mg/mL with DMSO: buffer (1:5) and diluted with a PAMPA buffer to 50 µg/mL in the PAMPA donor plate. These concentrations were chosen to be 100x lower than the ones tested from plant extracts because usually single constituents are found at lower concentrations in plant extracts and occurring at uncontrolled various levels [114]. Total DMSO concentration in each PAMPA donor well was 0.8%. All analyses were done in triplicate.
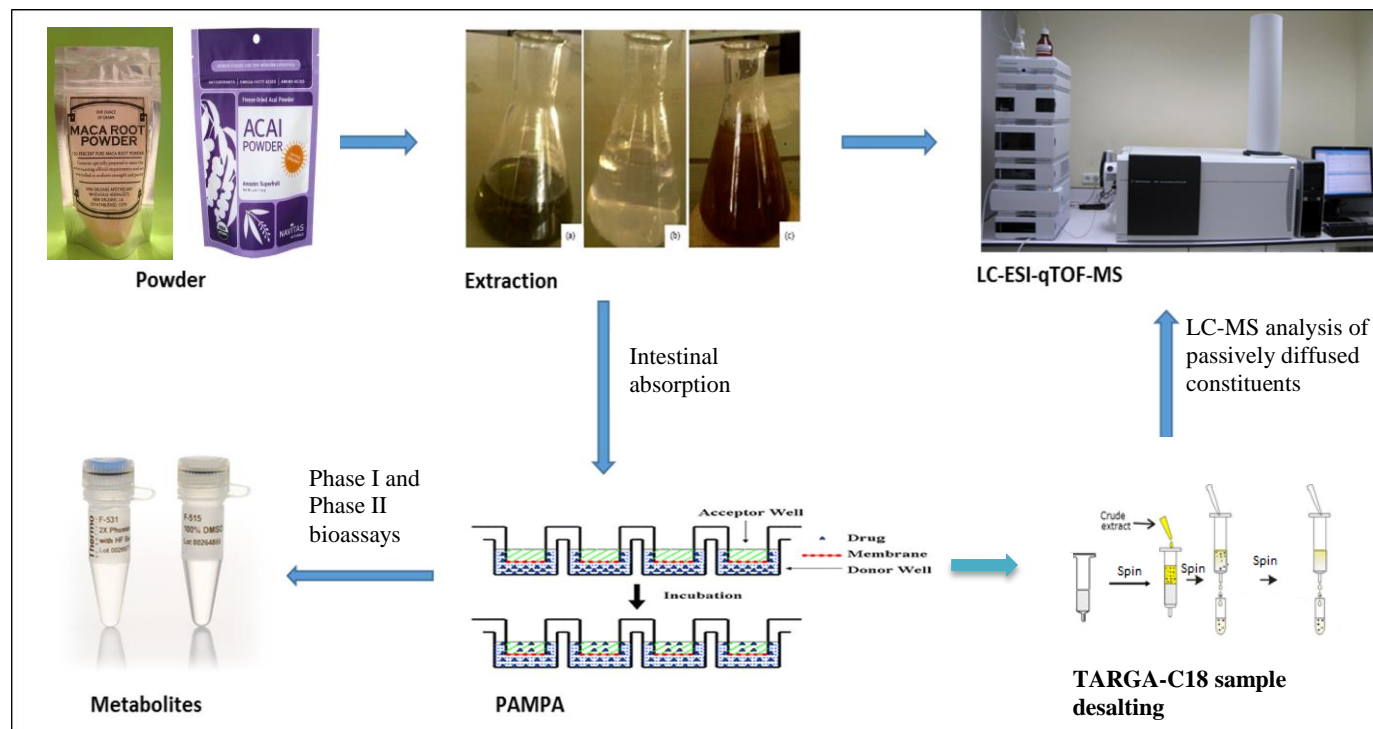
Fig. 2.1. Schematic representation for determination of passively absorbable constituents and formed metabolites

2.2.5 Phase I and Phase II metabolism screening studies for plant extracts and plant standard compounds

2.2.5.1 Development and optimization of Phase I and Phase II metabolism assays

Human liver microsomes (HLMs) selected for Phase I metabolism assay were pooled HLMs of a catalogue Gibco™ HMMC-PL from Thermo Fischer Scientific (Atlanta, GA). These were chosen based on the relatively high content of CYP450 (0.286 nmol CYP450 mg protein) reported on its certificate of analysis (https://tools.thermofisher.com/content/sfs/COAPDFs/2016/PL050B-B_HMMCPL.pdf)   since these are enzymes responsible for Phase I metabolism. Selection was also based on the high number of donors (50) from which HLMs were pooled and donors being of mixed gender as stated in the certificate of analysis to have a wide coverage of population that may

present different pharmacogenetic properties. A cofactor used in this assay was NADPH which enables formation of metabolites mainly by Phase I oxidation reaction [14]. Apart from oxidation, reduction, hydrolysis and oxidative demethylation [147] may also occur attaining the most common Phase I reactions [15].

For Phase II metabolism assay, HLMs from Sekisui XenoTech, LLC (H0610) (Kansas City, KS) (catalogue number: H0610) were chosen on the basis that they express wider range of both UGT1 and UGT2 subfamilies which are major enzymes responsible for glucuronidation [148]. Another critical point for this selection was the localization of UGTs; according to its certificate of analysis (https://www.xenotech.com/getattachment/84c67735-10f2-495b-958b-a6763f941c36) , H0610 is composed of UGTs expressed in both liver and intestine which are two main metabolic sites [149]. These are UGT1A1, 1A3, 1A6, 1A9 and UGT2B7 localized at both liver and intestinal tissues; UGT2B17 that is predominantly expressed in the small intestines [149]. The cofactors used in this assay was UDPGA alone or in combination with NADPH expected to enable the formation of glucuronides, main Phase II metabolites in adults [121]. Combination of UDPGA and NADPH was considered because apart from plant constituents that originally have nucleophilic functional groups (-OH, -NH$_2$, -SH, -COOH) that can readily undergo conjugation into a glucuronide, there are those than may need to undergo Phase I functionalization prior [150, 151]. NADPH would serve a purpose of functionalization while UDPGA would catalyze the glucuronidation process.

The highest concentration of the plant extracts from PAMPA donor (15 µg/µL) with its corresponding acceptor site concentration (0.3 µg/µL) were chosen for this study because it was anticipated that most metabolites would be found if higher concentration is used since some plant constituents are inherently minor [114] and the fact that passive absorption is concentration-dependent [144] means higher acceptor concentrations can be attained from higher donor concentrations of PAMPA. To estimate the concentration of plant extract delivered into the Phase I reaction mixture from either the PAMPA donor or acceptor site, a ratio suggested by the PAMPA supplier (acceptor concentration 50x lower than the initial donor concentration) [140] was used. This was described as a prediction of the plant extract concentration as the whole entity and not

individual constituents. The highest PAMPA acceptor concentration was therefore estimated to be 0.3 µg/µL which correlates with previously estimated blood concentrations from açaí and maca botanical dietary supplements' consumption above. The PAMPA donor site extract concentration was then estimated to have reduced to 14.7 µg/µL at the end of PAMPA experiment. The decision to screen both samples from both the acceptor and donor sites of PAMPA was made to acquire full spectrum of potential metabolites. The reason to include PAMPA donor site samples in metabolism assays was based on the principle that metabolism at the intestinal tract can affect absorption of a plant constituent [150, 152]. This means that, for example, if a constituent could not be absorbed because it was too nonpolar in its original form hence dissolution in the intestinal medium being a rate-limiting step, it may be absorbed after its polarity has been sufficiently increased by Phase I oxidation [153]. On the other hand, if a constituent could not be absorbed due to being originally too polar to cross lipid bilayer of the intestinal membrane, it may be absorbed after hydrolysis if that removes a polar group such as a glucose molecule [154-156].

2.2.5.1.1 Phase I metabolism assay

The HLMs were safely stored in -80 °C until use and reagents were kept in ice during the experiment execution. A solution of HLMs was generated in 0.1 M KH_2PO_4 buffer consisting of 1mM $MgCl_2$ (pH 7.4) at a stock concentration of 5 mg/mL. HLMs were added in the 1.5 mL Fisherbrand™ Premium microcentrifuge tubes (Thermo Fisher Scientific, Atlanta, GA) in the assay buffer to generate 0.5 mg HLMs in total 100 µL reaction. Plant extract from PAMPA acceptor site at concentrations 0.15 µg/µL was then added. Another experiment was carried out with the plant extract from PAMPA donor site. The mixture was then preincubated in a gentle shaking (75 rpm) VWR Water Bath (VWR International, Atlanta, GA) at 37°C for 5 min. After preincubation, NADPH (1 mM) was added to start a Phase I reaction while attaining 100 µl final volume and incubated at 37°C for 10 min in a gentle shaking (75 rpm) water bath. The reaction was stopped with 75 µl of ice-cold acetonitrile. After sitting on ice for 30 min, stopped reactions were centrifuged in Beckman Coulter Microfuge® 22R centrifuge at 13,000 x g at 4 °C for 15 min and supernatant collected for LC-MS analysis. Blank experiments, incubations with all reagents

except cofactors were also performed. These were used as controls from which the theoretical or predicted metabolites would also be extracted to identify new emerging peaks that formed only in the reaction sample.

Plant standard compounds used for chemical fingerprinting were also studied under Phase I metabolism assay. The same reaction conditions as above were used. Since PAMPA study with these standard compounds showed that a considerable number of them were not passively absorbed, a decision was made to study them in metabolism assay without going through PAMPA so that all of them could be analyzed and give a full spectrum of potential metabolites. This was also based on the literature that some plant constituents (i.e maca glucusinolates) may not be passively absorbed but their metabolites forming at the intestinal barrier be the ones absorbed [157]. Being pure compounds as opposed to constituents in the complex mixtures (extracts), they were studied at a concentration (0.05 µg/µL) lower than the one tested for plant extracts.

Control experiments were carried out with a CYP3A4 probe substrate midazolam (3µM) in place of the plant extract to confirm the integrity of this metabolic enzyme in the assays. All experiments were conducted in triplicate and triplicate LC-MS analysis was performed.

2.2.5.1.2 Phase II glucuronidation assay

Phase II enzymatic reactions with plant extracts and standard compounds were carried as above except that the microsomes were activated by adding alamethicin 20µg/ml and placed on ice for 15 min to allow pore formation by alamethicin after which a β-glucuronidase inhibitor, saccharolactone (5 mM) was added. The cofactor UDPGA (5 mM) alone or combined with NADPH (1 mM) was added to initiate the reactions after preincubation.

Control experiments were carried out with individual probe substrates covering both hepatic and intestinal UGTs; 17β-estradiol 100 µM (UGT1A1), zidovudine 500 µM (UGT2B7), testosterone 50 µM (UGT2B17) and 1-Naphthol 500 µM (UGT1A6). All experiments were conducted in triplicate and triplicate LC-MS analysis was performed.

2.2.5.2 Literature search for Phase I and Phase II metabolites

Extensive search of metabolites from individual plant constituents found in all 5 total extracts was done. These were searched for in Scifinder, PubMed, Sciencedirect and in databases like Human Metabolome Database.

2.2.5.3 Predictions of Phase I and Phase II metabolites using Biotransformation Mass Defects and online MetaPrint2D-React tools

For those açaí and maca plant constituents with no reported metabolites in the literature, scientific predictions were done using metabolite-predicting softwares. The reliable metabolite prediction is said to be crucial at the preclinical stage to identify metabolites that might have impact on safety and efficacy and to reduce the risk of expensive clinical-stage trials [118]. Two metabolite predicting tools, an Agilent Biotransformation Mass Defects and online MetaPrint2D-React were efficiently utilized for predicting metabolites. Agilent Biotransformation Mass Defects has been considered a powerful tool for metabolite identification [158] and online MetaPrint2D-React tool has been described as a statistical model for atom mapping enabling scientists to predict structural modifications by Phase I and Phase II biotransformation [118, 159, 160].

In this study, these two tools were used as complementary to each other for LC-MS-based metabolite identification from açaí and maca plant extracts. The MetaPrint2D-React tool was not just able to predict most probable metabolism sites on the chemical structures of plant constituents but would also generate chemical structures of the probable Phase I and Phase II metabolites considering physicochemical properties of the molecules such as stereochemistry, polarity and size (Fig. 2.2). This tool would then rank the metabolites assigning a value of 1.0 to the most favorable metabolite and less than 1.0 to the predicted minor metabolites. From here, Agilent Biotransformation Mass Defects could generate molecular formulas and accurate masses for all metabolites that could form when its Phase I and Phase II metabolic reactions (120 in total) are applied resulting into 120 biotransformations. With the background of anticipated metabolic reactions based on the cofactors used for the metabolic assays, the list was then reduced to a smaller

size by unchecking unexpected biotransformations. From the displayed list by Agilent Biotransformation Mass Defects, then the ones suggested by MetaPrint2D-React were chosen and their molecular formulas and accurate masses generated by Agilent Biotransformation Mass Defects B214.1 software were then taken directly to the Agilent MassHunter Qualitatative Analysis B.07.00 software for metabolite analysis by displaying extracted ion chromatogram (EIC) from the total ion chromatogram (TIC).

Colour	Normalized occurrence ratio (NOR)
Red	0.66 – 1.00
Orange	0.33 – 0.66
Green	0.15 – 0.33
White	0.00 – 0.15
Grey	Little/no data

NOR is based on how frequently a position/group on the chemical structure with a specific configuration has been reported as a site of metabolism, depending on the metabolic reaction selected.

Parent molecule: Dihydroconiferyl alcohol   Metabolite
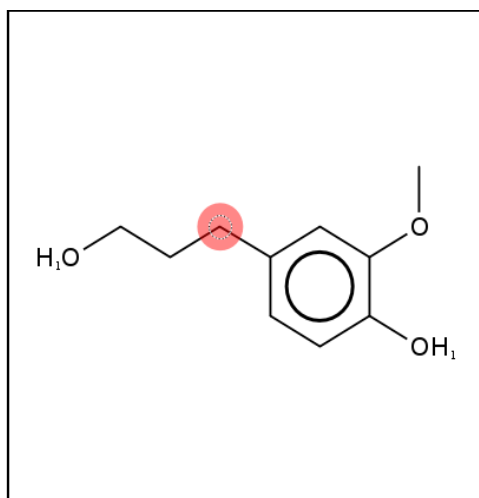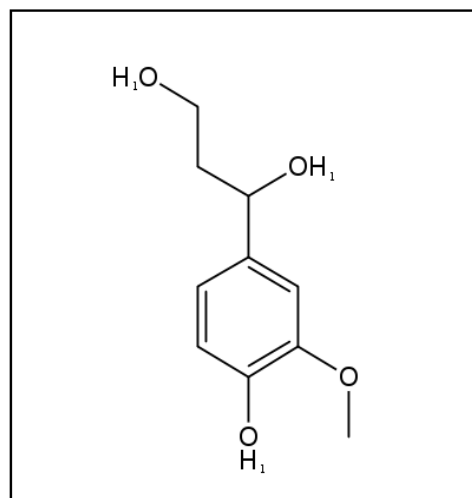
Reaction type: Hydroxylation
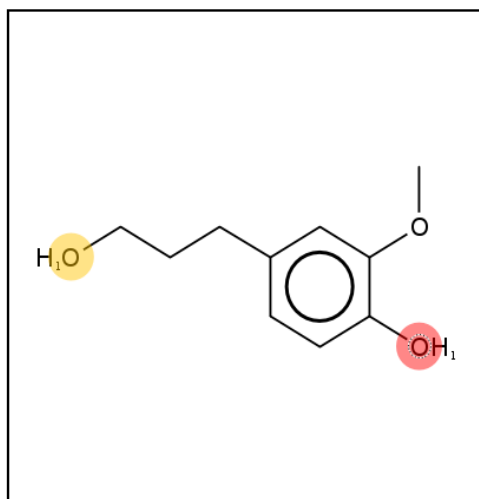
CYP450
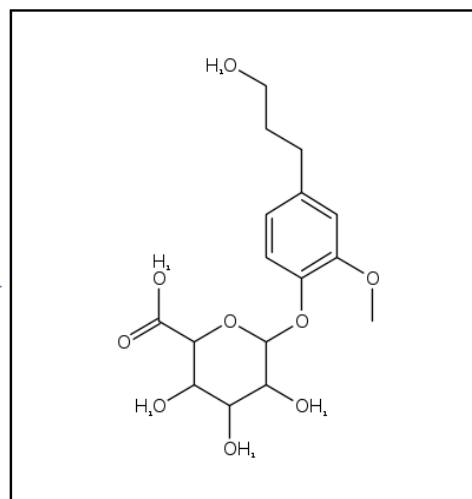
Reaction type: Glucuronidation

CYP450

Fig. 2.2. Phase I and Phase II metabolite predictions of dihydroconiferyl alcohol from açaí.

2.2.5.4 Predictions of MS fragmentation pathways of Phase I and Phase II metabolites

using ACD/MS Fragmenter softwares

To further predict the chemical structures of the projected metabolites, their fragmentation pattern was studied. The chemical structures of the predicted metabolites that were generated by MetaPrint2D-react were drawn in ACD/Chemsketch 2016.2.2 software and uploaded to the ACD/MS Fragmenter 2016.2.2 software where not only fragments were generated for a presented chemical structure but also the fragmentation pathways (Fig. 2.3).
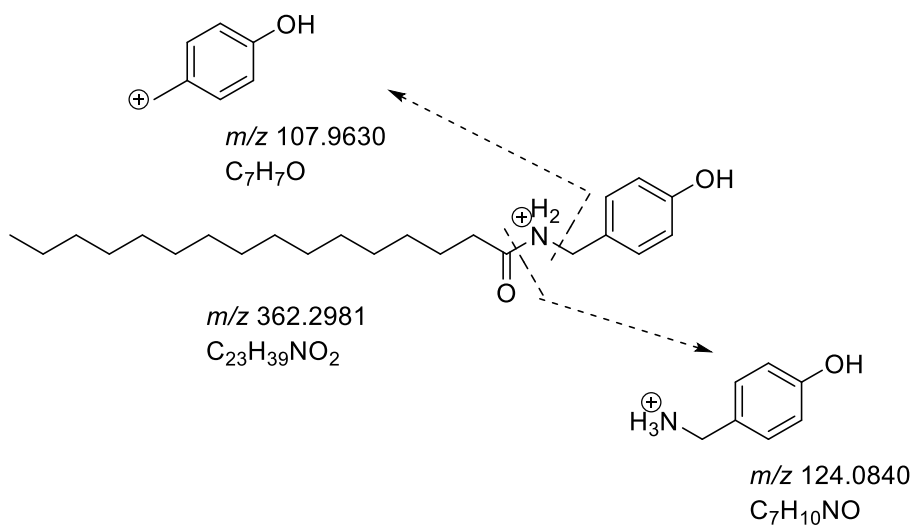
Fig. 2.3 Fragmentation pathway of the predicted oxidized *N*-benzylhexadecanamide from maca.

2.3 CYP3A4 inhibition studies for plant extracts, plant standard compounds and Phase I and Phase II metabolites of plant extracts

2.3.1 Development and optimization of the CYP3A4 inhibition assay

2.3.1.1 Optimization of CYP3A4 reaction incubation time

Incubation mixtures (100 µL) in 1.5 mL Fisherbrand™ Premium microcentrifuge tubes (Thermo Fisher Scientific, Atlanta, GA) contained 0.2 mg/mL HLMs in 100 mM potassium phosphate (K_2HPO_4) buffer (pH 7.4) containing 5 mM $MgCl_2$ and 1 mM EDTA. A stock solution of a CYP 3A4 substrate, 100 µM midazolam, was prepared in a solvent made of methanol: buffer (30:70 v/v). Methanol concentration in the final reaction was 0.9%. In the reactions, a CYP3A4 probe substrate midazolam at its Km concentration (3 µM) [132] was added and mixtures preincubated at 37 °C in a gentle shaking (75 rpm) water bath for 5 min. After the preincubation, the reactions were initiated by addition of 1 mM NADPH and mixtures incubated at 37 °C in a gentle shaking (75 rpm) water bath for 2, 6, 10, 15, 20, 30, 45 or 60 minutes. Each reaction was stopped by the addition of 20 µL water/acetonitrile/formic acid (92:5:3, v/v/v). The samples were vortexed for 1 min in Vortex-Genie 2 (Scientific Industries Inc., Bohemia, NY) and centrifuged at 13,000 x g at 4 °C for 15 min. After centrifugation, supernatant from each reaction time was injected into the LC-MS and quantitative analysis of a metabolite 1'-hydroxymidazolam done. All experiments were conducted in triplicate and triplicate LC-MS analysis was performed. The linearity of metabolite formation was evaluated.

2.3.1.1.1 Preparation of a calibration curve of 1'-hydroxymidazolam

Calibration curve experiments were conducted to obtain the accurate amount of 1'-hydroxymidazolam formed during the optimized reaction time (10 min) course. An experimental set had incubation mixture containing midazolam at 3 µM in 100 µL total volume and the assay was conducted as mentioned above. After 10 min incubation, the reaction was stopped by the addition of 20 µL water/acetonitrile/formic acid (92:5:3, v/v/v). A product 1'-hydroxymidazolam was monitored by LC-MS. In another set, a standard 1'-hydroxymidazolam at 1:2 serial dilution

concentrations (0.75, 1.5, 3.0, 6.0, 12.0, 24.0, 48.0 and 96.0 µM) was also incubated under the same conditions in a mixture that lacks a substrate midazolam. The reaction was stopped with the same quenching solution. From this set, a standard 1'-hydroxymidazolam ion was monitored by LC-MS. A calibration curve and peak area ratios between a product 1'-hydroxymidazolam and its standard were generated. This was used to calculate the accurate amount of a metabolite 1'-hydroxymidazolam produced in the assay and to guide a decision on selecting the concentration of internal standard $[^{13}C_3]$ 1'-hydroxymidazolam to be used for spiking in the CYP3A4 inhibition experiments. With the approximated internal standard (IS) concentration, calibration curve experiments were repeated under the same conditions but the reactions stopped by the addition of 20 µL water/acetonitrile/formic acid (92:5:3, v/v/v) with the stable isotope-labeled surrogate standard $[^{13}C_3]$ 1'-hydroxymidazolam at concentrations 0.024, 0.24, and 2.4 µM to optimize the IS concentration. All experiments were conducted in triplicate and triplicate LC-MS analysis was performed.

2.3.2 Optimized CYP3A4 inhibitory assay to test plant extract constituents and standard compounds

2.3.2.1 Assay conditions

To determine CYP3A4 inhibitory activity of the açaí and maca plant extracts, incubation mixtures (100 µL) in 1.5 mL Fisherbrand™ Premium microcentrifuge tubes contained 0.2 mg/mL HLMs in 100 mM potassium phosphate (K_2HPO_4) buffer (pH 7.4) containing 5 mM $MgCl_2$ and 1 mM EDTA. In the reaction mixtures, midazolam 3 µM was added and varying concentrations 0.05, 0.075, 0.1, and 0.15 µg/µL of plant extract from PAMPA acceptor site. The mixtures were then preincubated at 37 °C in a gentle shaking (75 rpm) water bath for 5 min. After the preincubation, the reactions were initiated by addition of 1 mM NADPH and mixtures incubated at 37 °C in a gentle shaking (75 rpm) water bath for 10 min. The reactions were stopped by the addition of 20 µL water/acetonitrile/formic acid (92:5:3, v/v/v) with the stable isotope-labeled surrogate standard $[^{13}C_3]$ 1'-hydroxymidazolam at concentrations 0.024 µM. The samples were each vortexed for 1 min and centrifuged at 13,000 x g at 4 °C for 15 min. After centrifugation,

supernatant from each sample was injected into the LC-MS and quantitative analysis of a metabolite 1'-hydroxymidazolam was done. The schematic representation of the CYP3A4 inhibition assay is displayed below (Fig. 2.4).

Plant standard compounds, at a fixed concentration of 0.05 µg/mL were also screened for CYP3A4 inhibition. The same reactions used for screening plant extracts for CYP3A4 inhibition above were applied.

A positive control experiment was carried out for a known inhibitor, ketoconazole under the same reaction conditions. In this reaction, the ketoconazole was used in place of the plant extracts. A stock solution, 100 µM ketoconazole was prepared in 10% methanol. In the reaction, ketoconazole was used at a low concentration (1 µM) and high concentration (10 µM) to establish a range of CYP3A4 inhibition to be used for assessment of plant extracts. Methanol concentration in the final reaction was 0.9%.

A negative control experiment was carried out under the same reaction conditions with only midazolam and no plant extracts or ketoconazole. This was done to confirm the integrity of the CYP3A4 enzyme in the assay. In this reaction, the assay buffer was used in place of the plant extracts. All the experiments were conducted in triplicate and triplicate LC-MS analysis of 1'-hydroxymidazolam was performed.
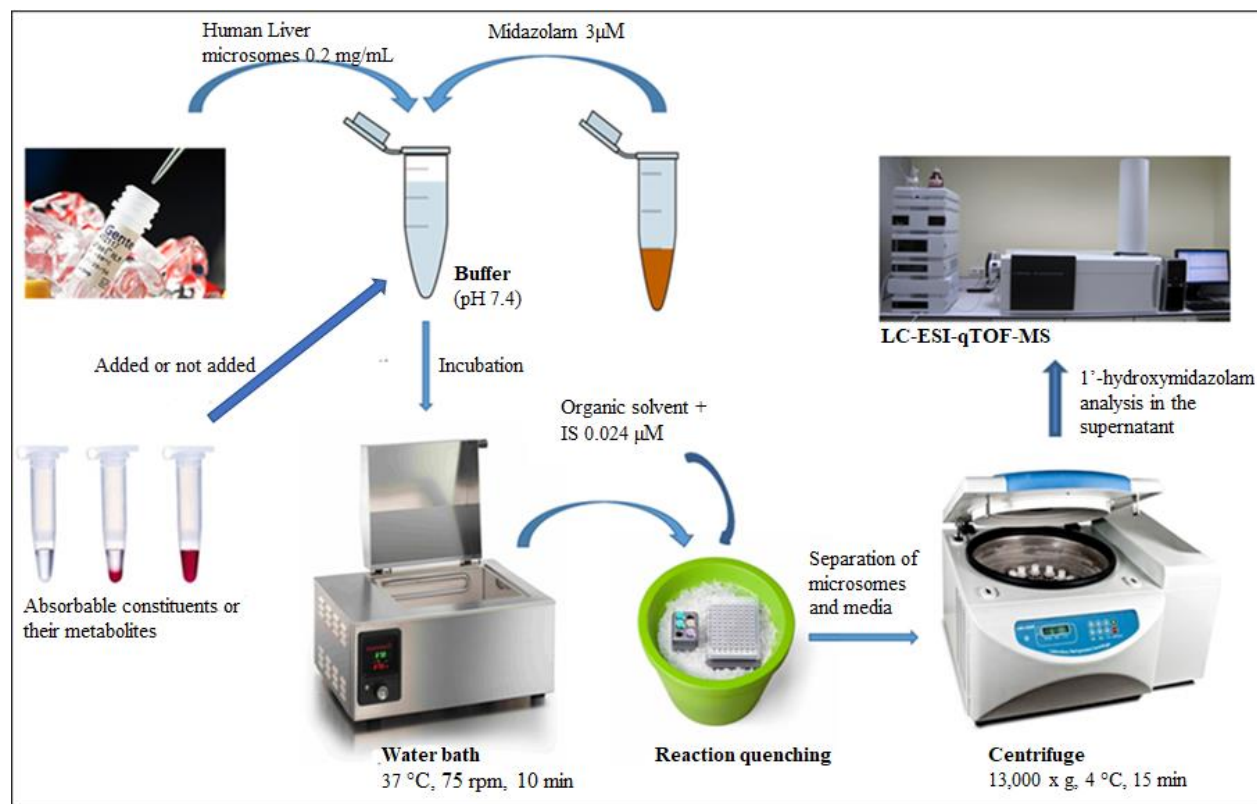
Fig. 2.4. Schematic representation of CYP3A4 Inhibition bioassay

2.3.2.2 IC$_{50}$ determination conditions

To determine the inhibitor's potency, once the potential (>50%) CYP3A4 inhibition was obtained by açaí and maca plant extracts, half maximal inhibitory concentration (IC$_{50}$) was determined. This was conducted through incubation mixtures with 2-fold increasing concentrations of the plant extract that covered the concentrations assayed in the initial CYP3A4 inhibition screening (0.0125, 0.025, 0.05, 0.1, 0.2 and 0.4 µg/µL). To attain these concentrations from PAMPA acceptor compartment using the estimation index suggested by the supplier [140], the initial concentrations used in the donor compartment ranged from 1.25 – 40 µg/µL in 1:2 ratio. The assay was carried out as described in section 2.3.2.1 above and triplicate analysis of 1'-hydroxymidazolam by LC-MS done.

2.3.2.3 LC-MS conditions

The LC-MS and electrospray ion (ESI) source was used for monitoring of a metabolite 1'-hydroxymidazolam. All samples were analyzed on a 4.6 x 100 mm, 3.5 µm ZORBAX Eclipse Plus C18 column. The flow rate was set at 0.4 mL/min and the sample injection volume at 5 µL while the acquisition rate was 1.41 scan/s with the complete mass scanning range from *m/z* 100–1000. The MS conditions were optimized with a positive ion ESI-MS analysis performed at a capillary voltage of 3200 V; drying gas temperature 350 °C; fragmentor voltage 175 V and skimmer 65 V. Nitrogen was supplied as a nebulizing gas at the pressure of 25 psig and as a drying gas at flow rate 10 L/min.

LC conditions consisted of a gradient mobile phase with (A) water containing 0.1% formic acid and (B) acetonitrile. A 4 min gradient from 75 - 100% of solvent B followed by 1 min post-run in 75% B with a flow rate of 0.4 mL/min and a column temperature of 40 °C was optimized. Detection was carried out in positive ESI mode.

2.3.3 CYP3A4 inhibition assay for Phase I and Phase II metabolites of plant constituents

2.3.3.1 Phase I assay conditions

Phase I metabolism experiment was carried out to produce Phase I metabolites prior to CYP3A4 inhibition assay. Phase I metabolism experiments with the highest concentration from PAMPA acceptor site were conducted as elaborated earlier (section 2.2.5.1.1). However, to avoid incorporating an organic solvent that would instantly denature HLMs in the following CYP3A4 inhibition assay, the reactions were not stopped by addition of acetonitrile during Phase I metabolism but were immediately centrifuged at high speed (13000 x g) and low temperature (4 °C) for 15 min to ensure that reactions stop. To further ensure that no further reactions take place, the supernatants were immediately separated from microsomes after centrifuge into the new microcentrifuge tubes for screening in the CYP3A4 inhibition assay. A control experiment was carried out whereby a reaction was stopped by addition of ice-cold acetonitrile before centrifuge as in section 2.2.5.1.1. The estimated concentration of plant extract metabolites delivered in the CYP3A4 inhibition assay was 0.12 µg/µL based on the initial extract concentration in the PAMPA donor compartment. The HLMs (0.2 mg) and midazolam (3 µM) were added and the mixtures were preincubated at 37 °C in a gentle shaking (75 rpm) water bath for 5 min.

After the preincubation, the reactions were initiated by addition of 1 mM NADPH and mixtures incubated at 37 °C in a gentle shaking (75 rpm) water bath for 10 min. The reactions were stopped by the addition of 20 µL water/acetonitrile/formic acid (92:5:3, v/v/v) with the stable isotope-labeled surrogate standard [$^{13}C_3$] 1'-hydroxymidazolam at concentrations 0.024 µM. The samples were each vortexed for 1 min and centrifuged at 13,000 x g at 4 °C for 15 min. After centrifugation, supernatant from each sample was injected into the LC-MS and quantitative analysis of a metabolite 1'-hydroxymidazolam done. The positive and negative control experiments were carried out as in section 2.3.2.1.

To confirm that the reaction had stopped during the quick centrifuging moment, after centrifuge and separation of supernatant from microsomes, the supernatant from a reaction stopped by ice-cold acetonitrile and one that was immediately centrifuged were analyzed by LC-MS. The

peak areas of the ions of Phase I metabolites produced in the reaction stopped by acetonitrile and one stopped by immediate centrifuge were compared.

2.3.3.1.1 LC-MS conditions

The standard LC-MS conditions for CYP3A4 inhibition assay by monitoring a decrease in the metabolite (1'-hydroxymidazolam) formation were used (section 2.3.2.1). LC conditions still consisted of a gradient mobile phase with (A) water containing 0.1% formic acid and (B) acetonitrile. A 4 min gradient from 75 - 100% of solvent B followed by 1 min post-run in 75% B with a flow rate of 0.4 mL/min and a column temperature of 40°C was optimized. Detection was carried out in positive ESI mode.

2.3.3.2 Phase II assay conditions

Phase II metabolism experiment was carried out assay as elaborated in section 2.2.5.1.2 prior to CYP3A4 inhibitory to generate Phase II metabolites. Then the assay conditions were kept as in section 2.3.3.1 above to evaluate the CYP3A4 inhibition by Phase II metabolites.

2.3.3.2.1 LC-MS conditions

The LC-MS conditions for CYP3A4 inhibition evaluation were similar to section 2.3.2.1.

Chapter 3: Results and discussion of the developed and optimized LC-MS-based strategy for screening of passively absorbed plant extract constituents for CYP3A4 inhibition

3.1 Chemical fingerprinting and profiling of plant extract constituents

The identification of açaí and maca plant extract constituents was carried out using Agilent MassHunter Qualitative Analysis B.07.00 software. The analysis of plant extract constituents was done by displaying extracted ion chromatogram (EIC) of each constituent from the total ion chromatogram (TIC). Further, a constituent was reliably identified by molecular feature whereby the accurate mass, *m/z* value, molecular formula and double-bond equivalence (DBE) should correlate to the chemical constituent with less error (<5 ppm) and high score. After individual component analysis, all identified constituents in each extract were documented with their characteristic structural properties generated by LC-MS (Table 3-7).

Six anthocyanins were identified in acidic methanol açaí plant extract. The identity of cyanidin-3-O-glucoside, cyanidin-3-O-rutinoside, cyanidin-3-O-sambubioside and pelargonidin-3-rutinoside were fully confirmed by comparison with the standards (Table 3). Out of twenty-one identified non-anthocyanin polyphenols in acidic methanol açaí plant extract at 10 mg/ml, eight were confirmed by comparison to standard compounds. The eight confirmed polyphenolic constituents were orientin, homo-orientin, vitexin, isovitexin, chrysoeriol, syringic acid, catechin and gallic acid (Table 3.1). Furthermore, twenty-five polyphenols were identified in the methanol açaí extract and eleven of these were confirmed by comparison with the standard compounds. These confirmed eleven were orientin, chrysoeriol, syringic acid, catechin, ferulic acid, quercetin 3-glucoside, quercetin rutinoside, quercetin, vanillic acid, catechol and gallic acid (Table 4).

Six glucosinolates were identified in the acidic methanol maca extract at 10 mg/ml (Table 5). Eleven phenolics were identified in the methanol maca extract at a concentration of 10 mg/ml. The identity of quercetin and L-Phenylalanine were confirmed by comparison with the standard compounds (Table 6). Eleven phenolics were identified in the methanol maca extract. The identity of L-tyrosine and L-tryptophan were confirmed by comparison with the standard compounds

(Table 6.1). Eight macamides were identified in the DCM maca extract at 10 mg/ml (Table 6.2). Seventeen macamides were identified in the DCM maca extract at 10 mg/ml. The identity of *N*-benzylhexadecanamide was confirmed by comparison with its standard compound (Table 7). Chemical structures of major constituents in açaí and maca were drawn using ChemDraw software (PerkinElmer, Akron, OH) and displayed in figures 3.1a-3.1b.

3.1.1 Chemical fingerprinting of açaí and maca plant extracts

3.1.1.1 Acidic methanol açaí plant extract

Table 3. ESI-LC-MS analysis of açaí anthocyanins

Analyte	Formula [M]	Ion Formula [M+H]+	[M+H]+ m/z	RT (min)	DBE	Diff (ppm)	Score
Cyanidin-3-O-glucoside	$C_{21}H_{20}O_{11}$	$C_{21}H_{21}O_{11}$	449.1091	7.01	12	-2.92	91.64
Cyanidin-3-O-sambubioside	$C_{26}H_{28}O_{15}$	$C_{26}H_{29}O_{15}$	581.1538	7.996	13	-4.93	79.84
Cyanidin-3-O-rutinoside	$C_{27}H_{30}O_{15}$	$C_{27}H_{31}O_{15}$	595.1693	7.394	13	-0.09	70.96
Peonidin-3-glucoside	$C_{22}H_{22}O_{11}$	$C_{22}H_{23}O_{11}$	463.1268	11.035	12	-1.46	90.36
Pelargonidin-3-rutinoside	$C_{27}H_{30}O_{14}$	$C_{27}H_{31}O_{14}$	579.1718	7.763	13	-0.15	68.69
Pelargonidin-3-glucoside	$C_{21}H_{20}O_{10}$	$C_{21}H_{21}O_{10}$	433.1137	10.934	12	-1.85	97.59

Table 3.1. ESI-LC-MS analysis of açaí non-anthocyanin polyphenols

Analyte	Formula [M]	Ion Formula [M+H]+	[M+H]+ m/z	RT (min)	DBE	Diff (ppm)	Score
Orientin	$C_{21}H_{20}O_{11}$	$C_{21}H_{21}O_{11}$	449.1099	9.689	12	-3.03	86.33
Homo-orientin	$C_{21}H_{20}O_{11}$	$C_{21}H_{21}O_{11}$	449.1054	9.875	12	5.96	82.85
Isovitexin	$C_{21}H_{20}O_{10}$	$C_{21}H_{21}O_{10}$	433.1135	10.631	12	-3.45	65.62

Analyte	Formula [M]	Ion Formula [M+H]$^+$	[M+H]$^+$ m/z	RT (min)	DBE	Diff (ppm)	Score
Vitexin	$C_{21}H_{20}O_{10}$	$C_{21}H_{21}O_{10}$	433.1125	10.737	12	0.95	81.25
Chrysoeriol	$C_{16}H_{12}O_6$	$C_{16}H_{13}O_6$	301.0704	18.22	11	1.8	91.51
Protocatechuic acid, methyl ester	$C_8H_8O_4$	$C_8H_9O_4$	169.0488	9.08	5	4.12	83.35
Syringic acid	$C_9H_{10}O_5$	$C_9H_{11}O_5$	199.059	8.615	5	2.31	76.7
Caffeic acid	$C_9H_8O_4$	$C_9H_9O_4$	181.9489	5.744	6	4.1	94.82
Syringaresinol	$C_{22}H_{26}O_8$	$C_{22}H_{27}O_8$	436.1961	8.301	10	5.16	72.84
Lariciresinol	$C_{20}H_{24}O_6$	$C_{20}H_{25}O_6$	378.1931 [M+NH$_4$]$^+$	11.292	9	-0.51	67.32
Isolariciresinol	$C_{20}H_{24}O_6$	$C_{20}H_{25}O_6$	383.149 [M+NH$_4$]$^+$	11.298	9	-5.39	83.9
Astilbin	$C_{21}H_{22}O_{11}$	$C_{21}H_{23}O_{11}$	473.107 [M+Na]$^+$	10.533	11	-1.93	96.38
Loliolide	$C_{11}H_{16}O_3$	$C_{11}H_{17}O_3$	219.098 [M+Na]$^+$	10.847	4	6.03	79.95
Menthiafolic acid	$C_{10}H_{16}O_3$	$C_{10}H_{17}O_3$	207.0993 [M+Na]$^+$	11.2	3	-0.1	84.43
2,6-dimethyl-1,4-benzoquinone	$C_8H_8O_2$	$C_8H_9O_2$	137.0531	8.542	5	-4.79	69.93
Dihydrodehydroconiferyl alcohol	$C_{20}H_{24}O_6$	$C_{20}H_{25}O_6$	361.165	13.423	9	0	93.3
(1R,3S)-(+)-camphoric acid	$C_{13}H_{20}O_2$	$C_{13}H_{21}O_2$	209.1534	15.842	4	1.6	93.74
Catechin	$C_{15}H_{14}O_6$	$C_{15}H_{15}O_6$	291.087	6.414	9	-4.34	64.31
Epicatechin	$C_{15}H_{14}O_6$	$C_{15}H_{15}O_6$	291.0853	6.27	9	5.71	62.75
Gallic acid	$C_7H_6O_5$	$C_7H_7O_5$	171.0268	5.353	5	4.3	77.05
p-coumaric acid	$C_9H_8O_3$	$C_9H_9O_3$	182.0812 [M+NH$_4$]$^+$	4.43	6	-0.33	85.57

Analyte	Formula [M]	Ion Formula [M+H]+	[M+H]+ m/z	RT (min)	DBE	Diff (ppm)	Score
3-oxo-alpha-ionol	$C_{13}H_{20}O_2$	$C_{13}H_{21}O_2$	209.1537	24.106	4	-0.19	86.62

3.1.1.2 Methanol açaí plant extract

Table 4. ESI-LC-MS analysis of açaí polyphenols

Analyte	Formula [M]	Ion Formula [M-H]-	[M-H]- m/z	RT (min)	DBE	Diff (ppm)	Score
Quercetin rhamnoside	$C_{21}H_{20}O_{11}$	$C_{21}H_{19}O_{11}$	447.0937	10.131	12	-0.73	99.07
Kaempferol 3-O-rutinoside	$C_{27}H_{30}O_{15}$	$C_{27}H_{29}O_{15}$	593.1508	9.798	12	0.53	98.72
Kaempferol 3-O-rhamnoside	$C_{21}H_{20}O_{10}$	$C_{21}H_{19}O_{10}$	431.0964	8.327	12	5.59	78.4
Quercetin rutinoside	$C_{27}H_{30}O_{16}$	$C_{27}H_{29}O_{16}$	609.146	10.79	13	0.21	99.02
Orientin	$C_{21}H_{20}O_{11}$	$C_{21}H_{19}O_{11}$	447.0926	10.341	12	1.63	98.05
Scoparin	$C_{22}H_{22}O_{11}$	$C_{22}H_{21}O_{11}$	461.1089	11.936	12	0.21	98.77
Chrysoeriol	$C_{16}H_{12}O_6$	$C_{16}H_{11}O_6$	299.0552	18.549	11	3.19	96.57
Quercetin	$C_{15}H_{10}O_7$	$C_{15}H_9O_7$	301.0355	16.112	11	-0.41	99.42
Quercetin 3-glucoside	$C_{21}H_{20}O_{12}$	$C_{21}H_{19}O_{12}$	463.0884	4.802	12	-0.46	98.4
Taxifolin	$C_{15}H_{12}O_7$	$C_{15}H_{11}O_7$	303.0499	10.757	10	3.43	95.27
p-Hydroxybenzoic acid	$C_7H_6O_3$	C_7H5O_3	137.0238	8.095	5	4.6	82.23
Vanillic acid	$C_8H_8O_4$	C_8H7O_4	167.0345	8.079	5	2.95	86.28
Gallic acid	$C_7H_6O_5$	C_7H5O_5	169.0128	3.689	5	4.4	62.65

Analyte	Formula [M]	Ion Formula [M-H]⁻	[M-H]⁻ m/z	RT (min)	DBE	Diff (ppm)	Score
3',4'-dihydroxy-3'-methoxypropiophenone	$C_{10}H_{12}O_4$	$C_{10}H_{11}O_4$	195.065	10.82	5	4.1	96.5
Beta-hydroxypropiovanillone	$C_{10}H_{12}O_4$	$C_{10}H_{11}O_4$	195.0651	10.384	5	5.61	91.95
Dihydroconiferyl alcohol	$C_{10}H_{12}O_3$	$C_{10}H_{11}O_3$	181.0652	8.325	5	6.89	85.11
Erythro and threo-1-(4-hydroxy-3-methoxyphenyl)-2-[4-(3-hydroxypropyl)-2-methoxyphenoxy]-1,3-propanediol	$C_{20}H_{26}O_7$	$C_{20}H_{25}O_7$	377.1593	10.46	8	4.15	90.01
Velutin	$C_{17}H_{14}O_6$	$C_{17}H_{13}O_6$	313.0712	25.336	11	2.36	82.45
Astilbin	$C_{21}H_{22}O_{11}$	$C_{21}H_{21}O_{11}$	449.109	10.647	11	-0.16	98.76
2,6-Dimethoxy-1,4-benzoquinone	$C_8H_8O_4$	$C_8H_7O_4$	167.0342	8.561	5	3.58	94.48
Resveratrol	$C_{14}H_{12}O_3$	$C_{14}H_{11}O_3$	227.0703	12.906	9	2.99	88.62
Ferulic acid	$C_{10}H_{10}O_4$	$C_{10}H_{11}O_4$	193.0498	9.69	6	4.19	83.05
Chlorogenic acid	$C_{16}H_{18}O_9$	$C_{16}H_{19}O_9$	353.0867	11.428	8	4.95	51.5
Catechin	$C_{15}H_{14}O_6$	$C_{15}H_{15}O_6$	289.0734	5.476	9	-5.16	91.3
Catechol	$C_6H_6O_2$	$C_6H_7O_2$	109.0299	7.103	4	-3.166	98.81

3.1.1.3 Acidic methanol maca plant extract

Table 5. ESI-LC-MS analysis of maca glucosinolates

Analyte	Formula [M]	Ion Formula [M-H]$^-$	[M-H]$^-$ m/z	RT (min)	DBE	Diff (ppm)	Score
3-hydroxybenzyl glucosinolate	$C_{14}H_{19}NO_{10}S_2$	$C_{14}H_{18}NO_{10}S_2$	424.0374	1.784	6	1.03	98.9
4-hydroxybenzyl glucosinolate	$C_{14}H_{19}NO_{10}S_2$	$C_{14}H_{18}NO_{10}S_2$	424.0373	1.7843	6	1.1	97.7
Glucotropaeolin	$C_{14}H_{19}NO_9S_2$	$C_{14}H_{18}NO_9S_2$	408.0447	4.128	6	-4.06	90.9
4-methoxybenzyl glucosinolate	$C_{15}H_{21}NO_{10}S_2$	$C_{15}H_{20}NO_{10}S_2$	438.053	1.708	6	1.52	96.17
3-methoxybenzyl glucosinolate	$C_{15}H_{21}NO_{10}S_2$	$C_{15}H_{20}NO_{10}S_2$	438.055	3.738	6	0.99	85.88
Hexyl glucosinolate	$C_{13}H_{27}NO_9S_2$	$C_{13}H_{26}NO_9S_2$	404.1094	7.956	1	-6.74	64

3.1.1.4 Methanol maca plant extract

Table 6. ESI-LC-MS analysis of maca phenolics

Analyte	Formula [M]	Ion Formula [M+H]$^+$	[M+H]$^+$ m/z	RT (min)	DBE	Diff (ppm)	Score
4-hydroxycinnamic acid	$C_9H_8O_3$	$C_9H_9O_3$	182.0804 [M+NH$_4$]$^+$	5.37	6	-2.29	73.05
(1R,3S)-1-methyltetrahydro-β-Carboline-3-carboxylic acid	$C_{13}H_{14}N_2O_2$	$C_{13}H_{15}N_2O_2$	253.0942 [M+Na]$^+$	10.751	8	-1.03	83.6

Analyte	Formula [M]	Ion Formula [M+H]$^+$	[M+H]$^+$ m/z	RT (min)	DBE	Diff (ppm)	Score
Benzyl alcohol	C_7H_8O	C_7H_9O	131.047 [M+Na]$^+$	5.029	4	-12.27	68.49
Benzaldehyde	C_7H_6O	C_7H_7O	124.0755	3.166	5	0.36	80.29
Benzylamine	C_7H_9N	$C_7H_{10}N$	108.0806	4.379	4	1.89	80.52
Malic acid benzoate	$C_{11}H_{10}O_6$	$C_{11}H_{11}O_6$	239.0538	7.383	7	0.42	55.81
5-hydroxymethylfurfural	$C_6H_6O_3$	$C_6H_7O_3$	127.0386	6.524	4	2.17	97.91
L-Phenylalanine	$C_9H_{11}NO_2$	$C_9H_{12}NO_2$	166.086	5.187	5	2.54	79.88
Quercetin	$C_{15}H_{10}O_7$	$C_{15}H_{11}O_7$	303.0498	16.109	11	0.11	98.13
5-oxo-6E,8E-octadecadienoic acid	$C_{18}H_{30}O_3$	$C_{18}H_{31}O_3$	295.2275	18.818	4	4	90.35
Tricin 4′-O-(erythro-β-guaiacyl-glyceryl) ether	$C_{27}H_{26}O_{11}$	$C_{27}H_{27}O_{11}$	527.1527	2.679	15	-2.64	69.49
Guanosine	$C_{10}H_{13}N_5O_5$	$C_{10}H_{14}N_5O_5$	301.1265 [M+NH$_4$]$^+$	7.063	7	-2.79	59.02
Lepidiline A	$C_{19}H_{20}N_2$	$C_{19}H_{21}N_2$	277.1695	9.985	11	1.41	94.17
Lepidiline B	$C_{20}H_{22}N_2$	$C_{20}H_{23}N_2$	291.1858	10.353	11	3.84	84.07

Table 6.1. ESI-LC-MS analysis of maca amino acids

Analyte	Formula [M]	Ion Formula [M+H]⁺	[M+H]⁺ m/z	RT (min)	DBE	Diff (ppm)	Score
Proline	$C_5H_9NO_2$	$C_5H_{10}NO_2$	116.0703	2.604	2	3.18	81.68
Uridine	$C_9H_{12}N_2O_6$	$C_9H_{13}N_2O_6$	267.0574 [M+Na]⁺	3.34	5	-2.52	46.24
Malic acid	$C_4H_6O_5$	$C_4H_{10}NO_5$	135.0274	3.368	2	-2.53	75.26
Leucine	$C_6H_{13}NO_2$	$C_6H_{14}NO_2$	132.101	4.448	1	8.14	90.22
Isoeucine	$C_6H_{13}NO_2$	$C_6H_{13}NO_2$	132.1003	4.254	1	12.59	73.31
Valine	$C_5H_{11}NO_2$	$C_5H_{12}NO_2$	156.0426 [M+K]⁺	2.51	1	-3.2	91.32
Tyrosine	$C_9H_{11}NO_3$	$C_9H_{12}NO_3$	182.0809	3.734	5	1.5	85.92
Methionine	$C_5H_{11}NO_2S$	$C_5H_{12}NO_2S$	199.1056[M+NH₄]⁺	4.601	5	9.13	74.39
Hydroxyproline	$C_5H_9NO_3$	$C_5H_{10}NO_3$	154.0488 [M+Na]⁺	2.78	2	-8.55	70.02
Tryptophan	$C_{11}H_{12}N_2O_2$	$C_{11}H_{12}N_2O_2$	205.0958	6.245	7	5.72	64.05
Arginine	$C_6H_{14}N_4O_2$	$C_6H_{15}N_4O_2$	175.5042	9.523	2	1.6	98.68

Table 6.2. ESI-LC-MS analysis of maca macamides

Analyte	Formula [M]	Ion Formula [M+H]$^+$	[M+H]$^+$ m/z	RT (min)	DBE	Diff (ppm)	Score
N-benzyl-13-oxo -9E,11E-octadecadienamide	$C_{25}H_{37}NO_2$	$C_{25}H_{38}NO_2$	384.2888	20.288	8	1.79	97.7
N-benzyl-5-oxo-*6E*,*8E*-octadecadienamide	$C_{25}H_{37}NO_2$	$C_{25}H_{38}NO_2$	384.2887	20.792	8	1.85	84.71
N-benzyl-9-oxo-12Z-octadecenamide	$C_{25}H_{39}NO_2$	$C_{25}H_{40}NO_2$	386.3024	19.575	7	0.68	96.4
N-benzyl-9-oxo-12Z,15Z-octadecadienamide	$C_{25}H_{37}NO_2$	$C_{25}H_{38}NO_2$	384.2887	20.792	8	1.81	93.63
N-benzyl-13-oxooctadeca-9E,11*E*-dienamide	$C_{25}H_{37}NO$	$C_{25}H_{38}NO$	368.394	19.789	8	2.27	94.82
N-benzyl-(9Z, 12Z, 15Z)-octadecatrienamide	$C_{25}H_{37}NO$	$C_{25}H_{38}NO$	368.2944	20.193	8	2.01	92.34
5-oxo-*6E*,*8E*-octadecadienoic acid	$C_{18}H_{30}O_3$	$C_{18}H_{31}O_3$	295.2257	19.65	4	-1.72	98.5
Macaridine	$C_{13}H_{13}NO_2$	$C_{13}H_{14}NO_2$	216.1006	11.97	8	5.05	92.56

3.1.1.5 DCM maca plant extract

Table 7. ESI-LC-MS analysis of maca macamides

Analyte	Formula [M]	Ion Formula [M+H]$^+$	[M+H]$^+$ m/z	RT (min)	DBE	Diff (ppm)	Score
N-benzylhexadecanamide	C$_{23}$H$_{39}$NO	C$_{23}$H$_{40}$NO	368.2922 [M+Na]$^+$	20.896	5	-0.62	81.17
N-benzyl-(9Z)-octadecenamide	C$_{25}$H$_{41}$NO	C$_{25}$H$_{42}$NO	394.309 [M+Na]$^+$	18.33	6	-0.96	72.76
N-phenethylhexadecanamide	C$_{24}$H$_{41}$NO	C$_{24}$H$_{42}$NO	382.3074 [M+Na]$^+$	19.232	5	-0.01	68.18
N-benzyloctadecanamide	C$_{25}$H$_{43}$NO	C$_{25}$H$_{44}$NO	391.3671 [M+NH$_4$]$^+$	11.312	5	3.03	93.11
N-(3,4-dimethoxybenzyl)-hexadecanamide	C$_{25}$H$_{43}$NO	C$_{25}$H$_{44}$NO	396.3249 [M+Na]$^+$	14.347	5	1.3	70.86
(9Z,12Z,15Z)-N-(3-Methoxybenzyl)-9,12,15-octadecatrienamide	C$_{26}$H$_{39}$NO$_2$	C$_{26}$H$_{40}$NO$_2$	398.3067	22.92	8	-3.69	75.22
N-benzyl-(9Z, 12Z)-octadecadienamide	C$_{25}$H$_{39}$NO	C$_{25}$H40NO	392.2934 [M+Na]$^+$	20.287	7	0.59	90.08
N-Benzyl-13-oxoocta deca-9E,11E-dienamide	C$_{25}$H$_{37}$NO	C$_{25}$H$_{38}$NO	368.2966	19.784	8	-5.05	72.77
N-benzyl-(9Z, 12Z, 15Z)-octadecatrienamide	C$_{25}$H$_{37}$NO	C$_{25}$H$_{38}$NO	390.2783 [M+Na]$^+$	23.138	8	-5.07	81.81
N-benzylpentadecanamide	C$_{22}$H$_{37}$NO	C$_{22}$H$_{38}$NO	332.2964	21.018	5	-5.26	83.02
N-benzyloctanamide	C$_{15}$H$_{23}$NO	C$_{15}$H$_{24}$NO	256.1683[M+Na]$^+$	16.752	5	-4.83	92.48
4´-Methoxy-N-benzyloctanamide	C$_{16}$H$_{25}$NO$_2$	C$_{16}$H$_{26}$NO$_2$	264.1944	8.596	5	6.13	72.94

Analyte	Formula [M]	Ion Formula [M+H]$^+$	[M+H]$^+$ m/z	RT (min)	DBE	Diff (ppm)	Score
4´-Methoxy-*N*-benzyloctadecanamide	$C_{26}H_{45}NO_2$	$C_{26}H_{46}NO_2$	442.312 [M+K]$^+$	22.305	5	-0.44	68.04
N-(3-methoxybenzyl)-hexadecanamide	$C_{24}H_{41}NO2$	$C_{24}H_{42}NO_2$	398.3073 [M+Na]$^+$	22.835	5	-3.85	85.28
(9Z,12Z)-*N*-(3-Methoxybenzyl)-9,12-octadecadienamide	$C_{26}H_{41}NO_2$	$C_{26}H_{42}NO_2$	400.3227	19.584	7	-4.4	88.29
N-benzyl-15Z-tetracosenamide	$C_{31}H_{53}NO$	$C_{31}H_{54}NO$	494.3737 [M+K]$^+$	14.479	6	2.54	65.56
4'-methoxy-*N*-benzyl-(9Z)-octadecanamide	$C_{26}H_{43}NO_2$	$C_{26}H_{44}NO_2$	402.3366	23.585	6	0.73	81.48
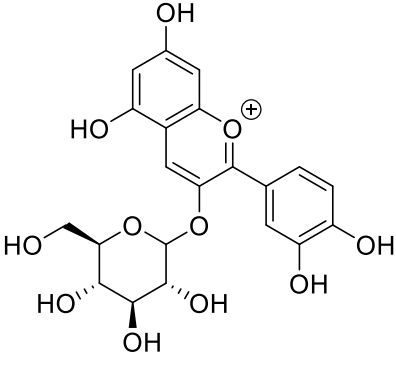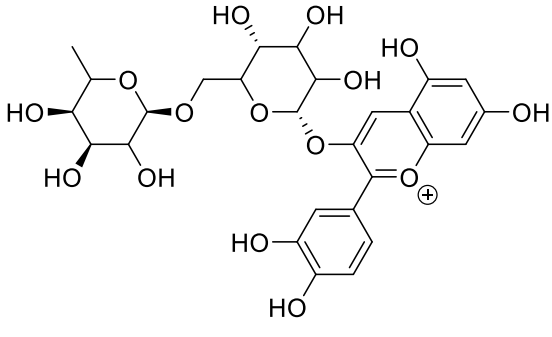
Açaí berry marker constituents	Name and class of compound
	Cyanidin-3-O-glucoside (anthocyanin)
	Cyanidin-3-O-rutinoside (anthocyanin)

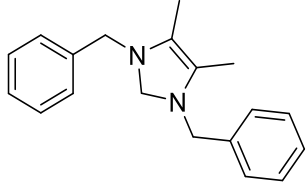**Fig. 3.1a.** Chemical structures of major constituents in açaí berry extract.
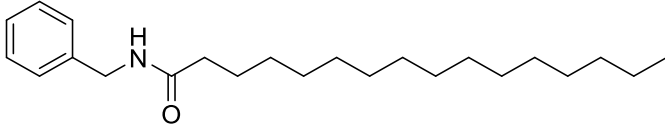
Maca root marker constituents	Name and class of compound
	Lepidiline A (alkaloid)
	N-benzylhexadecanamide (macamide)

Fig. 3.1b. Chemical structures of major constituents in maca root extract.

3.2 Identification of passively diffused plant extract constituents

The Agilent MassHunter Qualitative Analysis B.07.00 software was used for the identification of passively diffused açaí and maca plant constituents. This was done by extracting each constituent in the PAMPA acceptor solution after PAMPA assay and those that displayed the corresponding ions and their presence confirmed, were identified as passively absorbed. The confirmation was processed by molecular feature whereby the accurate mass, *m/z* value, molecular formula and DBE should correlate to the absorbed chemical constituent with less error (< 5 ppm) and high score. The EICs of the constituents in the donor site of PAMPA at the beginning of the PAMPA experiment (t0) were also displayed and their peak areas compared to the ones obtained after the PAMPA (t5 hrs). After the individual component analysis, whereby a change in original peak in terms of peak area was assessed after 5 hour period of incubation (Fig 3.2), all identified absorbed constituent ions in the PAMPA acceptor site were extracted and compared with the constituent ions left in the donor site (Fig. 3.3a – Fig. 3.3e).

Plant standard constituents were also analyzed in the same manner as the plant extracts. They were then used to compare the absorptivity of an individual constituent in a complex mixture (plant extract) and as a single entity (Table 3.1).

MeOH maca extract

5-hydroxymethylfurfural (PAMPA donor site) at t0

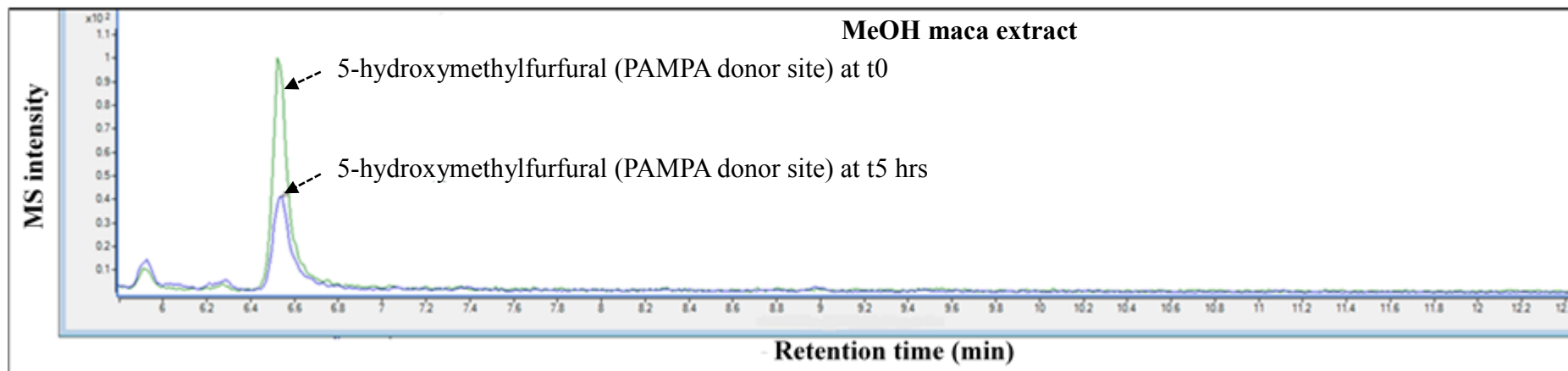5-hydroxymethylfurfural (PAMPA donor site) at t5 hrs

Fig. 3.2. Comparison of the overlaid EICs of maca plant constituent (5-hydroxymethylfurfural) before (t0) and after PAMPA (t5 hrs).
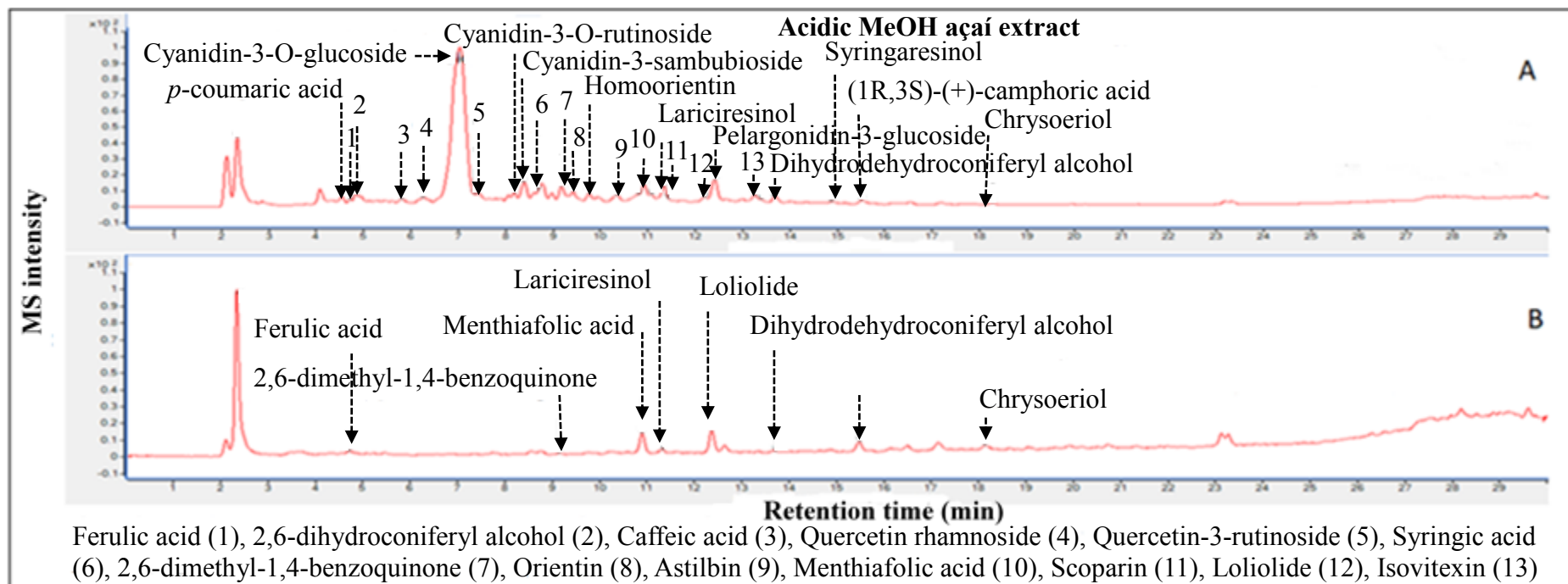
Fig. 3.3a. Comparison of EIC of acidic methanol açaí extract at 15 µg/µL after PAMPA test. (A) Compounds in donor site. (B)

Fig. 3.3b. Comparison of EIC of methanol açaí extract at 15 µg/µL after PAMPA test. (A) Compounds in donor site. (B) Compounds in acceptor site.

Fig. 3.3c. Comparison of EIC of acidic methanol maca extract at 15 µg/µL after PAMPA test. (A) Compounds in donor site. (B) Compounds in acceptor site.
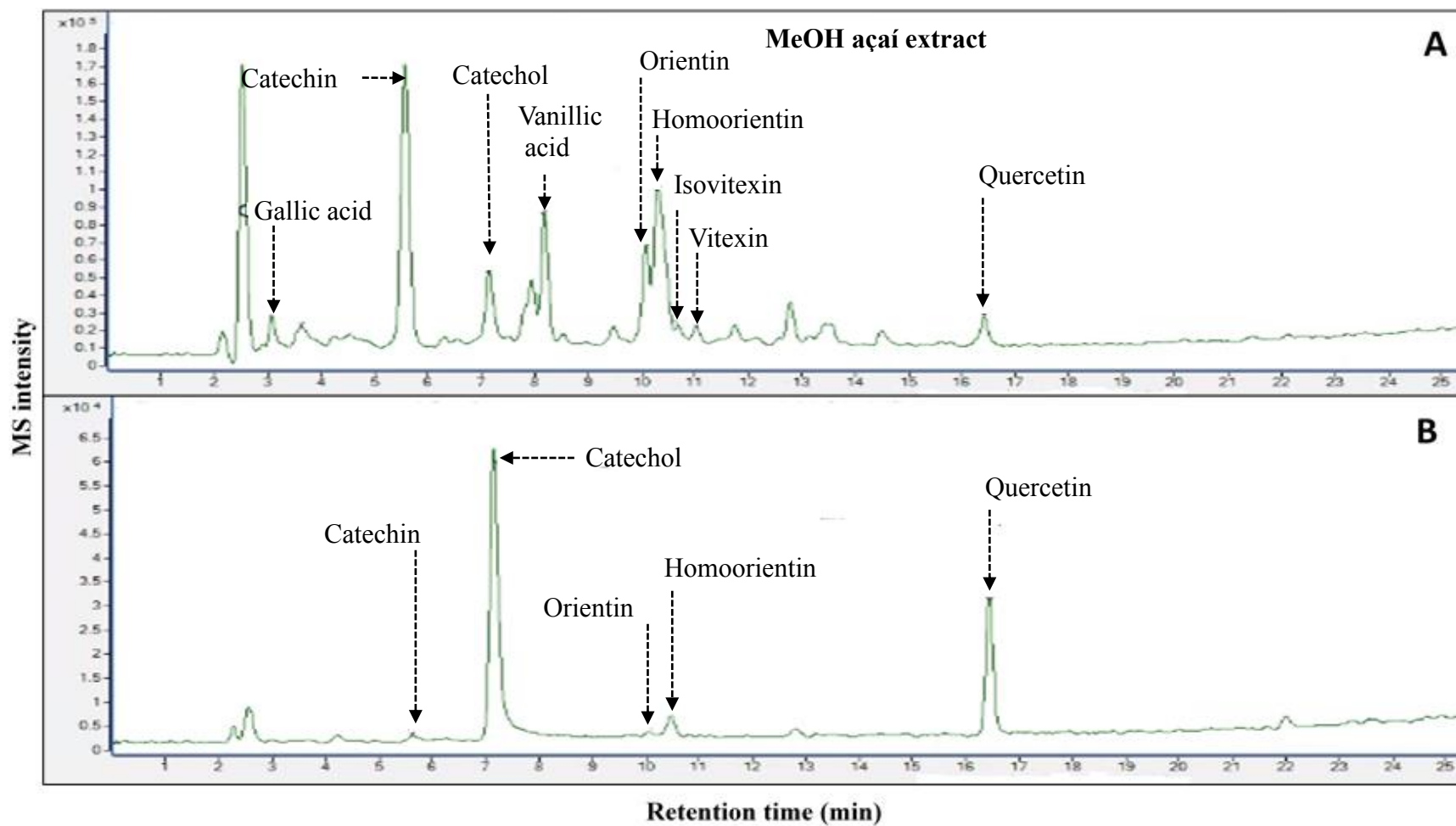
Fig. 3.3d. Comparison of EIC of methanol maca extract at 15 µg/µL after PAMPA test. (A) Compounds in donor site. (B) Compounds in acceptor site.

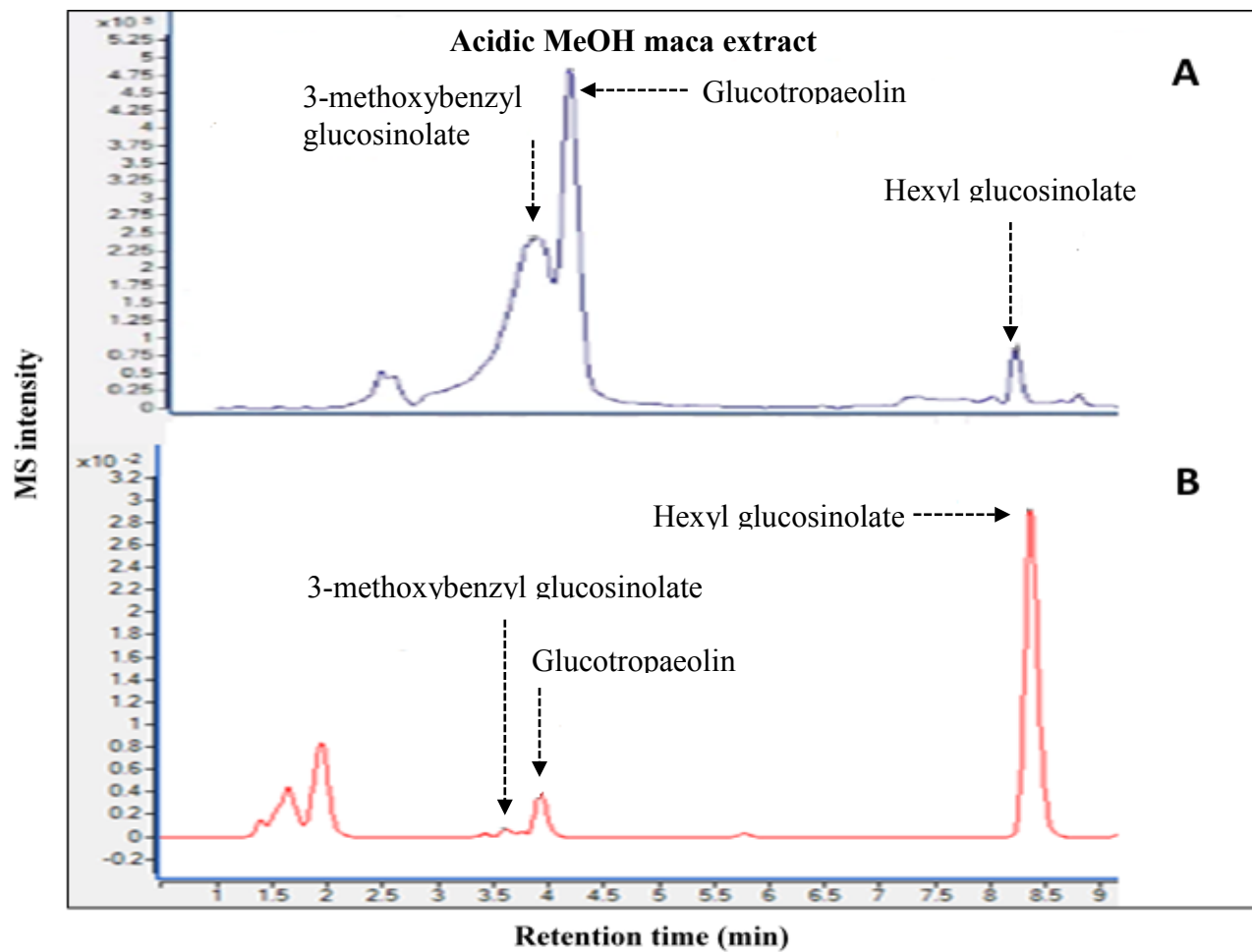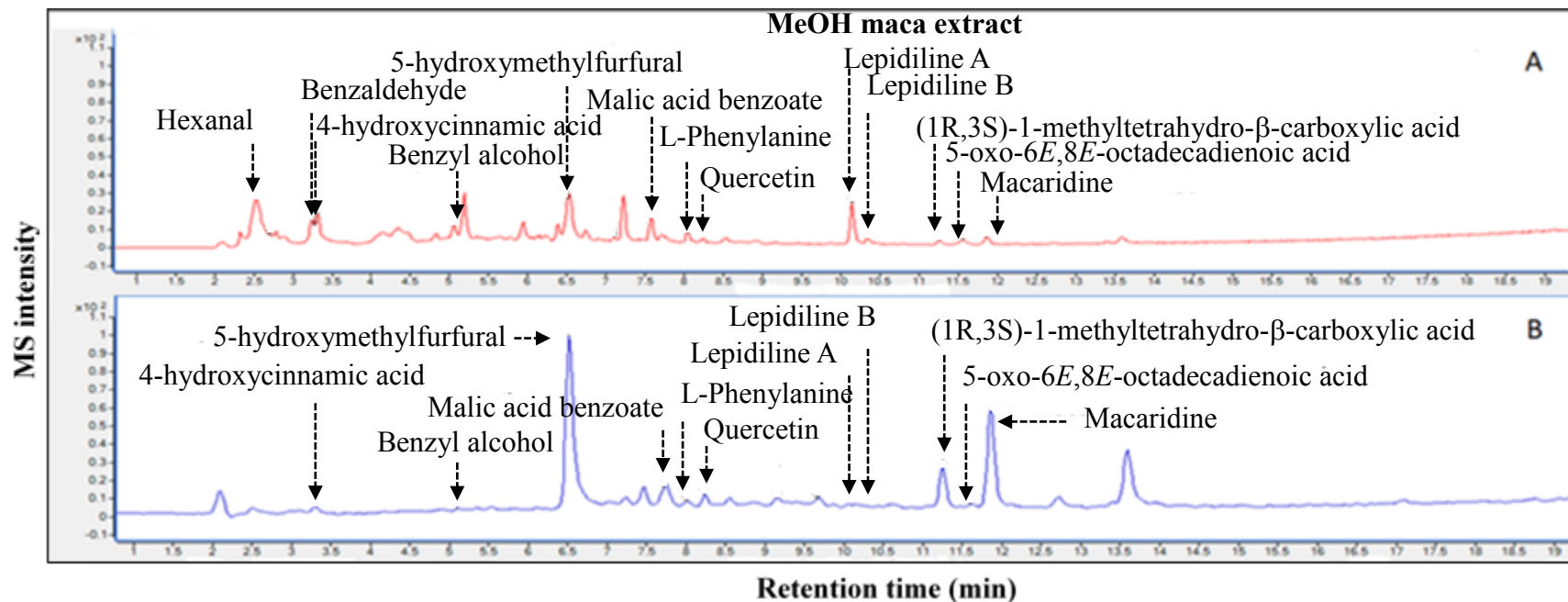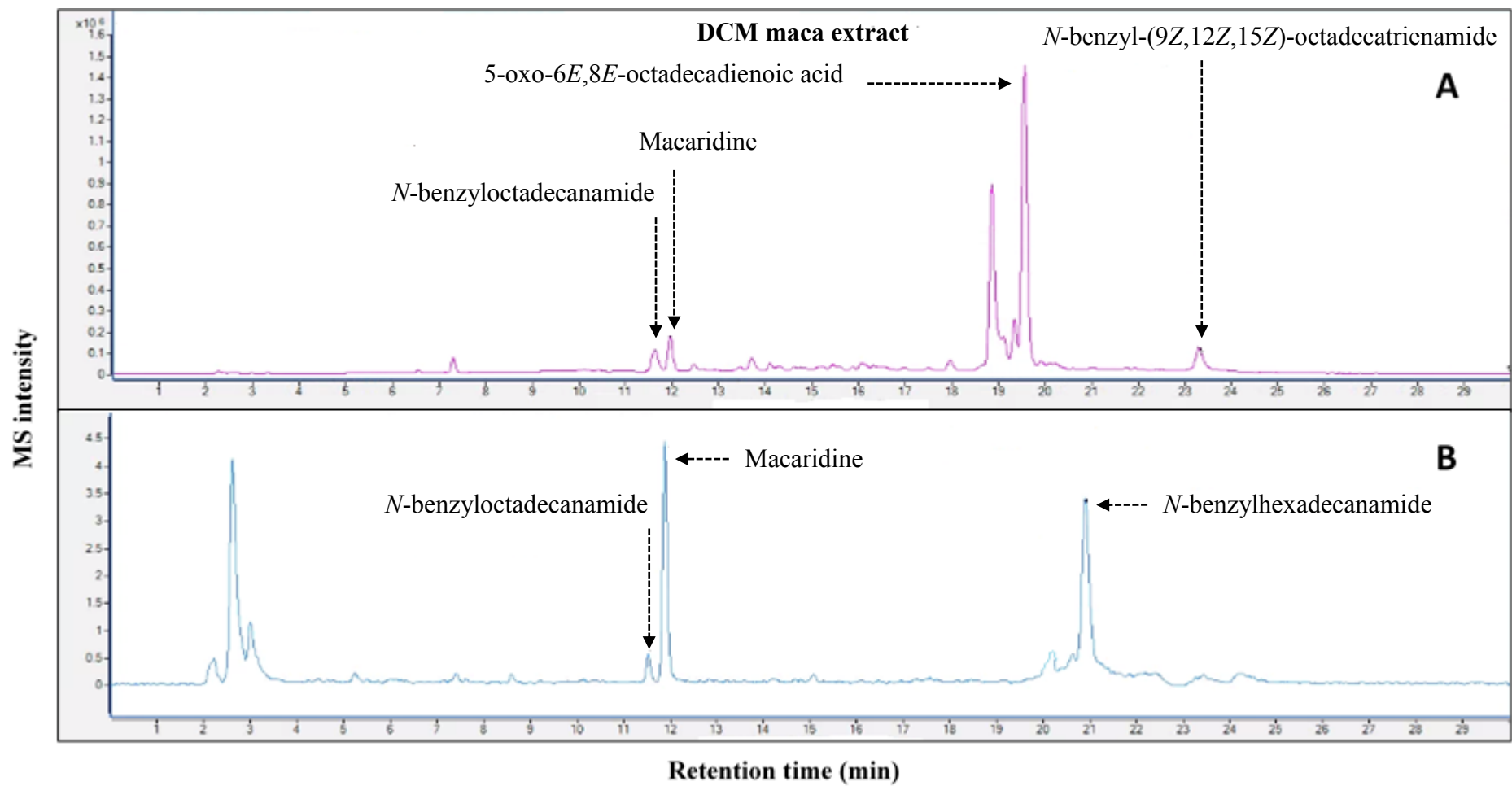**Fig. 3.3e**. Comparison of EIC of DCM maca extract at 15 µg/µL after PAMPA test. (A) Compounds in donor site. (B) Compounds in acceptor site.

The absorption extent (Table 3.1) was then quantified by using the peak areas of each constituent at the beginning ($C_D(0)$) and at the end of PAMPA in the donor site ($C_D(t)$) compared to the one in the PAMPA acceptor site at the end of PAMPA ($C_A(t)$). These were used in the equation (1) below for standard calculation of effective permeability (P_e) values adapted from Petit *et al* [114]:

Equation (1):

$$P_e = \frac{-2.303 V_D}{A(t - \tau_{ss})} \times (\frac{1}{1 + r_v}) \times \log[1 - (\frac{1 + r_v^{-1}}{(1 - R)}) \times \frac{C_A(t)}{C_D(0)}]$$

Where P_e represents the effective passive permeability coefficient (cm/s)

$$r_v = \frac{V_D}{V_A}$$

V_A and V_D represent the acceptor well volume (200 µL) and donor well volume (300 µL), respectively, A is the membrane area (0.3 cm^2), t is the time of incubation in seconds (18 000 s), and $C_A(t)$ and $C_D(t)$ is the concentration at time t in the acceptor and donor compartment, respectively. R is the membrane retention defined as:

$$(1 - R) V_D C_D(0) = V_D C_D(t) + V_A C_A(t)$$

Therefore, the P_e calculation considers the non-specific binding of constituents in the membrane by including membrane retention and the influence of gravity is eliminated in the assay by placing the donor compartment below the acceptor plate.

Thirty percent (30%) fraction absorbable calculated by using P_e equation is considered an acceptable starting point for predicting absorption in many drug discovery studies and it is used to classify absorption extent of plant constituents in PAMPA whereby log P_e value of -4.70 = 30% fraction absorbable [115]. Any log P_e value below -4.70, considered to have low potential for

passive absorption, is classified as low passive absorption category "GIT-" while a value above -4.70 is classified as high passive absorption category "GIT+" [114, 115].

The data from analysis of the three standards sulfasalazine, amiloride hydrochloride (HCl) and caffeine used in this study correlated with the literature that they are low-permeable, mid-permeable and high permeable by passive diffusion, respectively [141] indicating that the PAMPA membrane in this study was intact. As a result, a log P_e value obtained from sulfasalazine (-6.61) was arbitrarily assigned to any of the plant extract constituents that could not be detected in the PAMPA acceptor compartment. In correlation to the literature [161, 162], passively absorbable constituents of açaí and maca plant extracts were those that comply with Lipinski and Veber's rules. This was confirmed by The Metabolomics Innovation Center (TMIC) online tool (http://www.hmdb.ca/metabolites) that provides among others physicochemical properties of natural products and whether they abide by Lipinski and Veber's rules. In this exercise, it was realized that açaí anthocyanins and maca glucosinolates from acidic methanol extracts had log P values <2 and these did not show a potential for passive absorption probably due to extensive polarity (breaking Lipinski's rule) making it hard for them to traverse the nonpolar fatty acid esters "tails" of lipid bilayer. An exception was a hexyl glucosinolate from acidic methanol maca extract which displayed a potential for passive absorption which was assumed to be due to a nonpolar side-chain (hexyl) helping to balance the polarity of the glucosinolate. It has also been reported that glucosinolates are mostly not absorbed in their intact form but get hydrolyzed by colonic myrosinases and the resulting isothiocyanates get absorbed readily [157]. For acidic methanol açaí extract, consistent with the literature that anthocyanins are taken up by transporters, especially Na^+-dependent glucose transporters (SGLT) [163], all açaí anthocyanins were non-passively absorbable. All constituents that showed potential for intestinal passive absorption had molecular weights less than 500 Da.

Similarly, as generally known that L-amino acids are carried by Na^+-coupled amino acid transporters (NAT) across the intestinal membrane [164], the amino acids in methanol maca extract were all non-passively absorbable in either the extract or the standards. While lepidiline A and lepidiline B have a close structural similarity, an extra methyl group on lepidine B may be reducing its dissolution hence reducing its passive absorption potential as seen in this study. However, there was no data available in the literature supporting the potential intestinal passive absorption of lepidiline A, macaridine and (1R,3S)-1-methyltetrahydro-β-Carboline-3-carboxylic acid. On the other hand, 5-hydroxymethylfurfural (HMF) has been reported to be rapidly absorbed in rats and mice GIT at a concentration-dependent manner which indicates passive absorption [165, 166].

Moreover, most macamides from DCM maca extract could not pass the PAMPA membrane and this was presumed to be a result of their extensive nonpolar feature (log P >5 - breaking Lipinski's rule and rotatable bonds > 10 - breaking Veber's criterion). This means that their dissolution in the intestinal media and into the outer hydrophilic choline esters "heads". Indeed, the DCM maca extract could hardly dissolve in the PAMPA buffer system during this assay. It is believed that one macamide (*N*-benzylhexadecanamide) that has shown potential for passive absorption in this study as confirmed with its standard, is only because it had formed a salt in PAMPA buffer (detected as Na^+ adduct). The salt form of a macamide would have increased polarity hence better dissolution in PAMPA media and the outer hydrophilic layer of the lipid membrane.

Another factor observed in this study is that extent of absorption of açaí and maca plant constituents in complex mixtures was approximately equal to the one obtained when assayed as single compounds (Table 8). Therefore, as previously reported [114], passive absorption of plant constituents may not be altered by their natural occurrence as part of a complex mixture such as botanical dietary supplements.

In acidic açaí methanol extract, a compound protocatechuic acid (PCA) methyl ester was one of the few passively absorbable constituents. While PCA standard was not available as an ester form in this study, it also displayed a potential for passive absorption (Log P_e -4.61). This standard was less absorbed than its corresponding methyl ester and this may be due to relatively reduced polarity on the methyl ester. Apart from that, absorption of PCA has been attributed to the transporter system and P-gp efflux [117]. There was no data available in the literature related to intestinal passive absorption the other four compounds (loliolide, menthiafolic acid, Dihydroconiferyl alcohol and 3-oxo-alpha-ionol) observed in this extract.

In correlation to the literature, orientin and homoorientin in methanol açaí extract were passively absorbed in the assay [167]. However, the absorption profile of orientin has been reported to be diminished by its susceptibility to P-glycoprotein efflux transport [167]. This means that its observed absorption extent in this study where the transporters are not included, may be exaggerated when compared to the one from *in vivo* models. Although no literature was available depicting the intestinal passive absorption of catechol, its high passive absorption profile has been demonstrated on *in vitro* and *in vivo* skin models [168].

Most flavonoids including quercetin 3-glucoside, quercetin 3-rutinoside, kaempferol 3-O-rutinoside, quercetin, scoparin, vitexin, isovitexin and taxifolin could not show a potential for passive absorption. This shows the importance of metabolism in influencing absorption of flavonoids whereby these flavonoids are mentioned to be hydrolyzed prior to metabolism at the intestinal barrier [169, 170]. It is supposed that this hydrolysis reduces the extensive polarity of flavonoids and enhance their potential for passive absorption. Also, for catechin and epicatechin, these are said to O-methylated and glucuronidated extensively and none of their intact forms were detected in the human plasma [171].

To reliably confirm the passively absorbed constituents, after samples from the PAMPA acceptor compartment were analyzed by LC-MS, their TICs were uploaded into the ACD/Spectrus Processor 2016.2.2 software for confirmatory analysis. Before analysis, the background was subtracted on the TICs by the ACD/Spectrus Processor software. Being known compounds, the constituent structures were loaded from the ACD/Dictionary included in the ACD/Spectrus

Processor software after which the ACD/Spectrus Processor performed a search for their presence in the uploaded TICs. When a constituent was passively absorbed, the ACD/Spectrus Processor displayed its extracted ion chromatogram (abbreviated as XIC for this software), retention time, *m/z* value and confidence level with 'Excellent and green color' denoting the highest confidence (Table 8.1). Those with highest confidence were assumed to be denote high potential for passive absorption.

Using the highly nonpolar maca constituents (macamides), the importance of structural polarity in passive absorption was proved by comparing a constituent macamide that has an alkyl amide made of 17 carbons (*N*-benzyloctadecanamide) with its synthetic analog that is made into a polar ester by attaching a hydrophilic group 3-pyridylcarbinol (Table 8.2). The passive absorption extent was significantly increased in the ester form (log P_e -4.36) as opposed to the intact macamide (log P_e -4.70).

Table 8: PAMPA: Intestinal Absorption Analysis

Standard ranking margin: Log P$_e$ -4.7 = 30% absorbable [114]

Log Pe	Absorption extent
<-4.70	High permeable
>-4.70	Low permeable

Açaí plant extracts				
Acidic methanol açaí extract constituents	**Extract log P$_e$**	**Standard compound log P$_e$**	**Absorption extent in extract**	**Absorption extent as a single standard compound**
Anthocyanins				
Cyanidin 3-glucoside	-6.61	-6.30	GIT -	GIT -
Cyanidin 3-sambubioside	-6.61	-6.61	GIT -	GIT -
Cyanidin 3-rutinoside	-6.61	-6.61	GIT -	GIT -
Peonidin 3-glucoside	-6.61	ND	GIT -	ND
Pelargonidin-3-rutinoside	-6.61	-5.55	GIT -	GIT -
Pelargonidin 3-glucoside	-6.61	-5.77	GIT -	GIT -
Non-anthocyanin polyphenols				
Kaempferol 3-O-rutinoside	-6.61	ND	GIT-	ND
Quercetin rutinoside	-6.61	-6.61	GIT-	GIT -

72

Scoparin	-6.61	ND	GIT-	ND
Ferulic acid	-6.61	-6.61	GIT-	GIT -
Syringic acid	-5.02	-5.19	GIT-	GIT -
Caffeic acid	-6.61	ND	GIT-	ND
p-coumaric acid	-6.61	ND	GIT-	ND
Chrysoeriol	-4.73	-5.73	GIT-	GIT -
Menthiafolic acid	-4.45	ND	GIT+	ND
Dihydrodehydroconiferyl alcohol	-5.38	ND	GIT-	ND
Dihydroconiferyl alcohol	-4.45	ND	GIT+	ND
2,6-dimethyl-1,4-benzoquinone	-6.61	ND	GIT-	ND
3-oxo-alpha-ionol	-4.31	ND	GIT+	ND
Loliolide	-4.40	ND	GIT+	ND
Syringaresinol	-6.61	ND	GIT-	ND
Lariciresinol	-6.61	ND	GIT-	ND
Isolariciresinol	-6.61	ND	GIT-	ND
Catechin	-6.35	-6.61	GIT -	GIT -
Epicatechin	-6.61	ND	GIT -	ND
Protocatechuic acid (PCA), methyl ester	-4.31	ND	GIT+	ND
Astilbin	-6.61	ND	GIT -	ND
Methanol açaí extract constituents				
Phenolics				
Catechol	-4.29	-4.59	GIT+	GIT +
Quercetin	-5.28	-6.57	GIT -	GIT -
Taxifolin	-5.33	-6.61	GIT -	GIT -
Gallic acid	-6.61	-6.61	GIT -	GIT -
Orientin	-4.35	-4.29	GIT+	GIT +
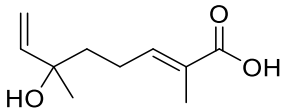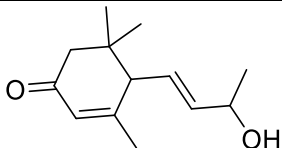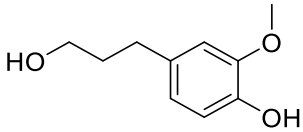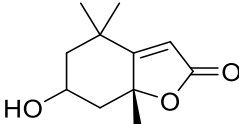
Homoorientin	-4.47	-4.35	GIT+	GIT +
Vitexin	-6.61	-6.61	GIT -	GIT -
Isovitexin	-6.61	-6.61	GIT -	GIT -
Vanillic acid	-6.61	-6.61	GIT -	GIT -
Maca plant extract				
Acidic methanol maca extract constituents				
Glucosinolates				
Glucotropaeolin	-5.86	ND	GIT -	ND
3-methoxybenzyl glucosinolate	-6.6	ND	GIT -	ND
Hexyl glucosinolate	-4.29	ND	GIT +	ND
Methanol maca extract constituents				
Phenolics				
Lepidiline A	-4.42	ND	GIT +	ND
Lepidiline B	-6.35	ND	GIT -	ND
4-Hydroxycinnamic acid	-5.91	ND	GIT -	ND
(1R,3S)-1-methyltetrahydro-β-Carboline-3-carboxylic acid	-4.29	ND	GIT +	ND
Benzyl alcohol	-4.93	ND	GIT -	ND
Malic Acid Benzoate	-4.83	ND	GIT -	ND
5-hydroxymethyl furfural	-4.39	ND	GIT +	ND
Macaridine	-4.29	ND	GIT +	ND
Quercetin	-5.3	-4.83	GIT -	GIT -
Uridine	-4.94	ND	GIT -	ND
5-Oxo-6*E*,8*E*-octadecadienoic acid	-5.84	ND	GIT -	ND
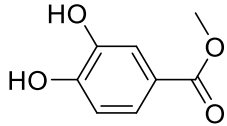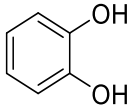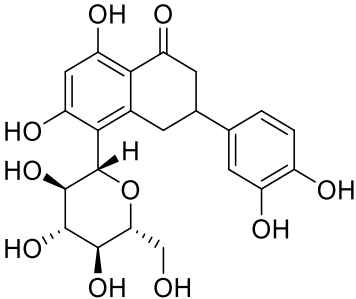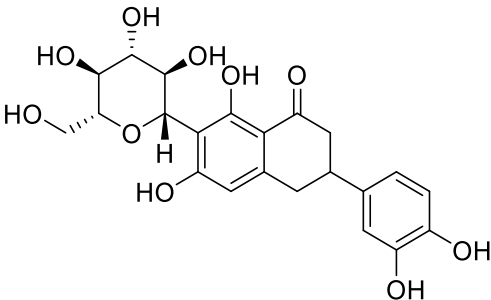
Amino acids				
L-Phenylanine	-6.61	-6.61	GIT -	GIT -
L-tyrosine	-5.68	-5.76	GIT -	GIT -
L-tryptophan	-6.61	-5.47	GIT -	GIT -
Proline	-6.04	ND	GIT -	ND
Leucine	-5.55	ND	GIT -	ND
Isoleucine	-5.16	ND	GIT -	ND
Valine	-5.03	ND	GIT -	ND
DCM maca extract constituents				
Macamides				
N-benzylhexadecanamide	-4.59	-4.57	GIT +	GIT +
N-benzyloctadecanamide	-4.70	ND	GIT -	ND
N-Benzyl-13-oxooctadeca-9E,11E-dienamide	-6.61	ND	GIT -	ND
N-(3-methoxybenzyl)-hexadecanamide	-6.61	ND	GIT -	ND
4'-methoxy-*N*-benzyl-(9Z)octadecanamide	-6.61	ND	GIT -	ND
N-(3-methoxybenzyl)-hexadecanamide	-6.61	ND	GIT -	ND
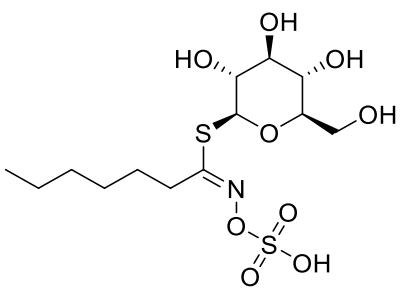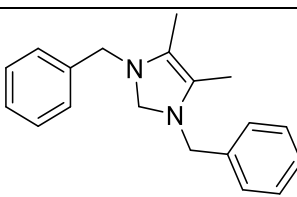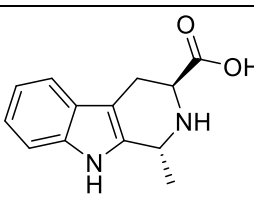
N/A – Not available

Controls	Log Pe	Absorption extent
Positive: Caffeine	-3.81	GIT +
Mid-permeable: Amiloride	-4.34	GIT +
Negative: Sulfasalazine	-6.61	GIT -

Table 8.1. ACD/Spectrus analysis of passively absorbed açaí and maca constituents

Molecular Formula	Molecular Mass (Da)	[M+H]$^+$ *m/z*	Structure	Name	Compound presence confirmation by ACD Spectrus
1. Acidic methanol açaí extract					
$C_{10}H_{16}O_3$	184.2320	185.0891		Menthiafolic acid	Good
$C_{13}H_{20}O_2$	208.2967	209.1537		3-oxo-alpha-ionol	Excellent
$C_{10}H_{12}O_3$	182.2190	183.0652		Dihydroconiferyl alcohol	Good
$C_{11}H_{16}O_3$	196.2460	197.1030		Loliolide	Excellent

$C_8H_8O_4$	168.1480	169.0488		Protocatechuic acid, methyl ester	Good

2. Methanol açaí extract

$C_6H_6O_2$	110.1120	109.0299		Catechol	Good
$C_{21}H_{20}O_{11}$	448.3800	447.0926		Orientin	Excellent
$C_{21}H_{20}O_{11}$	448.3800	447.0934		Homoorientin	Excellent

3. Acidic methanol maca extract					
$C_{13}H_{27}NO_9S_2$	403.4610	404.1094		Hexyl glucosinolate	Good
4. Methanol maca extract					
$C_{19}H_{20}N_2$	276.7410	277.1695		Lepidiline A	Good
$C_{13}H_{14}N_2O_2$	230.2642	231.0942		(1R,3S)-1-methyltetra-hydro-β-Carboline-3-carboxylic acid	Excellent
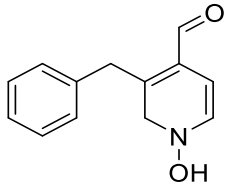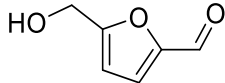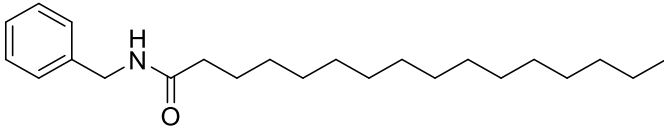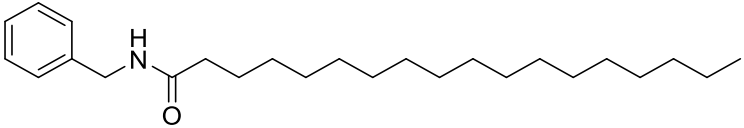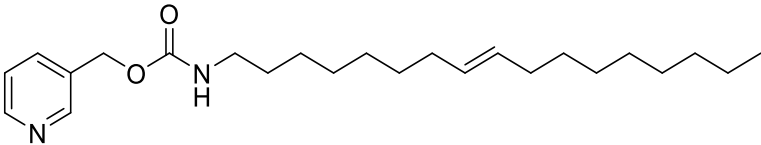
Formula	Mass	m/z	Structure	Name	Rating
$C_{13}H_{13}NO_2$	215.252	216.1006		Macaridine	Excellent
$C_6H_6O_3$	126.111	127.0386		5-hydroxy-methylfurfural	Excellent
5. DCM maca extract					
$C_{23}H_{39}NO$	345.7210	368.2922 $[M+Na]^+$		*N*-benzyl-hexadecanamide	Good

Table 8.2. Comparison of passive absorption extent between a nonpolar intact macamide and a relatively polar synthetic macamide ester

Name	Structure	Log P_e
N-benzyloctadecanamide		-4.70 GIT-
N-(8Z-Heptadecen-1-yl)-O-(3-pyridylmethyl) carbamate		-4.36 GIT+

3.3 Identification of Phase I and Phase II metabolites of plant extract constituents

Analysis of LC-MS data followed both targeted (theoretical) and untargeted (prediction) approaches. A known or predicted metabolite was extracted from reaction samples with background subtraction to ensure that it forms only in the reaction sample. However, working with complex mixtures implied the possibility that a formed metabolite could produce a chemical formula and exact mass similar to one or more of the pre-existing compounds. In these cases, the significant increase in abundance of such a pre-existing ion would give some impression that it was not just an original constituent but with a formed metabolite added on it. Despite that, the general procedure considered with confidence the new chromatographic peaks forming only in the test samples and not in the controls as possible formed metabolites. The LC-MS analysis of these metabolites was supported by the literature search and the predictions suggested by MetaPrint2D-React online tool and Agilent Biotransformation Mass Defects B214.1 software.

Formation of the theoretical and predicted metabolites was analyzed by the Agilent MassHunter Qualitatative Analysis B.07.00 software by displaying EICs of the metabolites from the TIC. Further, a metabolite was confidently predicted by molecular feature whereby the accurate mass, *m/z* value, molecular formula and DBE should correlate to the chemical structure of the predicted metabolite with less error (< 5 ppm) and high score. Chromatograms of the known (Fig. 3.4a) and predicted (Fig. 3.5a) metabolites were displayed.

To perform the structural elucidation of the formed known and predicted metabolites, targeted MS/MS experiments were run. This collision-induced dissociation (CID) fragmentation of the parent ions corresponding to produced metabolites was carried out at 3 different fixed collision energies (5, 20 and 40 eV) to study the fragmentation pathways and identify the main fragments. The MS/MS conditions were set as follows: mass range $50 - 1700$ *m/z*, acquisition time 709.2 ms/spectra, acquisition rate 1 spectra/sec, medium isolation width and charge state of 1. The generated fragments of a known metabolite [172] (Fig. 3.4b) and for confirmation of predicted metabolites (Fig. 3.5b) were displayed. The fragmentation pathway for a known glucuronide (catechol glucuronide) followed the reported pattern [173]. A major fragment was a released catechol from breaking of a relatively more labile glycosidic bond. A radical fragment was

observed in this metabolite fragmentation. While radical formation during CID fragmentation may be uncommon, it has been reported various times [174, 175]. Furthermore, the proposed fragmentation pattern for the putative macamide metabolite agreed with the reported fragmentation pathway of macamides whereby the main fragment ion was from breaking of a labile amide bond [92, 176].

To further perform the structural elucidation of the formed predicted metabolites, their predicted chemical structures previously generated by the MetaPrint2D-React online tool were drawn in ACD/ChemSketch 2016.2.2 software then uploaded to the ACD/Spectrus Processor 2016.2.2 together with the TIC obtained from LC-MS analysis. At this stage, ACD/Spectrus Processor could report if a predicted metabolite was formed and display its extracted ion chromatogram (abbreviated as XIC for this software), retention time, *m/z* value and confidence level with 'Excellent and green color' denoting the highest confidence in the identification (Table 8.3). Those with highest confidence were assumed to be the major metabolites. Interestingly the ACD/Spectrus Processor could even eliminate the background on the TIC enhancing the identification of the metabolite peaks with little or no matrix interference. Owing to the usefulness of the ACD/Spectrus Processor software, it was also used to confirm the formation of theoretical metabolites (Table 8.4). Since these were known compounds, their structures were loaded directly from the ACD/Dictionary included in the ACD/Spectrus Processor.

Among the identified Phase I and Phase II metabolites were the confirmed ten known metabolites in açaí and eight in maca (Table 8.5). Except for kaempferol-3-O-rutinoside in the açaí plant extract, the formation of all metabolites was also confirmed by conducting metabolism experiment with its corresponding single standard compound. This fully eliminated the complexity in the plant extract where a metabolite may also be a pre-existing constituent.

Nineteen putative chemical structures were predicted for the unknown metabolites detected from açaí extracts and four chemical structures of unknown metabolites from maca extracts (Table 8.6). The formed metabolites were confirmed with standard compounds where available. The formation of Phase I and Phase II metabolites from pelargonidin 3-rutinoside, pelargonidin 3-glucoside, vitexin, isovitexin, syringic acid, chrysoeriol, vanillic acid and taxifolin in açaí plant

extracts was confirmed by conducting metabolism experiments with their corresponding single standard compound. The formation of the *N*-benzylhexadecanamide metabolite in maca plant extract was also confirmed by conducting metabolism experiment with its corresponding single standard compound.

In general, retention times of all confirmed and predicted hydroxylated Phase I metabolites were earlier than their original compounds indicating that they have become more polar. Phase II metabolites with more polar groups added came even earlier than their corresponding Phase I metabolites. The opposite was observed for those Phase I metabolites attained by hydrolysis as most became more nonpolar upon removal of a hydrophilic group such as a sugar moiety by hydrolysis.

The MS/MS experiments were also carried out for some of the predicted metabolites and the obtained fragments (Table 8.7) matched those that were predicted by ACD/MS Fragmenter. The first fragments (*m/z* 305.1254 and 168.9426 for taxifolin and vanillic acid, respectively) suggest that the displayed predicted glucuronides in açaí plant extract were first fragmented back to their original forms releasing a glucuronic acid portion. After these, the molecules seem to follow their reported fragmentation patterns [177, 178].

Apart from predictions from ACD/MS Fragmenter, a formed metabolism was also identified based on the known fragments of the original macamides [92, 176]. For *N*-benzylhexadecanamide, the fragment representing a long alkyl chain (*m/z* 165.0886) did not change, while a benzylamine usual fragment from the literature (*m/z* 108) was the only one that increased by 16 Da giving *m/z* 124.0840 indicating hydroxylated metabolite. Apart from having been a predicted metabolite by MetaPrint2D-React online tool, it is of course known that hydroxylation on the aromatic ring prefers a *para* position [13], a *para*-hydroxilated *N*-benzylhexadecanamide metabolite was presumed to be the most probable form. On the contrary, *N*-benzyloctadecanamide with a longer alkyl-amide chain seemed to be oxidized on the terminal carbon as predicted by MetaPrint2D-React online tool and shown by intact fragment *m/z* 277.6584 (Table 8.7).
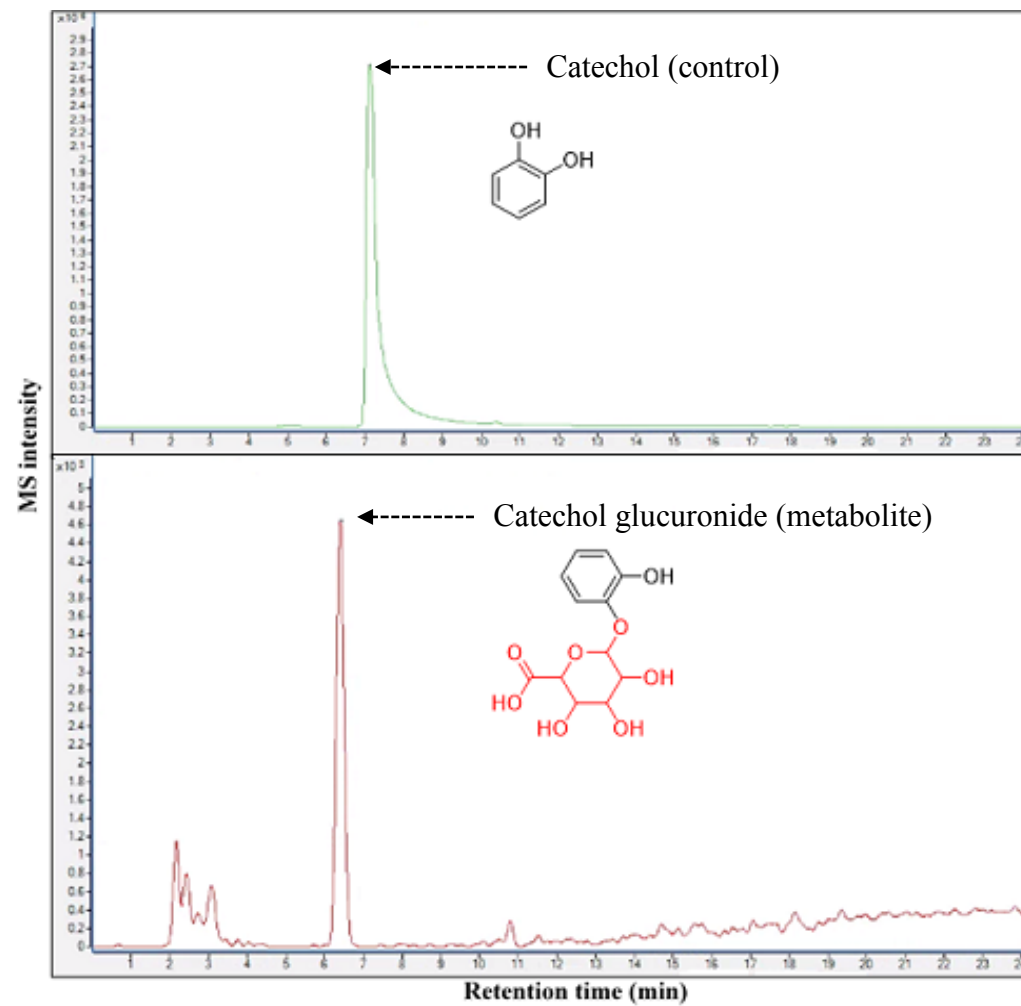
Fig. 3.4a. EIC of a Phase II metabolite of açaí phenolic constituent, catechol.
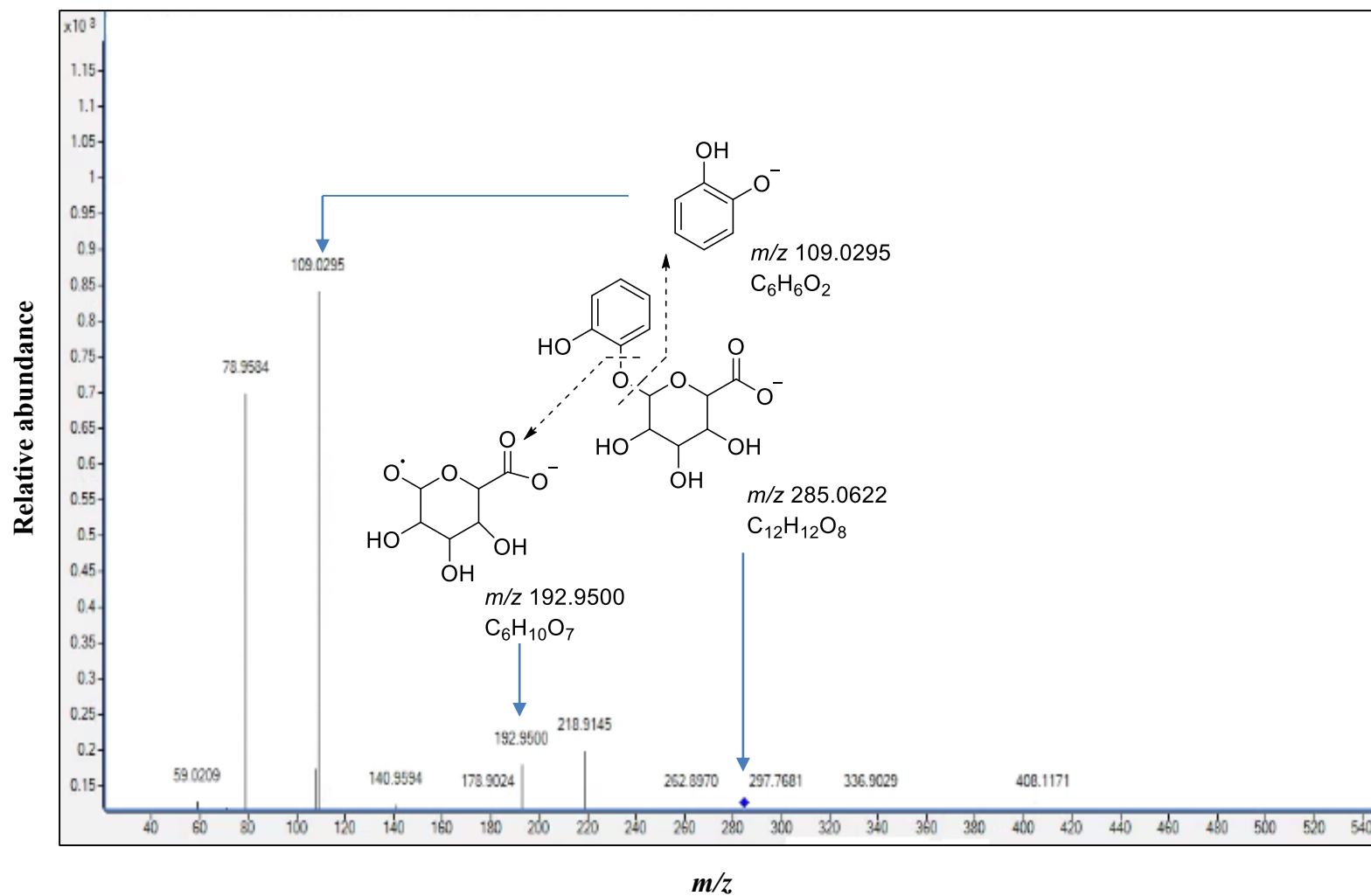
Fig. 3.4b. ESI-MS/MS fragmentation of a known catechol glucuronide at collision energy 40 eV.

85

Fig. 3.5a. EIC of a Phase I metabolite of a macamide, *N*-benzylhexadecanamide.
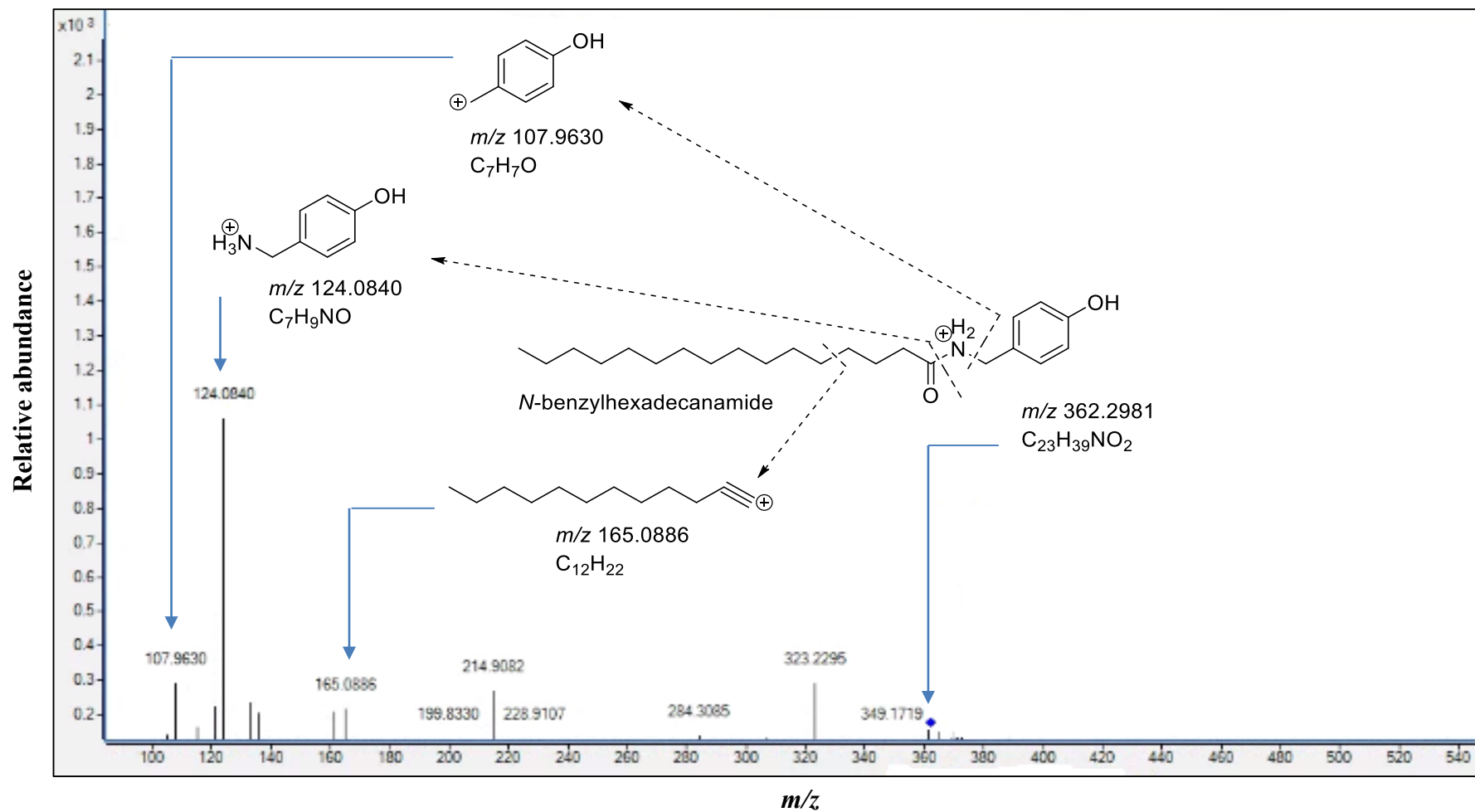
Fig. 3.5b. ESI-MS/MS fragmentation to confirm the chemical structure of a predicted oxidized *N*-benzylhexacanamide metabolite at collision energy 40 eV.
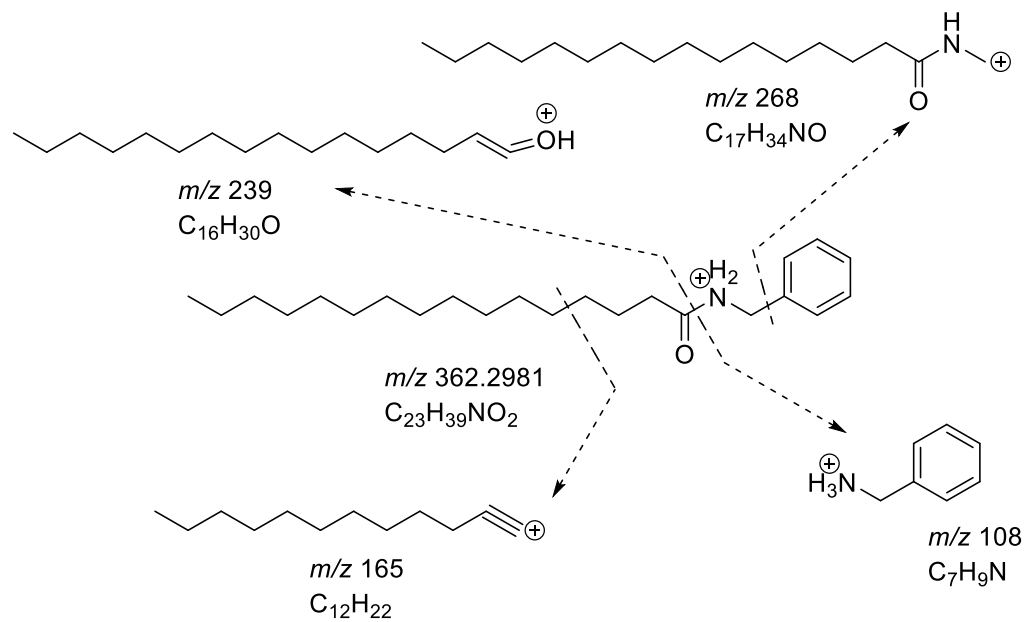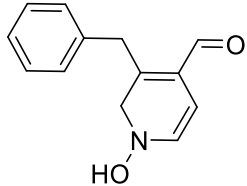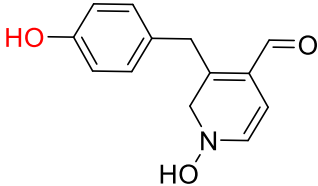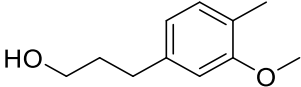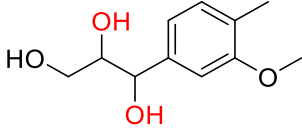
Fig. 3.5c. Literature-based MS/MS fragmentation of the parent macamide, *N*-benzylhexacanamide [92].

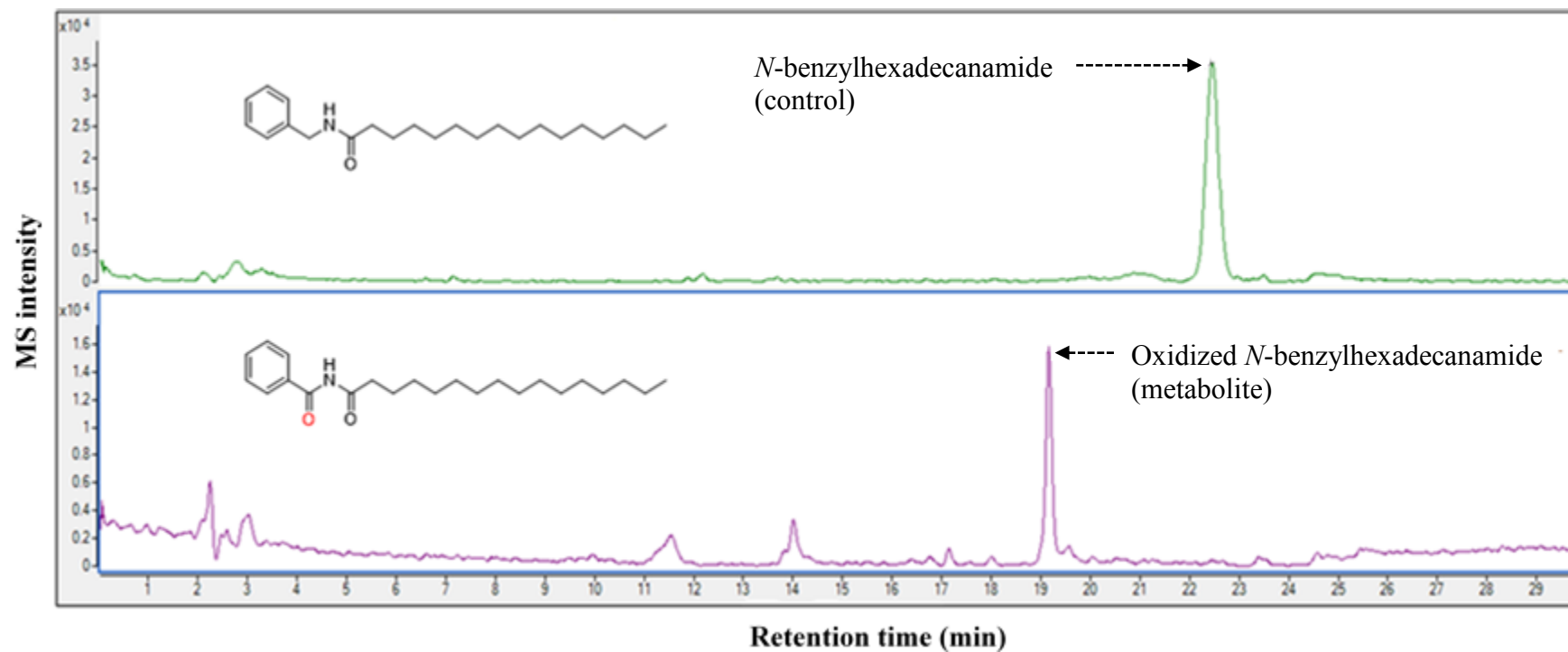**Table 8.3: ACD/Spectrus analysis of predicted açaí and maca metabolites**

Parent constituent	Parent structure	Metabolite structure	Molecular Formula	Molecular Mass (Da)	[M+H]⁺ m/z	Compound presence confirmation by ACD Spectrus
Macaridine (maca extract). *Metabolic reaction*: hydroxylation			$C_{13}H_{13}NO_3$	231.251	232.123	Excellent
Dihydroconiferyl alcohol (açaí extract). *Metabolic reaction*: dihydroxylation			$C_{10}H_{14}O_5$	214.084	215.091	Excellent
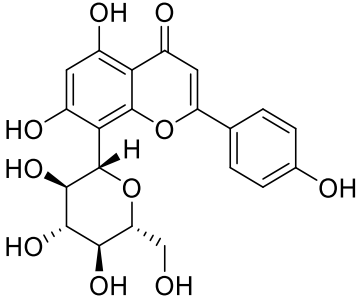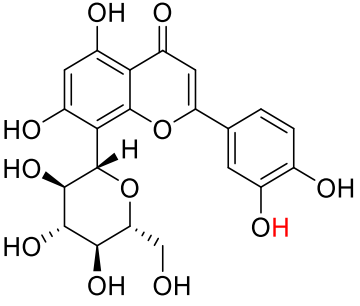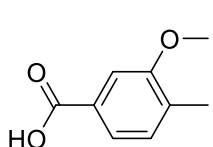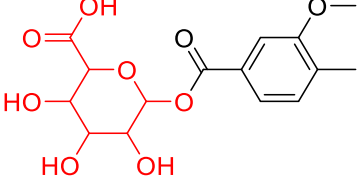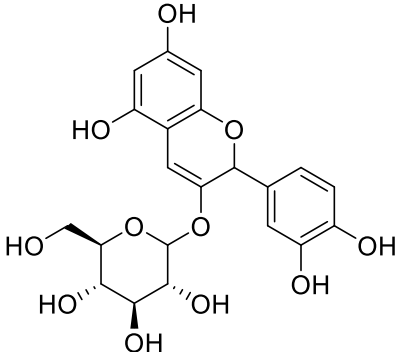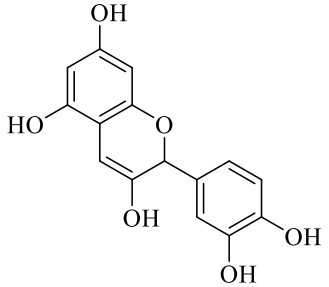
Parent constituent	Parent structure	Metabolite structure	Molecular Formula	Molecular Mass (Da)	[M+H]$^+$ m/z	Compound presence confirmation by ACD Spectrus
Scoparin (açaí extract). *Metabolic reaction*: oxidative demethylation			$C_{14}H_{16}O_{10}$	448.101	449.108	Excellent
Vanillic acid (açaí extract). *Metabolic reaction*: glucuronidation			$C_{14}H_{16}O_{10}$	344.0743	353.0587 (M+Na)$^+$	Excellent

Table 8.4: ACD/Spectrus analysis of known açaí and maca metabolites

Parent constituent	Parent structure	Metabolite structure and name	Molecular Formula	Molecular mass (Da)	[M+H]⁺ m/z	Compound presence confirmation by ACD Spectrus
Cyanidin-3-O glucoside (açaí extract). *Metabolic reaction*: *hydrolysis*		**Cyanidin**	$C_{15}H_{10}O_6$	286.198	287.055	Excellent
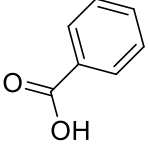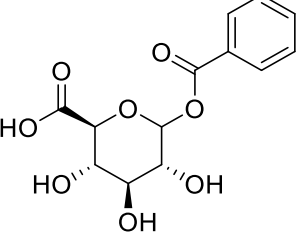
Benzoic acid (maca extract). *Metabolic reaction*: glucuronidation		**Benzoyl glucuronide**	$C_{13}H_{14}O_8$	298.247	299.857	Excellent

Table 8.5. Confirmed Phase I and Phase II metabolites

Parent compound	Phase I or Phase II reaction	Metabolite formed [literature]	Metabolite m/z $[M+H]^+$	RT (min)	DBE	Diff (ppm)	MS/MS $[M+H]^+$ (relative abundance, %)	Fragments correlation to literature
Açaí plant sample								
Cyanidin-3-O-glucoside	Hydrolysis (Phase I)	Cyanidin [179]	287.0555	15.271	11	-3.16	230.8792 (50), 185.1181 (20), 151.0936 (100)	[180, 181]
• Cyanidin	Glucuronidation (Phase II)	Cyanidin glucuronide [179]	501.0411 $[M+K]^+$	2.728	12	5.23	287.0363 (80), 125.0162 (100)	[182]

Parent compound	Phase I or Phase II reaction	Metabolite formed [literature]	Metabolite m/z [M+H]$^+$	RT (min)	DBE	Diff (ppm)	MS/MS [M+H]$^+$ (relative abundance, %)	Fragments correlation to literature
Cyanidin-3-O-rutinoside	Hydrolysis (Phase I)	Cyanidin [179]	287.0553	16.138	11	-3.09	257.2552 (55), 230.8792 (50), 185.1181 (20), 151.0936 (100)	[181]
Cyanidin-3-O-sambubioside	Hydrolysis (Phase I) then glucuronidation (Phase II)	Cyanidin glucuronide [179]	485.0701 [M+Na]$^+$	2.46	12	-1.61	287.0105 (50), 174.8979 (100)	[182]
Pelargonidin-3-glucoside	Hydrolysis (Phase I)	Perlagonidin [179]	271.0634	13.379	11	-1.42	226.9470 (30), 191.0932 (20), 173.0766 (100), 145.1042 (20)	[183]
Kaempferol-3-O-rutinoside	Hydrolysis (Phase I)	Kaempferol [184]	285.0421 [M-H]$^-$	17.089	6	4.8	119.0487 (100), 168.9968 (20), 239.0752 (50), 255.9322 (30)	[185]
Catechol	Glucuronidation (Phase II)	Catechol glucuronide [186]	285.0622 [M-H]$^-$	6.398	6	-.1.67	75.9584 (85), 109.0295 (100), 192.9500 (8), 210.9145 (10)	[172]
Orientin & Homoorientin	Hydrolysis (Phase I)	Luteolin [187]	287.0561	7.189	11	-4.27	285.0381 (100), 256.9439 (40), 242.9767 (35), 211.0925 (40)	[185]
	Hydrolysis (Phase I) then	Luteolin-7-glucuronide [188]	501.0439 [M+K]$^+$	2.497	13	-0.94	449.3170 (100), 365.0970 (25),	[185]

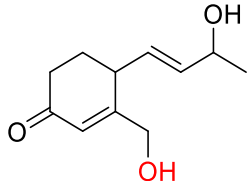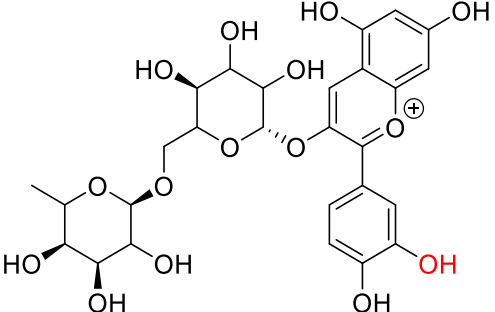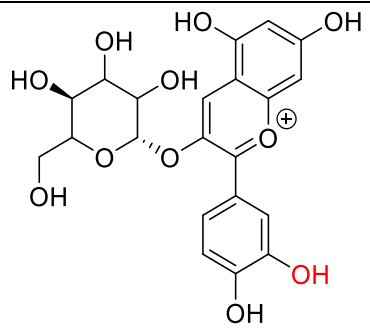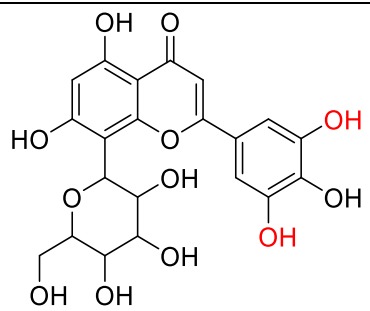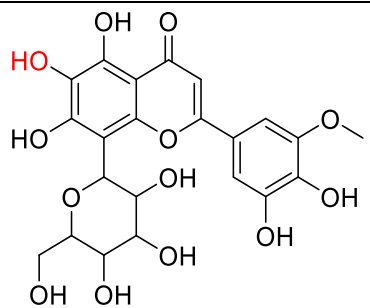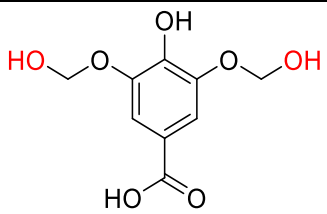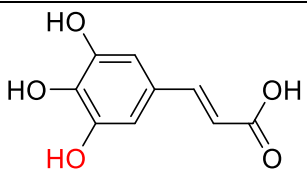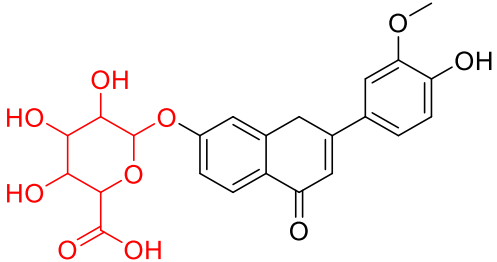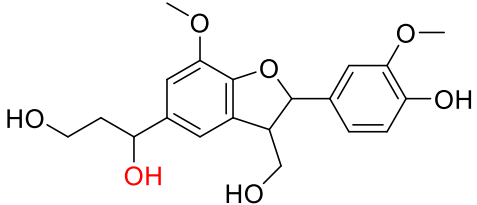| Parent compound	Phase I or Phase II reaction	Metabolite formed [literature]	Metabolite *m/z* [M+H]+	RT (min)	DBE	Diff (ppm)	MS/MS [M+H]+ (relative abundance, %)	Fragments correlation to literature
	glucuronidation (Phase II)						274.7900 (10), 203.0455 (100)	
Quercetin	Glucuronidation (Phase II)	Quercetin-7-glucuronide [189]	479.0843	11.142	13	-0.667	349.769 (70), 302.8750 (50), 169.0634 (50), 103.0167 (100)	[189]
	Glucuronidation (Phase II)	Quercetin-4'-glucuronide [189]	479.0839	11.676	13	-1.79	302.9986 (50), 227.0212 (100), 170.9209 (50), 103.0151 (90)	[189]
	Glucuronidation (Phase II)	Quercetin-3'-glucuronide [189]	479.0844	11.507	13	-4.29	302.8844 (80), 244.9562 (60), 147.0040 (100), 103.0115 (40)	[190]
Quercetin 3-rutinoside & Quercetin-3-glucoside	Hydrolysis (Phase I)	Quercetin [191]	303.0505	14.535	11	-2.42	240.9352 (95), 153.2650 (90), 107.9698 (100)	[192]
Maca plant sample								
Benzyl alcohol	Oxidation (Phase I)	Benzaldehyde [193]	107.0491	4.443	5	3.62	89.0311 (10), 80.0475 (100)	[194]
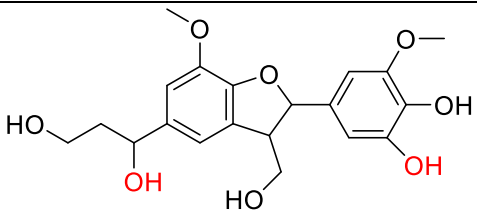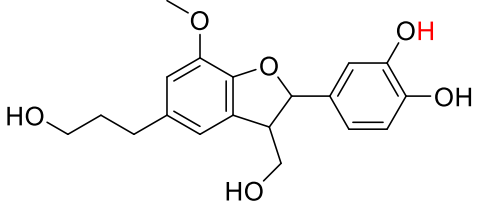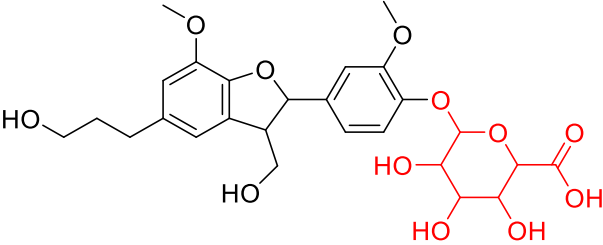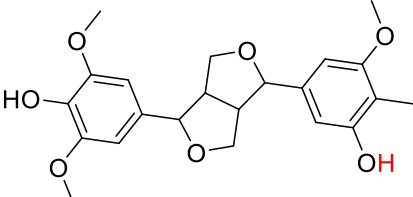
Parent compound	Phase I or Phase II reaction	Metabolite formed [literature]	Metabolite *m/z* [M+H]$^+$	RT (min)	DBE	Diff (ppm)	MS/MS [M+H]$^+$ (relative abundance, %)	Fragments correlation to literature
• Benzaldehyde	Oxidation (Phase I)	Benzoic acid [193]	140.0705 [M+NH$_4$]$^+$	2.104	5	1.34	79.0447 (100)	[195]
• Benzoic acid	Glucuronidation (Phase II)	Benzoyl glucuronide [196]	321.0595 [M+Na]$^+$	2.0212	7	-0.73	123.0547 (50), 79.0247 (100)	[195]
Malic acid benzoate	Hydrolysis (Phase I)	Malic acid [197]	135.0295	2.944	2	0.94	116.9163 (100), 98.0963 (60), 77.2163 (40)	[198]
Hexanal	Oxidation (Phase I)	Hexanoic acid [199]	155.0457 [M+Na]$^+$	18.416	1	1.93	107.0595 (30), 91.0595 (20), 83.0573 (100), 77.0386 (40)	[200]
5-Hydroxymethylfurfural	Glucuronidation (Phase II)	Methylfurfural glucuronide [201]	303.0701	4.985	6	0.01	127.0371 (100), 91.0521 (20)	[202]
Benzylamine	Oxidation (Phase I)	Benzamide [203]	139.0843 [M+NH$_4$]$^+$	4.992	4	4.52	120.0442 (50), 104.0486 (10), 91.0513 (80), 80.0471 (80), 77.0371 (100)	[204]
4-Hydroxycinnamic acid	Glucuronidation (Phase II)	*p*-coumaric acid glucuronide [205]	363.0685 [M+Na]$^+$	2.756	8	1.64	163.0576 (95), 145.0471 (100), 118.0842 (95), 97.0550 (90)	[206]
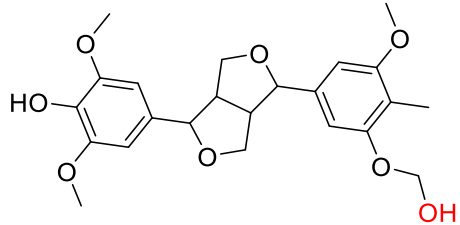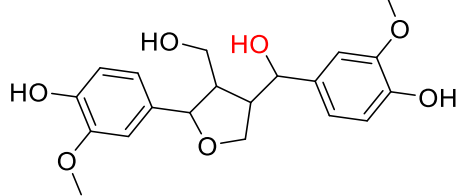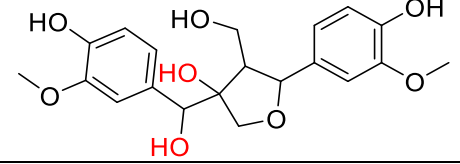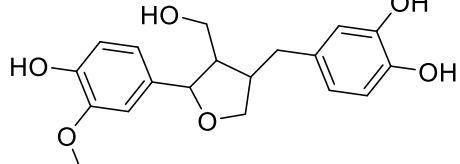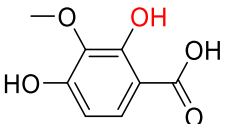
Table 8.6. Predicted Phase I and Phase II metabolites
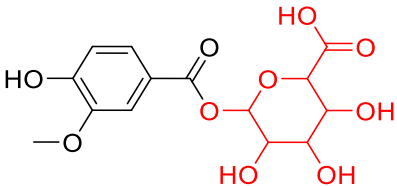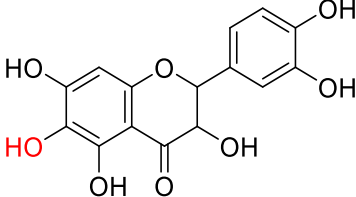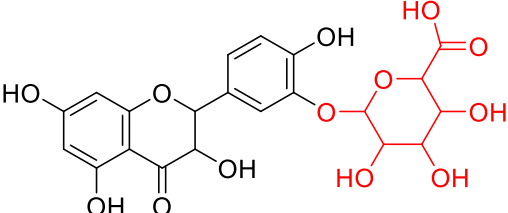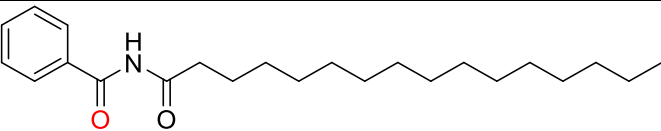
Parent compound	Phase I or Phase II reaction	Putative metabolite as predicted by MetaPrint2D-React online tool	Metabolite *m/z* [M+H]⁺	RT (min)	DBE	Diff (ppm)
Açaí plant sample						
3-oxo-alpha-ionol	Hydroxylation (Phase I)		247.1315	10.769	4	-3.72
Pelargonidin 3-rutinoside	Hydroxylation (Phase I)		613.1998	11.183	13	1.55

Parent compound	Phase I or Phase II reaction	Putative metabolite as predicted by MetaPrint2D-React online tool	Metabolite *m/z* [M+H]⁺	RT (min)	DBE	Diff (ppm)
Pelargonidin 3-glucoside	Hydroxylation (Phase I)		450.116	7.123	12	-1.53
Vitexin	Dihydroxylation (Phase I)		465.103	7.91	12	-0.15
Scoparin	Hydroxylation (Phase I)		496.1434	6.931	12	3.64

Parent compound	Phase I or Phase II reaction	Putative metabolite as predicted by MetaPrint2D-React online tool	Metabolite m/z [M+H]$^+$	RT (min)	DBE	Diff (ppm)
Syringic acid	Dihydroxylation (Phase I)		231.0489	2.611	5	2.16
Caffeic acid	Hydroxylation (Phase I)		197.0468	8.78	6	0.89
Chrysoeriol	Glucuronidation (Phase II)		477.1069	8.819	13	-3.28
Dihydrodehydro-coniferyl alcohol	Hydroxylation (Phase I)		399.1409	10.959	9	0.55

Parent compound	Phase I or Phase II reaction	Putative metabolite as predicted by MetaPrint2D-React online tool	Metabolite m/z $[M+H]^+$	RT (min)	DBE	Diff (ppm)
	Dihydroxylation (Phase I)		431.1118	8.652	9	-4.45
	Oxidative O-demethylation (Phase I)		347.1478	10.979	9	3.88
	Glucuronidation (Phase II)		554.2222	8.186	11	3.02
Syringaresinol	Oxidative O-demethylation (Phase I)		427.1366	13.417	10	-0.55

Parent compound	Phase I or Phase II reaction	Putative metabolite as predicted by MetaPrint2D-React online tool	Metabolite *m/z* [M+H]$^+$	RT (min)	DBE	Diff (ppm)
	Hydroxylation (Phase I)		457.1482	13.226	10	-2.47
Lariciresinol & isolariciresinal	Hydroxylation (Phase I)		399.1414	13.063	9	0.33
	Dihydroxylation (Phase I)		415.1358	11.382	9	1.81
	Oxidative O-demethylation (Phase I)		347.1487	11.919	9	-0.48
Vanillic acid	Hydroxylation (Phase I)		183.0297 (M-H)$^-$	7.619	5	0.81

Parent compound	Phase I or Phase II reaction	Putative metabolite as predicted by MetaPrint2D-React online tool	Metabolite m/z $[M+H]^+$	RT (min)	DBE	Diff (ppm)
	Glucuronidation (Phase II)		353.0587 $(M+Na)^+$	5.8	7	-4.72
Taxifolin	Hydroxylation (Phase I)		319.047 $(M-H)^-$	9.583	10	-0.66
	Glucuronidation (Phase II)		481.1023	6.689	12	-4.94
Maca plant sample						
N-benzyl-hexadecanamide	Oxidation (Phase I)		362.305	19.192	6	0.86
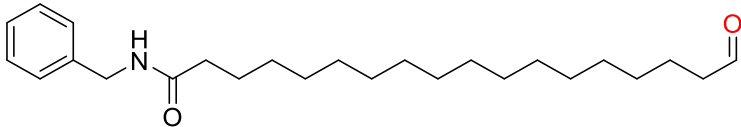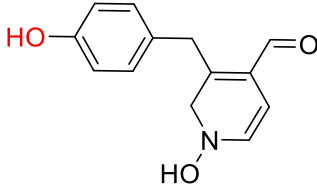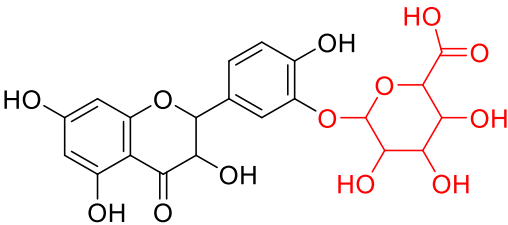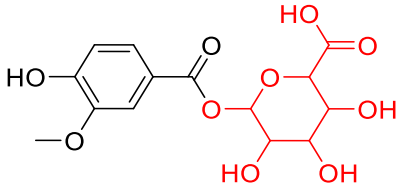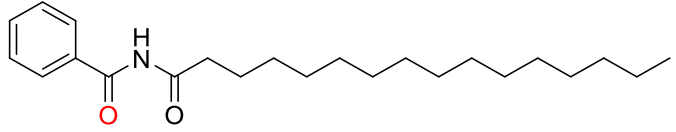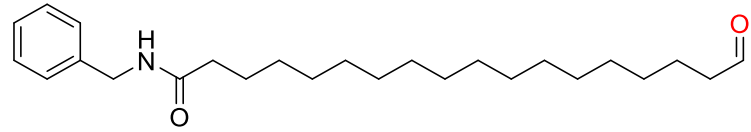
Parent compound	Phase I or Phase II reaction	Putative metabolite as predicted by MetaPrint2D-React online tool	Metabolite m/z [M+H]+	RT (min)	DBE	Diff (ppm)
N-benzyl-octadecanamide	Oxidation (Phase I)		428.2923	20.859	6	0.52
Macaridine	Hydroxylation (Phase I)		232.123	4.925	8	2.61

Table 8.7. MS/MS studies for predicted açaí and maca Phase I and Phase II metabolites

Parent compound	Phase I or Phase II reaction	Putative metabolite formed	MS/MS [M+H]+ (relative abundance, %)
Açaí plant extract			

Parent compound	Phase I or Phase II reaction	Putative metabolite formed	MS/MS [M+H]$^+$ (relative abundance, %)
Taxifolin	Glucuronidation (Phase II)		305.1254 (50), 254.8450 (100), 180.9043 (90), 140.9201 (40). 105.0656 (60)
Vanillic acid	Glucuronidation (Phase II)		168.9426 (30), 156.8884 (40), 145.1077 (100), 125.2125 (30), 118.3005 (50)
Maca plant extract			
N-benzylhexadecanamide	Oxidation (Phase I)		323.2295 (40), 284.3085 (20), 214.9085 (20), 165.0886 (30), 124.0840 (100), 107.9630 (40)
N-benzyloctadecanamide	Oxidation (Phase I)		341.1109 (100), 277.6584 (2), 147.9185 (20)

3.4 Optimization of parameters for CYP3A4 inhibition studies

3.4.1 Optimal incubation time of the enzymatic reaction

The CYP3A4 incubation experiment had a metabolite 1'-hydroxymidazolam formed most linearly during the first 10 min (Fig. 3.6). Therefore, 10 min was used as the incubation time in this study.
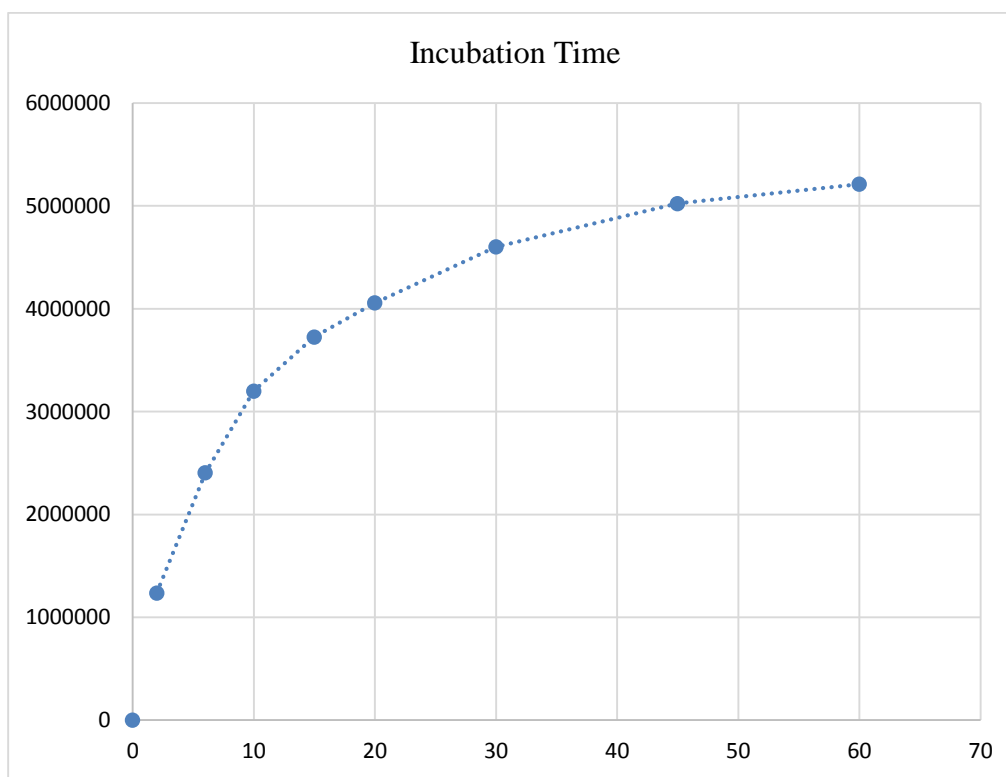
Fig. 3.6. Incubation time optimization for 1'-hydroxymidazolam formation

3.4.2 Calibration curve concentration range of 1'-hydroxymidazolam

Calibration curves in the range (2 – 60 min) were carried out to quantify the amount of 1'-hydroxymidazolam produced in the CYP3A4 incubation assay (Fig. 3.7). The amount of a

metabolite 1'-hydroxymidazolam formed in the assay was 5.83 µM with a good correlation coefficient (R^2) of > 0.99.
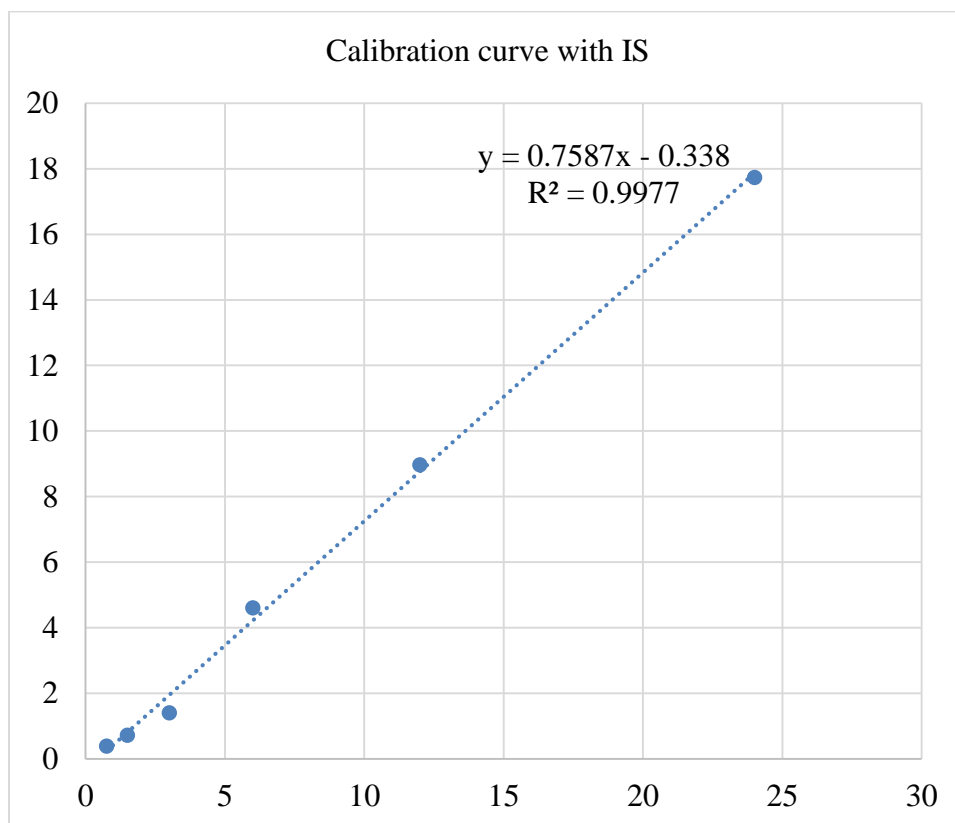
Fig. 3.7. Calibration curve for 1'-hydroxymidazolam quantification

3.5 Evaluation of CYP3A4 inhibition by plant extracts, plant standard compounds and Phase I and Phase II metabolites

3.5.1 Evaluation of CYP3A4 inhibition by açaí and maca plant extracts

The four açaí and maca plant extract concentrations 0.05, 0.075, 0.1, and 0.15 µg/µL were screened for CYP3A4 inhibition to assess their potential for botanical-drug interactions in clinical concomitant dose with chemotherapeutic agents. The plant standard compounds were screened for CYP3A4 activity at a concentration of 50 µg/mL. The metabolite 1'-hydroxymidazolam generated from hydroxylation of a CYP3A4 probe substrate, midazolam, was quantified by comparison of peak areas with those of the calibration curve and the accurate quantities used to calculate the extent of CYP3A4 inhibition (Fig. 3.8). The CYP3A4 inhibition by açaí and maca plant extracts and their available standard compounds was also calculated in percentages by using the equation (2) below. The extent of CYP3A4 inhibition calculated by either method was consistent.

Equation (2):

% CYP3A4 inhibition = 100 x (control peak area - peak area in test compound presence)/control peak area.
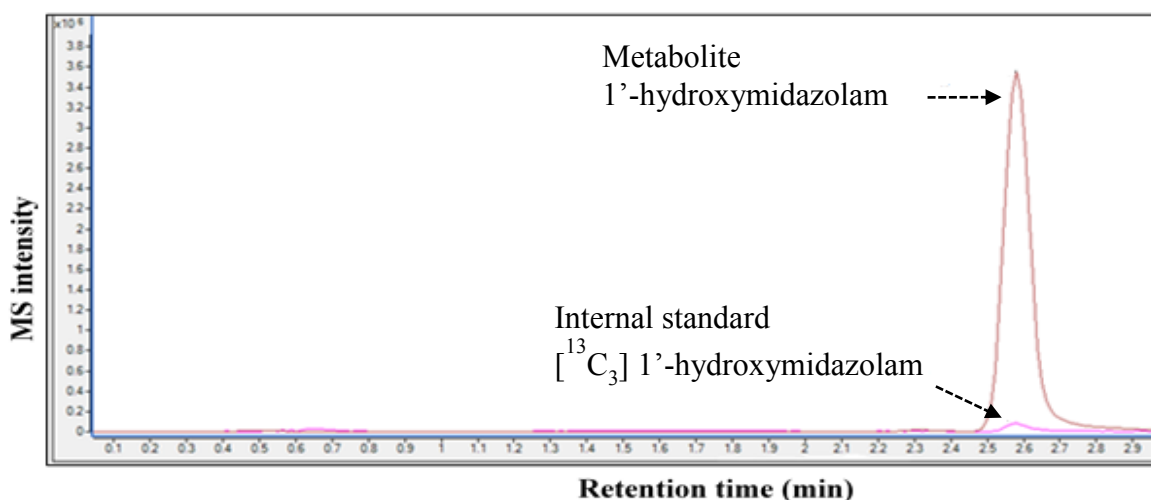
Fig. 3.8. EICs of I'-hydroxymidazolam used to monitor CYP3A4 inhibition extent.

Based on FDA classification [207], all extracts showed moderate inhibition (Table 8.8) and the standard compounds assayed separately (Table 8.9) were used to identify potential CYP3A4 inhibitors in açaí and maca extracts.

FDA classification of CYP Enzyme inhibitors [207]

Inhibitor	Substrate metabolic clearance
A Strong inhibitor	> 80% decrease
A Moderate inhibitor	50-80% decrease
A Weak inhibitor	20-50% decrease

Table 8.8: CYP3A4 inhibition profile by plant extracts and standard compounds:

CYP3A4 Inhibition	
Açaí plant extracts	
Acidic methanol açaí plant extract (µg/µL)	**% CYP3A4 Inhibition**
0.05	46.9
0.075	54.9
0.1	57.4
0.15	58.2
Methanol açaí plant extract (µg/µL)	
0.05	13.2
0.075	20.6
0.1	28.1
0.15	50.2

Maca plant extracts	
Acidic methanol maca plant extract (µg/µL)	
0.05	58.7
0.075	66.8
0.1	68.0
0.15	69.0
Methanol maca plant extract (µg/µL)	
0.05	67.7
0.075	70
0.1	73.6
0.15	76.7
DCM maca plant extract (µg/µL)	
0.05	50.3
0.075	54.2
0.1	57.7
0.15	68.9

Even though all extracts displayed moderate (50-80%) CYP3A4 inhibition, they showed different strengths whereas the methanol açaí extract was towards the lower limit (50%) while the methanol maca extract was towards the higher limit of moderate inhibition.

Table 8.9. CYP3A4 inhibition profile by plant standard compounds:

Standard compounds	
Acidic methanol açaí standard compounds	**% CYP3A4 Inhibition**
Cyanidin-3-O-glucoside	20.2
Cyanidin-3-O-rutinoside	0
Cyanidin-3-sambubioside	0
Pelargonidin-3-glucoside	0
Pelargonidin-3-rutinoside	0
Orientin	37.9
Homoorientin	0

	% CYP3A4 Inhibition
Vitexin	18.5
Isovitexin	25.8
Methanol açaí standard compounds	
Catechin	33.8
Catechol	66.9
Chrysoeriol	4.1
Ferulic acid	11.5
Gallic acid	96.1
Protocatechuic acid	34.8
Quercetin	8.6
Quercetin-3-glucoside	38
Quercetin-3-rutinoside	8.2
Syringic acid	40.5
Vanillic acid	27.7
Taxifolin	19.5
Maca DCM standard compounds	**% CYP3A4 Inhibition**
N-(8Z-Heptadecen-1-yl)-O-(3-pyridylmethyl) carbamate	95.6
N-benzylhexadecanamide	77.5

Positive control	
[Ketoconazole, µM]	**% CYP3A4 Inhibition**
1	55.3
10	92.9

N-(8Z-Heptadecen-1-yl)-O-(3-pyridylmethyl) carbamate, showing a potential for strong CYP3A4 inhibition, is a synthetic analog of macamides from *L. meyenii* [208] and used in this study due to the unavailability of commercial standard compounds of maca. However, it has not been reported for CYP3A4 inhibition before but for antiproliferative activity in many cancer cell lines [209].

Studies with standard compounds showed that none of the açaí anthocyanins inhibited CYP3A4 which correlates to the literature that generally anthocyanins, with exception of cyanidin 3-O-rhamnoside which was not detected in this extract, have not displayed any CYP3A4 inhibition activities [210]. Even though anthocyanins were reported as weak CYP3A4 inhibitors on the study conducted by Dreiseitel *et al* [211], they were still considered to pose only a limited risk of botanical-drug interactions. This risk may be even further negligible in the clinical setting since apart from anthocyanins not being passively absorbed in this study, their plasma concentrations have always been reported to be extremely low in the clinical studies. In the study conducted on human healthy volunteers that consumed açaí pulp containing 972 mg/L total anthocyanins or açaí juice containing 531 mg/L total anthocyanins, only 2321.35 ng/L and 1138.51 ng/L anthocyanins respectively were detected which is approximately 0.0002% bioavailability [79]. Del Pozo-Insfran *et al* reported that the major açaí anthocyanin, cyanidin-3-O-glucoside, could reach at maximum 0.008% in human plasma [59]. However, the very low detection of anthocyanins in human plasma may be explained by reports that they are instantly metabolized into their corresponding aglycones and other smaller molecules *in vivo* whereby some studies even suggest that the observed antioxidant activities may not be from intact anthocyanins but their metabolites [155, 212].

3.5.2 Calculation of IC_{50} values for açaí and maca plant extracts with potential for CYP3A4 inhibition

After all plant extracts displayed moderate (50-80%) CYP3A4 inhibition, IC_{50} studies were carried out at 6 concentrations ($0.0125 - 0.4\ \mu g/\mu L$) covering those assayed in the initial screening. The extent of inhibition at each concentration was calculated and the log dose-response curves plotted using GraphPad Prism 5.02 software (Mountain View, CA, USA) that also generated the IC_{50} values (Fig. 3.9).

The studied plant extracts displayed the IC_{50} values per each extract for CYP3A4 inhibition. The estimated IC_{50} values were 0. 0248 and 0.0688 µg/µl for acidic methanol and methanol açaí

extracts, respectively. The estimated IC_{50} values for acidic methanol, methanol and DCM maca extracts were 0.0431, 0.0873 and 0.0632 µg/µl, respectively.
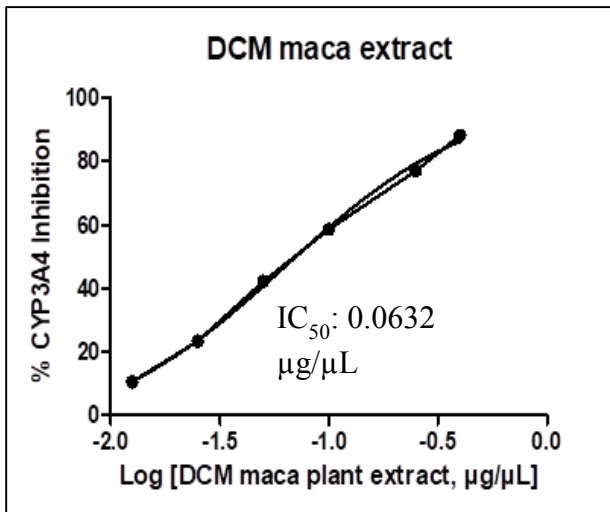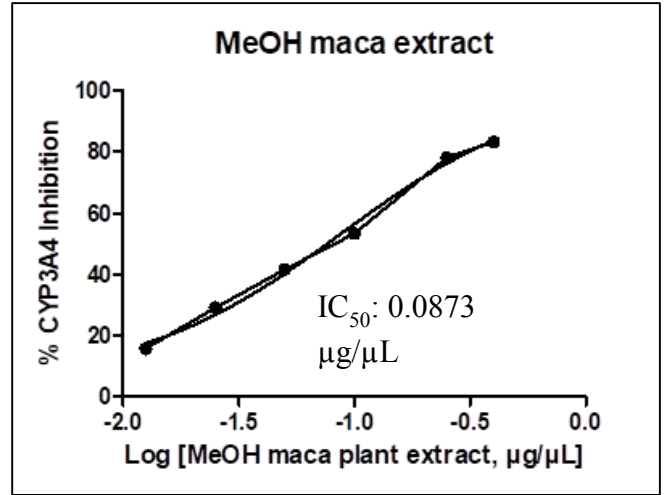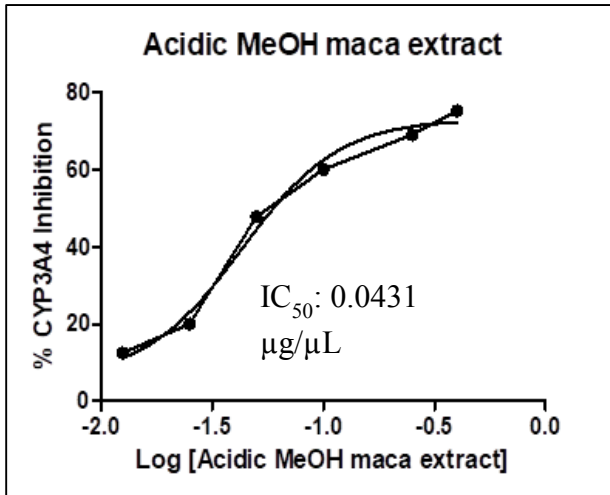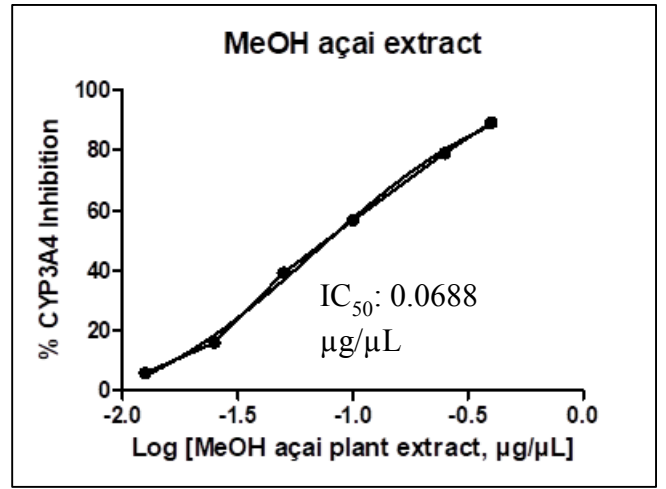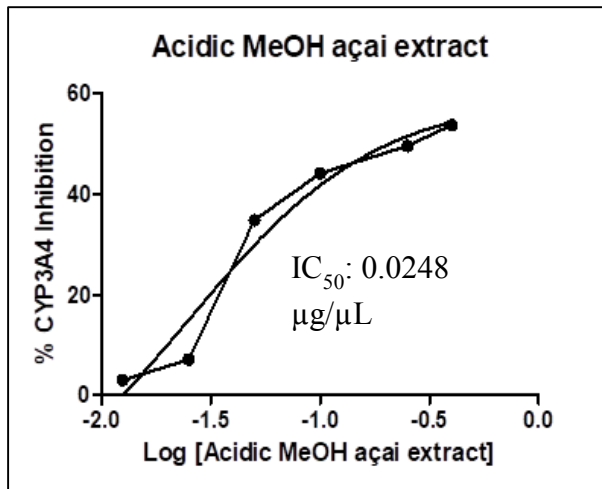
Fig. 3.9. Açaí and maca log dose-response curves at 0.0125, 0.025, 0.05, 0.1, 0.2 and 0.4 µg/µL.

The methanol açaí extract at 0.4 µg/µL was comparable to the DCM maca extract in that they displayed the highest CYP3A4 inhibitory activities (89.2 and 88.2%, respectively). Methanol maca extract at 0.4 µg/µL followed with 83.3% CYP3A4 inhibition and acidic methanol maca extract with 75.3%. The acidic methanol açaí extract, giving the lowest inhibitory activity, could only reach at maximum 53.7% CYP3A4 inhibition even at this highest concentration, 0.4 µg/µL. Based on these results and the maximum extract concentration studied, it could be observed that acidic methanol extracts of açaí and maca stayed as moderate CYP3A4 inhibitors. On the other hand, methanol extracts of açaí and maca together with DCM maca extract increased from moderate inhibition that was observed in the initial screening at 0.15 µg/µL to strong CYP3A4 inhibition at at 0.4 µg/µL.

3.5.3 Evaluation of CYP3A4 inhibition by Phase I and Phase II metabolites of açaí and maca plant constituents

Prior to screening for CYP3A4 inhibition, confirmation was made that the level of metabolite production in a reaction stopped by immediate centrifugal spinning was consistent with the level obtained in the reaction stopped by ice-cold ACN (Fig. 4.0). This confirmed that the reaction had stopped during the quick centrifuging moment where an organic solvent had been avoided to eliminate its interference with the microsomes in the then following CYP3A4 inhibition assay.

The açaí and maca plant extract Phase I and Phase II metabolites at concentration 0.12 µg/µL were screened for CYP3A4 inhibition to assess their potential for botanical-drug interactions in clinical concomitant dose with chemotherapeutic agents. The CYP3A4 inhibition by these metabolites was calculated in percentages by using the equation (2) listed in section 3.5.1.

All Phase I metabolites of plant extracts showed weak CYP3A4 inhibition (Table 9). These results suggested that Phase I metabolism was adequate to detoxify the inhibiting compounds and that the observed weak inhibition was most likely from the trace amounts of the original compounds that stayed intact.
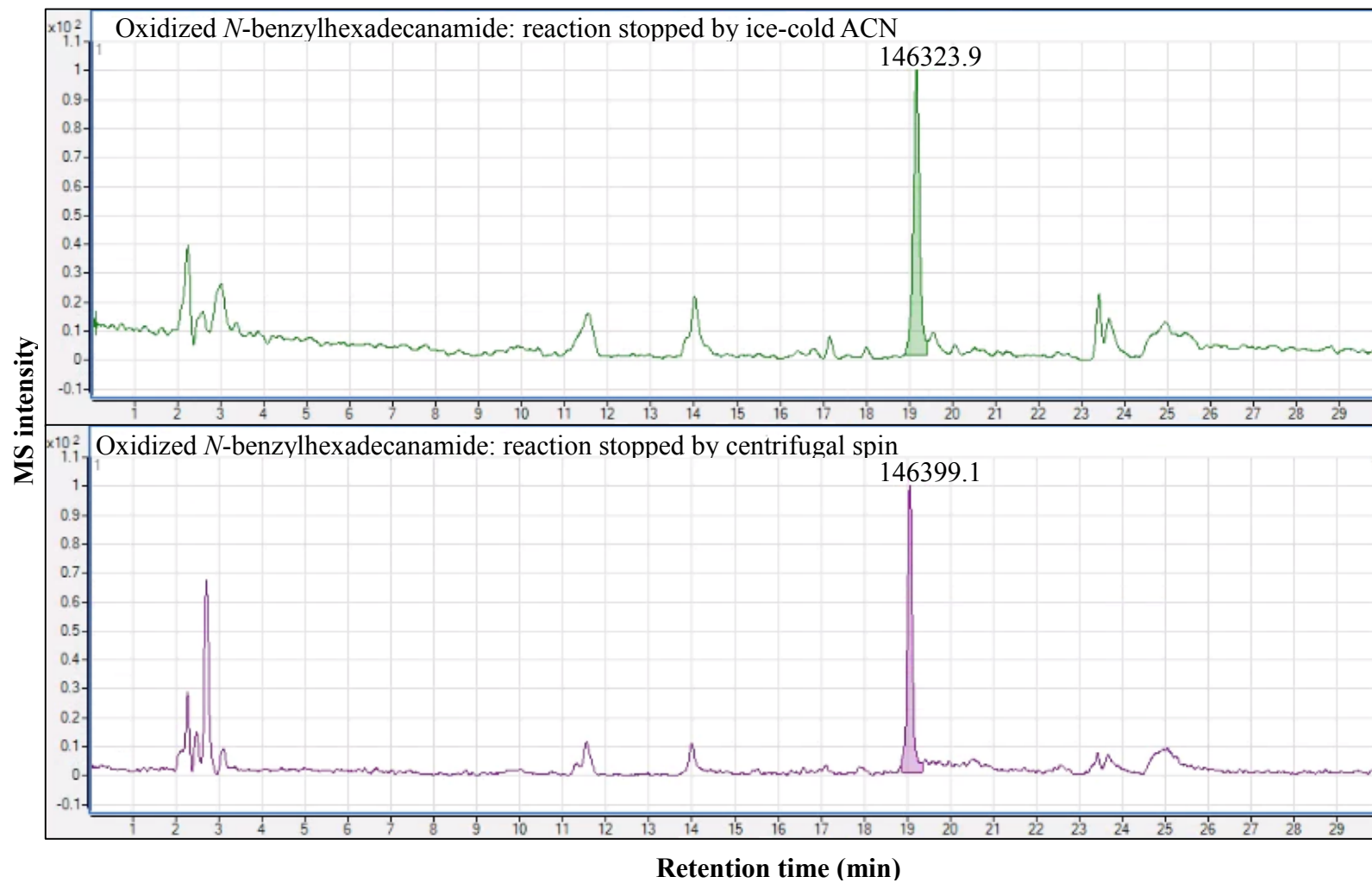
Fig. 4.0. Comparison of the peak areas of the metabolite oxidized *N*-benzylhexadecanamide in a reaction stopped by ice-cold acetonitrile and one stopped by immediate centrifuge.

Table 9. CYP3A4 inhibition profile by açaí and maca Phase I metabolites

CYP3A4 Inhibition	
Açaí Phase I metabolites	
Acidic methanol açaí Phase I metabolites (µg/µL)	**% CYP3A4 Inhibition**
0.12	19.7
Methanol açaí Phase I metabolites (µg/µL)	
0.12	8.13
Maca Phase I metabolites	
Acidic Methanol maca Phase I metabolites (µg/µL)	
0.12	23.2
Methanol maca Phase I metabolites (µg/µL)	
0.12	22.2
DCM maca Phase I metabolites (µg/µL)	
0.12	29.4

All açaí Phase II metabolites obtained by using only UDPGA as a cofactor showed weak CYP3A4 inhibition indicating sufficient detoxification by metabolism while those of maca displayed moderate CYP3A4 inhibition (Table 9.1). These were presumed to be the glucuronides formed from constituents with pre-existing nucleophilic groups such as a hydroxyl (-OH). Based on their chemical structures, the identified passively absorbed polyphenols in acidic methanol and methanol açaí extracts can form glucuronides should they be UGT substrates. The results show that these glucuronides could not exert their CYP3A4 inhibitory activity anymore. It is worth noting that, if it could happen that these glucuronides are substrates of β-glucuronidases, they could be hydrolysed back into their original structures [213] that displayed CYP3A4 inhibition. Their susceptibility to β-glucuronidases was not studied in this work.

For the maca extracts that all exhibited moderate CYP3A4 inhibition, making even more sense is the DCM extract that contains a macamide that according to its structure, is not susceptible to direct glucuronidation [214]. The percent of CYP3A4 inhibition displayed here is closer to the one displayed in the original extract screening which gives an impression that the identified macamide stayed intact. In acidic methanol maca extract that contains hexyl glucosinolate, while its chemical

structure would allow glucuronidation to take place, there was no glucuronide of any glucosinolate reported in the literature nor identified in this study. Therefore, it is presumed that hexyl glucosinolate may have stayed intact.

Table 9.1. CYP3A4 inhibition profile by açaí and maca Phase II metabolites from a cofactor UDPGA

CYP3A4 Inhibition	
Açaí Phase II UDPGA metabolites	
Acidic methanol açaí Phase II UDPGA metabolites (µg/µL)	**% CYP3A4 Inhibition**
0.12	48.2
Methanol açaí Phase II UDPGA metabolites (µg/µL)	
0.12	34.3
Maca Phase II UDPGA metabolites	
Acidic methanol maca Phase II UDPGA metabolites (µg/µL)	
0.12	52
Methanol maca Phase II UDPGA metabolites (µg/µL)	
0.12	57.1
DCM maca Phase II UDPGA metabolites (µg/µL)	
0.12	79.2

For açaí, Phase II metabolites obtained by using NADPH and UDPGA cofactors in acidic methanol açaí extract showed weak CYP3A4 inhibition while those from methanol açaí extract displayed moderate CYP3A4 inhibition. On the other hand, Phase II metabolites obtained by using these cofactors in acidic methanol and DCM açaí extract showed weak CYP3A4 inhibition but those from methanol maca extract displayed moderate CYP3A4 inhibition (Table 9.2). These were expected to be the glucuronides formed from constituents required both the functionlization such as the addition of a hydroxyl group by Phase I metabolism and glucuronidation by Phase II enzymes. However, since constituents in these methanol extracts are predominantly phenolics, the

order of Phase I and Phase II metabolism may not matter unless glucuronidation occurs directly on the newly inserted hydroxyl group.

From these results, it may be assumed that the macamide in DCM maca extract has undergone activation and glucuronidation phases which resulted in its loss of CYP3A4 inhibitory activity. If metabolized, then one or some of the absorbed constituents in methanol açaí and maca extracts may still have CYP3A4 inhibitory activity after hydroxylation and glucuronidation.

Table 9.2. CYP3A4 inhibition profile by açaí and maca Phase II metabolites from the cofactors NADPH and UDPGA

Açaí Phase II UDPGA + NADPH metabolites	
Acidic methanol açaí Phase II UDPGA + NADPH metabolites (μg/μL)	**% CYP3A4 Inhibition**
0.12	44.0
Methanol açaí Phase II UDPGA + NADPH metabolites (μg/μL)	
0.12	52.7
Maca Phase II UDPGA + NADPH metabolites	
Acidic Methanol maca Phase II UDPGA + NADPH metabolites (μg/μL)	
0.12	26.2
Methanol maca Phase II UDPGA + NADPH metabolites (μg/μL)	
0.12	66.9
DCM maca Phase II UDPGA + NADPH metabolites	
0.12	25.3

3.6 Identification of CYP3A4 inhibitors in açaí and maca plant extract constituents

Identification of constituents possibly exerting the CYP3A4 inhibitory effects from the assayed plant extracts was based on the absorption data from PAMPA study since only the passively diffused ones (GIT+ plus confirmation by ACD/Spectrus software) were screened. Five non-anthocyanin polyphenols (loliolide, dihydroconiferyl alcohol, menthiafolic acid, PCA methyl ester and 3-oxo-alpha ionol), were passively absorbed from acidic methanol açaí extract. None of them were available as a pure compound in our lab and in such case the information from literature was utilized for estimating the identity of the CYP3A4 inhibitor. Among these, PCA methyl ester is an ester of a prominent anthocyanin metabolite, PCA, reported to have mild CYP3A4 inhibition effects [211]. The PCA standard compound was of course screened for CYP3A4 inhibition in this study and only weak (34.8%) inhibition could be attained. Interestingly, de Faria *et al* [215] screened a series of PCA alkyl esters and suggested that an increase in the carbon chain of the ester, which decreases the hydrophilicity of the original PCA, is accompanied by proportional increase in the inhibition of NADPH-dependent oxidase. This behavior, according to de Faria, is true only up to 7 carbons ester [215]. It is supposed therefore, in this study that PCA methyl ester may be responsible for the observed CYP3A4 inhibition.

In the methanol açaí extract, only 3 constituents (catechol, orientin and homoorientin) were absorbed. All these were available as standard compounds and only catechol displayed moderate CYP3A4 inhibition at 0.05 µg/µL. This suggested catechol as the CYP3A4 inhibitor in methanol açaí plant extract. While gallic acid standard compound displayed strong CYP3A4 inhibition at the same concentration, it was not passively bioavailable either in the MeOH açaí extract, acidic MeOH açaí extract or as a single standard compound. This data agreed with the literature that catechol inactivates cytochrome protein in rat and human liver microsomes [216, 217] and that gallic acid strongly inhibits CYP3A4 [218, 219]. These passive absorption profiles and CYP3A4 inhibitory activities were confirmed by plant standard compounds.

For acidic methanol maca extract, the only one glucosinolate (hexyl glucosinolate) that was passively absorbed was therefore estimated to be the one responsible for the observed CYP3A4 inhibition. This was based on the vast literature reporting that glucosinolates and their degradation

products (isothiocyanates) inhibit various cytochrome enzymes which is a feature attributed to their chemopreventive activity [121, 220-222]. Among compounds potentially absorbed from methanol maca extract, 5-hydroxymethylfurfural (HMF), has of course been reported to be rapidly absorbed in rats and mice GIT at a concentration-dependent manner suggesting passive absorption [165, 166]. Although no literature reporting HMF as an inhibitor of CYP3A4, it has been reported for CYP2C8 inhibition [223]. HMF is a known potent cytotoxic molecule having been reported to exert direct tissue damage to the gastrointestinal mucosa and other mucous membranes [224, 225]. Based on this, the prediction in this study is that if not binding to CYP3A4 and inhibiting it, HMF in methanol maca extract may have directly damaged human liver microsomes in the assay leading to the observed CYP3A4 inhibition.

Furthermore, among two macamides that showed potential for passive absorption from DCM maca extract, *N*-benzylhexadecanamide which has been reported as a major macamide in *L. meyenii* [92] was commercially available. In the CYP3A4 screening, *N*-benzylhexadecanamide displayed moderate inhibition of the midazolam 1-hydroxylation. The was no data available in the literature suggesting *N*-benzylhexadecanamide effects on CYP3A4 at the time of writing this paper.

3.7 Identification of CYP3A4 inhibitors among Phase I and Phase II metabolites of açaí and maca plant constituents

Phase II metabolites from a cofactor UDPGA that showed moderate CYP3A4 inhibition were only maca extracts. Since the hexyl glucosinolate and macamide in acidic methanol and DCM maca extracts were presumed to have stayed intact, then only glucuronides identified in methanol maca extracts would be considered. In this extract, an identified glucuronide was only a methylfurfural glucuronide from a compound 5-hydroxymethylfurfural. There is no extensive literature on this glucuronide but it is possible that it may be responsible for the observed CYP3A4 inhibition.

In the case where both UDPGA and NADPH cofactors were used, only methanol extracts of açaí and maca displayed moderate CYP3A4 inhibition. This pointed at the type of metabolites that have undergone both Phase I reactions and Phase II metabolism. Such metabolites identified in methanol açaí extract were cyanidin glucuronide and luteolin-7-glucuronide. While both cyanidin and luteolin have been reported for CYP3A4 inhibition [210, 226], there is no data suggesting that any of these retain that activity after glucuronidation and due to their parent compounds being non-absorbable, they were formed only in the sample from PAMPA donor site. Therefore, they could not be responsible for the CYP3A4 inhibition observed in this study. No such metabolite was identified in methanol maca extract due to the lack of literature on the compounds that were identified as passively diffused in this extract.

3.8 Potential of açaí- or maca-anticancer drug interactions

Açaí and maca products, possessing constituents with antioxidant, chemopreventive, cytotoxic and anti-inflammatory activities are not only considered for cancer prevention but also discussed as potential botanical dietary supplements for patients undergoing chemotherapy [227-231]. This study demonstrates the potential of açaí and maca plant extracts to inhibit a major metabolic enzyme CYP3A4 responsible for metabolism and excretion of more than 70% medicines in the market [232], including chemotherapeutic agents [12]. This work also identifies some single constituents notably catechol, *N*-benzylhexadecanamide and gallic acid which displayed a significant CYP3A4 inhibition potential. This work does not just report an *in vitro* CYP3A4 inhibition but for the data to be more clinically relevant, the study also estimates the intracellular passive absorption potential of each identified constituent. Passive absorption is considered a major absorption mechanism for conventional medicines [112]. Even though gallic acid could not be passively diffused in this study, this does not exclude its absorption by transporter-mediated mechanisms as reported [233]. Again, the possibility of passive diffusion at excessively high concentrations and longer times (~1 h.) of gallic acid exposure have been reported [233, 234]. A passively absorbed compound from acidic methanol maca extract, hexyl glucosinolate, has also been identified as a potential CYP3A4 inhibitor in this study.

The study further estimated the IC_{50} values per each extract for CYP3A4 inhibition. The estimated IC_{50} values were 0. 0248 and 0.0688 µg/µl for acidic methanol and methanol açaí extracts, respectively. The estimated IC_{50} values for acidic methanol, methanol and DCM maca extracts were 0.0431, 0.0873 and 0.0632 µg/µl, respectively.

The current research also identifies metabolites from açaí and maca constituent with potential CYP3A4 inhibition. The Phase II metabolites methylfurfural glucuronide, cyanidin glucuronide and luteolin-7-glucuronide have also been identified in extracts that displayed significant CYP3A4 inhibition. Among these, methylfurfural glucuronide was identified in the passively absorbed methanol maca extract. These metabolites may be of concern since the localization of UGTs in the epithelial cells of intestines [235] suggests that the potential toxic glucuronides formed prior to reaching the liver will therefore possibly exert their inhibiting effects on liver CYP3A4 enzymes. Therefore, the CYP3A4 inhibitory glucuronides from açaí and maca extracts formed via UGTs in the endoplasmic reticulum (ER) of the liver may also have ability to show these effects.

Furthermore, while in most cases glucuronidation results in bioinactivation due to increased polarity and weight that favor excretion, there are vast cases of bioactivation and biointoxication [236-238]. Increased weight is generally considered to make glucuronides more susceptible to P-glycoproten (P-gp) exporters in the canalicular domain of hepatocytes and in the luminal site of enterocytes [239, 240]. However, it is known that not all glucuronides become P-gp substrates as this may involve many factors ranging from structural polarity to required configuration for binding P-gp protein apart from size [240, 241]. It is also known that glucuronides are generally reversible due to hydrolysis by β-glucuronidases located in the intestinal tract liberating the original compound that gets reabsorbed leading to enterohepatic circulation of those compounds secreted in bile [Regan, Sophie L.], a feature reported for açaí [242]. This enterohepatic circulation could therefore expose a patient to a toxic botanical dietary supplement constituent for longer periods. This therefore suggests that the CYP3A4 inhibitory glucuronides formed from açaí and maca plant constituents may be as critical original constituents with CYP3A4 inhibitory effects in botanical-drug interactions in chemotherapy.

Further supporting the potential for botanical-anticancer drug interactions, cyanidin, the prominent metabolite of açaí anthocyanins cyanidin-3-O-glucoside, cyanidin-3-O-rutinoside and cyanidin-3-O-sambubioside identified in this work and other studies [58, 179], has been been documented for CYP3A4 inhibition as well as pelargonidin from pelargonidin-3-glucoside [210]. These anthocyanin metabolites, having been reported with significant levels in human plasma as opposed to their corresponding anthocyanins [154, 212], have not only been reported for metabolic interaction but also mechanistic interaction with anticancer agents [243, 244].

The mechanistic interaction for anthocyanin metabolites has been mentioned to be from their advantageous chemopreventive feature of protecting cells against oxidative stress. Aichinger and co-workers [245] proposed a different view that these may also protect cancer cells from cytotoxic anticancer drugs posing a critical botanical-drug interaction. This was of course reported for anthocyanin metabolites whereby they suppressed deoxyribonucleic acid (DNA)-damaging effects of camptothecin and doxorubicin in HT29 colon carcinoma cells [243] posing a risk of treatment failure. Apart from this antagonistic interaction, they have also been reported for synergism with erlortinib by inhibiting the epidermal growth factor receptor (EGFR) [244] as erlotinb does in treatment of pancreatic cancer and non-small cell lung cancer [246] hence increasing the risk of erlotinib toxicity.

3.9 Conclusions

Based on considerable possibilities of concomitant use of açaí and maca botanical dietary supplements with anticancer medicines, this study reports for the first time, the potential metabolic interaction in concomitant use of açaí and maca botanical dietary supplements with anticancer drugs. In this work, botanical constituents in açaí and maca plant extracts with potential for passive absorption were identified. These included five non-anthocyanin polyphenols from acidic methanol açaí extract and one phenolic and two polyphenols in methanol açaí extract. In acidic methanol maca extract, only one glucosinolate with potential for passive absorption was identified, three phenolics and 1 alkaloid in methanol maca extract and one macamide in DCM maca extract.

The initial screening of açaí and maca extracts for CYP3A4 inhibitory effects and followed by IC$_{50}$ studies suggest that all the extracts tested in this study (acidic methanol açaí, methanol açaí, acidic methanol maca, methanol maca and DCM maca extracts) can be categorized as moderate CYP3A4 inhibitors based on the tested concentrations from clinical doses of commercial açaí and maca botanical dietary supplements. Identified passively bioavailable açaí constituent with potential for CYP3A4 inhibition is catechol. This was confirmed with a catechol standard. Another passively bioavailable açaí constituent estimated to be responsible for the observed CYP3A4 inhibition but not confirmed due to unavailability of a standard compound is protocatechuic acid methyl ester. Without a standard compound, the assignment was based on the literature. For maca plant extracts, *N*-benzylhexadecanamide was identified as the CYP3A4 inhibitor confirmed with its standard. Based on the literature, hexyl glucosinolate and 5-hydroxymethylfurfural were also estimated to have CYP3A4 inhibitory activities.

Phase I and Phase II metabolism studies revealed eleven confirmed known metabolites in açaí and eight in maca plant extracts. After CYP3A4 inhibition was observed from screening of açaí and maca metabolites, a literature search was done but none of the identified metabolites had been previously reported with CYP3A4 inhibition. However, based on the individual sample of extract metabolites that was being screened at a time, the two Phase II metabolites in açaí plant extract (cyanidin glucuronide and luteolin-7-glucuronide) and one Phase II metabolite from maca plant extract (methylfurfural glucuronide) may be responsible for the observed CYP3A4 inhibition. The structural elucidation of the unknown metabolites led to twenty-one chemical structures being predicted for the detected putative metabolites of açaí constituents. The structural assignment was also done for the three detected putative metabolites from maca plant extract.

Based on the identified passively absorbable açaí and maca constituents that in turn displayed CYP3A4 inhibition, this research suggests the potential botanical-drug interactions in people taking açaí and maca botanical supplements together with their prescribed anticancer medicines that are metabolized by CYP3A4 *in vivo*. The type of interaction predicted by this study is the CYP3A4 inhibition by the constituents of açaí and maca botanical supplements which would lead to decreased metabolism of the anticancer agent and its increase in concentration in the systemic

circulation. A case with anticancer agents that have narrow therapeutic range would therefore put a patient at an elevated risk of toxicity by a chemotherapeutic agent or a group of chemotherapeutic agents being used at a time. The high concentration in the systemic circulation and decreased clearance of an anticancer drug implies multi-organ exposure to a cytotoxic agent which may be fatal to the patient's health.

Mainly, this research establishes an LC-MS-based strategy for better investigation of botanical-drug interactions in the preclinical studies that is intended to avoid the discrepancy between the *in vitro* and *in vivo* botanical-drug interaction data. Crucial factors included in this work to mimic closely the clinical situation were; establishing concentration ranges that match the dose of the commercial botanical extracts and establishment of the intestinal barrier model (PAMPA) to eliminate the non-absorbable constituents and screen only those with potential to reach the liver *in vivo*. The data found in this study therefore, is expected to correlate well with the botanical-drug interaction data that could be obtained from the clinical trials. It is proposed in this study that, after the method validation by the *in vivo* models, this LC-MS-based strategy to study botanical-drug interactions by CYP3A4 inhibition, may be a better route to avoid the discrepancy and unnecessary clinical trials in the cases where the absorbable constituents of the botanical supplement do not exert CYP3A4 inhibition.

References

[1] World Health Organization. (**2017**) Media centre: Cancer Fact Sheet. World Health Organization

[2] Centers for Disease Control and Prevention. (**2016**) Cancer Prevention and Control: Statistics for different kinds of cancer. Centers for Disease Contrl and Prevention.

[3] Miller KD, Siegel RL, Lin CC, Mariotto AB, Kramer JL, Rowland JH, Stein KD, Alteri R and Jemal A. (**2016**) Cancer treatment and survivorship statistics, 2016. *CA: A Cancer Journal for Clinicians*, **66**, 271-289.

[4] Siegel RL, Miller KD and Jemal A. (**2017**) Cancer statistics, 2017. *CA: A Cancer Journal for Clinicians*, **67**, 7-30.

[5] National Institutes of Health. (**2017**) Types of cancer treatment. National Cancer Institute at the National Institutes of Health.

[6] Akhdar H, Legendre C, Aninat C and More F. (**2012**) Anticancer drug metabolism: chemotherapy resistance and new therapeutic approaches. In *Topics on Drug Metabolism*, InTech.

[7] Tepler I, Elias L, Smith JW, 2nd, Hussein M, Rosen G, Chang AY, Moore JO, Gordon MS, Kuca B, Beach KJ, Loewy JW, Garnick MB and Kaye JA. (**1996**) A randomized placebo-controlled trial of recombinant human interleukin- 11 in cancer patients with severe thrombocytopenia due to chemotherapy. *Blood*, **87**, 3607.

[8] Verstappen CCP, Heimans JJ, Hoekman K and Postma TJ. (**2003**) Neurotoxic complications of chemotherapy in patients with cancer. *Drugs*, **63**, 1549-1563.

[9] Sun CC, Bodurka DC, Weaver CB, Rasu R, Wolf JK, Bevers MW, Smith JA, Wharton JT and Rubenstein EB. (**2005**) Rankings and symptom assessments of side effects from chemotherapy: insights from experienced patients with ovarian cancer. *Supportive Care in Cancer*, **13**, 219-227.

[10] Bahirwani R and Rajender Reddy K. (**2014**) Drug-induced liver injury due to cancer chemotherapeutic agents. *Seminars in Liver Disease*, **34**, 162-171.

[11] Cairo MS. (**2000**) Dose reductions and delays: limitations of myelosuppressive chemotherapy. *Oncology*, **14**, 21-31.

[12]   Scripture CD and Figg WD. (**2006**) Drug interactions in cancer therapy. *Natural Reviews Cancer*, **6**, 546-558.

[13]   Dahal UP, Joswig-Jones C and Jones JP. (**2011**) Comparative study of the affinity and metabolism of type I and type II binding quinoline carboxamide analogues by cytochrome P450 3A4. *Journal of Medicinal Chemistry*, **55**, 280-290.

[14]   Guengerich FP. (**2007**) Mechanisms of cytochrome P450 substrate oxidation: MiniReview. *Journal of Biochemical and Molecular Toxicology*, **21**, 163-168.

[15]   Hartiala K. (**1973**) Metabolism of hormones, drugs and other substances by the gut. *Physiological Reviews*, **53**, 496-534.

[16]   Peng Y-S, Liu B, Wang R-F, Zhao Q-T, Xu W and Yang X-W. (**2015**) Hepatic metabolism: a key component of herbal drugs research. *Journal of Asian Natural Products Research*, **17**, 89-106.

[17]   Guillemette C. (**2003**) Pharmacogenomics of human UDP-glucuronosyltransferase enzymes. *The Pharmacogenomics Journal*, **3**, 136-158.

[18]   Molassiotis A, Fernadez-Ortega P, Pud D, Ozden G, Scott JA, Panteli V, Margulies A, Browall M, Magri M and Selvekerova S. (**2005**) Use of complementary and alternative medicine in cancer patients: a European survey. *Annals of Oncology*, **16**, 655-663.

[19]   Tascilar M, de Jong FA, Verweij J and Mathijssen RH. (**2006**) Complementary and alternative medicine during cancer treatment: beyond innocence. *The Oncologist*, **11**, 732-741.

[20]   National Center for Complementary and Integrative Health. (**2016**) Complementary, alternative, or integrative health: What's in a name? National Institutes of Health.

[21]   Alkhateeb FM, Doucette WR and Ganther-Urmie JM. (**2006**) Influences on consumer spending for herbal products. *Research in Social and Administrative Pharmacy*, **2**, 254-265.

[22]   Kumar NB, Allen K and Bell H. (**2005**) Perioperative herbal supplement use in cancer patients: potential implications and recommendations for presurgical screening. *Cancer control: journal of the Moffitt Cancer Center*, **12**, 149-157.

[23] Meijerman I, Beijnen JH and Schellens JH. (**2006**) Herb-drug interactions in oncology: focus on mechanisms of induction. *The Oncologist*, **11**, 742-752.

[24] Flexner C and Piscitelli CS. (**2000**) Managing Drug-Drug Interactions in HIV Disease. Medscape.

[25] Barnes PM, Bloom B and Nahin RL. (**2008**) Complementary and alternative medicine use among adults and children: United States, 2007. US Department of Health and Human Services, Centers for Disease Control and Prevention, National Center for Health Statistics Hyattsville, MD.

[26] Kennedy J, Wang C-C and Wu C-H. (**2008**) Patient disclosure about herb and supplement use among adults in the US. *Evidence-Based Complementary and Alternative Medicine*, **5**, 451-456.

[27] Clarke TC, Black LI, Stussman BJ, Barnes PM and Nahin RL. (**2015**) Trends in the use of complementary health approaches among adults: United States, 2002–2012. *National Health Statistics Reports*, **79**, 1-16.

[28] Qato DM, Wilder J, Schumm LP, Gillet V and Alexander GC. (**2016**) Changes in prescription and over-the-counter medication and dietary supplement use among older adults in the United States, 2005 vs 2011. *JAMA Internal Medicine*, **176**, 473-482.

[29] Velicer CM and Ulrich CM. (**2008**) Vitamin and mineral supplement use among US adults after cancer diagnosis: a systematic review. *Journal of Clinical Oncology*, **26**, 665-673.

[30] Patterson RE, Neuhouser ML, Hedderson MM, Schwartz SM, Standish LJ, Bowen DJ and Marshall LM. (**2002**) Types of alternative medicine used by patients with breast, colon, or prostate cancer: predictors, motives, and costs. *The Journal of Alternative and Complementary Medicine*, **8**, 477-485.

[31] Molassiotis A, Fernandez-Ortega P, Pud D, Ozden G, Platin N, Hummerston S, Scott JA, Panteli V, Gudmundsdottir G and Selvekerova S. (**2005**) Complementary and alternative medicine use in colorectal cancer patients in seven European countries. *Complementary Therapies in Medicine*, **13**, 251-257.

[32] Tough SC, Johnston DW, Verhoef MJ, Arthur K and Bryant H. (**2002**) Complementary and alternative medicine use among colorectal cancer patients in Alberta, Canada. *Alternative Therapies in Health and Medicine*, **8**, 54.

[33] Willison KD, Williams P and Andrews GJ. (**2007**) Enhancing chronic disease management: a review of key issues and strategies. *Complementary Therapies in Clinical Practice*, **13**, 232-239.

[34] Saydah SH and Eberhardt MS. (**2006**) Use of complementary and alternative medicine among adults with chronic diseases: United States 2002. *The Journal of Alternative and Complementary Medicine*, **12**, 805-812.

[35] Centers for Disease Control and Prevention. (**2010**) National Center for Health Statistics: National health interview survey. Centers for Disease Control and Prevention.

[36] TechNavio. (**2015**) Global dietary supplements market 2015-2019. *Market Research Reports® Inc*, 1-84.

[37] Cohen MH. (**2003**) Complementary and integrative medical therapies, the FDA, and the NIH: definitions and regulation. *Dermatologic Therapy*, **16**, 77-84.

[38] Gardiner P, Phillips R and Shaughnessy AF. (**2008**) Herbal and dietary supplement–drug interactions in patients with chronic illnesses. *American Family Physician*, **77**, 73-78.

[39] United States Food and Drug Administration. (**2008**) Current good manufacturing practice in manufacturing, packaging, labeling, or holding operations for dietary supplements. Federal Register June 25, 2007:34752-958. Quality Circle Institute, Inc.

[40] Morris KT, Johnson N, Homer L and Walts D. (**2000**) A comparison of complementary therapy use between breast cancer patients and patients with other primary tumor sites. *The American Journal of Surgery*, **179**, 407-411.

[41] Deng G and Cassileth BR. (**2005**) Integrative oncology: complementary therapies for pain, anxiety, and mood disturbance. *CA: A Cancer Journal for Clinicians*, **55**, 109-116.

[42] Kosty MP. (**2004**) PC-SPES: hope or hype?, American Society of Clinical Oncology.

[43] Straus SE. (**2002**) Herbal medicines—what's in the bottle? *New England Journal of Medicine*, **347**, 1997-1998.

[44]   Kappauf H, Leykauf-Ammon D, Bruntsch U, Horneber M, Kaiser G, Büschel G and Gallmeier WM. (**2000**) Use of and attitudes held towards unconventional medicine by patients in a department of internal medicine/oncology and haematology. *Supportive Care in Cancer*, **8**, 314-322.

[45]   Sewitch MJ and Rajput Y. (**2010**) A literature review of complementary and alternative medicine use by colorectal cancer patients. *Complementary Therapies in Clinical Practice*, **16**, 52-56.

[46]   Helyer LK, Chin S, Chui BK, Fitzgerald B, Verma S, Rakovitch E, Dranitsaris G and Clemons M. (**2006**) The use of complementary and alternative medicines among patients with locally advanced breast cancer--a descriptive study. *BMC Cancer*, **6**, 39.

[47]   Lafferty WE, Tyree PT, Devlin SM, Andersen MR and Diehr PK. (**2008**) CAM provider use and expenditures by cancer treatment phase. *The American Journal of Managed Care*, **14**, 326.

[48]   McGahey KE and Weiss GJ. (**2017**) Reviewing concomitant medications for participants in oncology clinical trials. *American Journal of Health-System Pharmacy*, **74**.

[49]   Sawyer MG, Gannoni AF, Toogood IR, Antoniou G and Rice M. (**1994**) The use of alternative therapies by children with cancer. *The Medical Journal of Australia*, **160**, 320-322.

[50]   Lippert MC, McClain R, Boyd JC and Theodorescu D. (**1999**) Alternative medicine use in patients with localized prostate carcinoma treated with curative intent. *Cancer*, **86**, 2642-2648.

[51]   Roe AL, Paine MF, Gurley BJ, Brouwer KR, Jordan S and Griffiths JC. (**2016**) Assessing natural product–drug interactions: an end-to-end safety framework. *Regulatory Toxicology and Pharmacology*, **76**, 1-6.

[52]   Davis EL, Oh B, Butow PN, Mullan BA and Clarke S. (**2012**) Cancer patient disclosure and patient-doctor communication of complementary and alternative medicine use: a systematic review. *The Oncologist*, **17**, 1475-1481.

[53] Yamaguchi KKdL, Pereira LFR, Lamarão CV, Lima ES and da Veiga-Junior VF. (**2015**) Amazon açaí: Chemistry and biological activities: A review. *Food Chemistry*, **179**, 137-151.

[54] Lee S-EL, Hoi-Seon; Lee, Young-Haeng; Park, Byoung-Soo; Choi, Won-Sik; . (**1998**) Antioxidative activities of methanol extracts of tropical and oriental medicinal plants. *Agricultural Chemistry and Biotechnology*, **41**, 556-559.

[55] Muñiz-Miret N, Vamos R, Hiraoka M, Montagnini F and Mendelsohn RO. (**1996**) The economic value of managing the açaí palm (*Euterpe oleracea* Mart.) in the floodplains of the Amazon estuary, Pará, Brazil. *Forest Ecology and Management*, **87**, 163-173.

[56] Rodrigues RB, Lichtenthäler R, Zimmermann BF, Papagiannopoulos M, Fabricius H, Marx F, Maia JG and Almeida O. (**2006**) Total oxidant scavenging capacity of *Euterpe oleracea* Mart. (açaí) seeds and identification of their polyphenolic compounds. *Journal of Agricultural and Food Chemistry*, **54**, 4162-4167.

[57] Trevisan ACD, Fantini AC, Schmitt-Filho AL and Farley J. (**2015**) Market for Amazonian açaí (*Euterpe oleraceae*) stimulates pulp production from Atlantic Forest Juçara Berries (*Euterpe edulis*). *Agroecology and Sustainable Food Systems*, **39**, 762-781.

[58] Del Pozo-Insfran D, Brenes CH and Talcott ST. (**2004**) Phytochemical composition and pigment stability of Açaí (*Euterpe oleracea* Mart.). *Journal of Agricultural and Food Chemistry*, **52**, 1539-1545.

[59] Del Pozo-Insfran D, Percival SS and Talcott ST. (**2006**) Açai (*Euterpe oleracea* Mart.) polyphenolics in their glycoside and aglycone forms induce apoptosis of HL-60 leukemia cells. *Journal of Agricultural and Food Chemistry*, **54**, 1222-1229.

[60] Mulabagal V, Keller WJ and Calderon AI. (**2012**) Quantitative analysis of anthocyanins in *Euterpe oleracea* (açaí) dietary supplement raw materials and capsules by Q-TOF liquid chromatography/mass spectrometry. *Pharmaceutical Biology*, **50**, 1289-1296.

[61] Gouvêa ACMS, Araujo MCPd, Schulz DF, Pacheco S, Godoy RLdO and Cabral LMC. (**2012**) Anthocyanins standards (cyanidin-3-O-glucoside and cyanidin-3-O-rutinoside) isolation from freeze-dried açaí (*Euterpe oleraceae* Mart.) by HPLC. *Food Science and Technology*, **32**, 43-46.

[62] Rocha A, Carvalho L, Sousa M, Madeira SF, Sousa P, Tano T, Schini-Kerth V, Resende A and De Moura RS. (**2007**) Endothelium-dependent vasodilator effect of *Euterpe oleracea* Mart. (Açaí) extracts in mesenteric vascular bed of the rat. *Vascular Pharmacology*, **46**, 97-104.

[63] Schauss AG, Wu X, Prior RL, Ou B, Huang D, Owens J, Agarwal A, Jensen GS, Hart AN and Shanbrom E. (**2006**) Antioxidant capacity and other bioactivities of the freeze-dried Amazonian palm berry, *Euterpe oleraceae* Mart. (açaí). *Journal of Agricultural and Food Chemistry*, **54**, 8604-8610.

[64] Gordon A, Cruz APG, Cabral LMC, de Freitas SC, Taxi CMAD, Donangelo CM, de Andrade Mattietto R, Friedrich M, da Matta VM and Marx F. (**2012**) Chemical characterization and evaluation of antioxidant properties of Açaí fruits (*Euterpe oleraceae* Mart.) during ripening. *Food Chemistry*, **133**, 256-263.

[65] Hassimotto NMA, Genovese MI and Lajolo FM. (**2005**) Antioxidant activity of dietary fruits, vegetables, and commercial frozen fruit pulps. *J Agric Food Chem*, **53**, 2928-2935.

[66] Pacheco-Palencia LA, Duncan CE and Talcott ST. (**2009**) Phytochemical composition and thermal stability of two commercial açai species, *Euterpe oleracea* and *Euterpe precatoria*. *Food Chemistry*, **115**, 1199-1205.

[67] Chin YW, Chai HB, Keller WJ and Kinghorn AD. (**2008**) Lignans and other constituents of the fruits of *Euterpe oleracea* (Açai) with antioxidant and cytoprotective activities. *Journal of Agricultural and Food Chemistry*, **56**, 7759-7764.

[68] Kang J, Li Z, Wu T, Jensen GS, Schauss AG and Wu X. (**2010**) Anti-oxidant capacities of flavonoid compounds isolated from açai pulp (*Euterpe oleracea* Mart.). *Food Chemistry*, **122**, 610-617.

[69] Hoesel B and Schmid JA. (**2013**) The complexity of NF-κB signaling in inflammation and cancer. *Molecular Cancer*, **12**, 86.

[70] Hu J, Zhao J, Khan SI, Liu Q, Liu Y, Ali Z, Li XC, Zhang SH, Cai X, Huang HY, Wang W and Khan IA. (**2014**) Antioxidant neolignan and phenolic glucosides from the fruit of *Euterpe oleracea*. *Fitoterapia*, **99**, 178-183.

[71]   Fragoso MF, Romualdo GR, Ribeiro DA and Barbisan LF. (**2013**) Açai (*Euterpe oleracea* Mart.) feeding attenuates dimethylhydrazine-induced rat colon carcinogenesis. *Food and Chemical Toxicology*, **58**, 68-76.

[72]   Ribeiro JC, Antunes LMG, Aissa AF, Darin JDaC, De Rosso VV, Mercadante AZ and Bianchi MdLP. (**2010**) Evaluation of the genotoxic and antigenotoxic effects after acute and subacute treatments with açai pulp (*Euterpe oleracea* Mart.) on mice using the erythrocytes micronucleus test and the comet assay. *Mutation Research/Genetic Toxicology and Environmental Mutagenesis*, **695**, 22-28.

[73]   Spada PD, Dani C, Bortolini GV, Funchal C, Henriques JA and Salvador M. (**2009**) Frozen fruit pulp of *Euterpe oleraceae* Mart. (Açai) prevents hydrogen peroxide-induced damage in the cerebral cortex, cerebellum, and hippocampus of rats. *Journal of Medicinal Food*, **12**, 1084-1088.

[74]   Sowers JL, Johnson KM, Conrad C, Patterson JT and Sowers LC. (**2014**) The role of inflammation in brain cancer. In *Inflammation and Cancer*, B. B. Aggarwal, B. Sung and S. C. Gupta (Eds.), Springer Basel, Basel, 75-105.

[75]   Hogan S, Chung H, Zhang L, Li J, Lee Y, Dai Y and Zhou K. (**2010**) Antiproliferative and antioxidant properties of anthocyanin-rich extract from açai. *Food Chemistry*, **118**, 208-214.

[76]   Silva DF, Vidal FC, Santos D, Costa MC, Morgado-Diaz JA, do Desterro Soares Brandao Nascimento M and de Moura RS. (**2014**) Cytotoxic effects of *Euterpe oleracea* Mart. in malignant cell lines. *BMC Complementary and Alternative Medicine*, **14**, 175.

[77]   Sadowska-Krępa E, Kłapcińska B, Podgórski T, Szade B, Tyl K and Hadzik A. (**2015**) Effects of supplementation with açai (*Euterpe oleracea* Mart.) berry-based juice blend on the blood antioxidant defence capacity and lipid profile in junior hurdlers. A pilot study. *Biology of Sport*, **32**, 161.

[78]   Jensen GS, Wu X, Patterson KM, Barnes J, Carter SG, Scherwitz L, Beaman R, Endres JR and Schauss AG. (**2008**) *In vitro* and *in vivo* antioxidant and anti-inflammatory capacities of an antioxidant-rich fruit and berry juice blend. Results of a pilot and randomized,

double-blinded, placebo-controlled, crossover study. *Journal of Agricultural and Food Chemistry*, **56**, 8326-8333.

[79] Mertens-Talcott SU, Rios J, Jilma-Stohlawetz P, Pacheco-Palencia LA, Meibohm B, Talcott ST and Derendorf H. (**2008**) Pharmacokinetics of anthocyanins and antioxidant effects after the consumption of anthocyanin-rich açai juice and pulp (*Euterpe oleracea* Mart.) in human healthy volunteers. *Journal of Agricultural and Food Chemistry*, **56**, 7796-7802.

[80] Quiroz C, Aliaga R, Hermann M and Hellers J. (**1997**) Maca (*Lepidium meyenii* Walp.). Andean roots and tubers: ahipa, arracacha, maca and yacon.: Promoting the conservation and use of underutilized neglected crops 21. *International Plant Genetic Resources InstituteRome,* 173-179.

[81] Sandoval M, Okuhama NN, Angeles FM, Melchor VV, Condezo LA, Lao J and Miller MJ. (**2002**) Antioxidant activity of the cruciferous vegetable Maca (*Lepidium meyenii*). *Food Chemistry*, **79**, 207-213.

[82] Muhammad I, Zhao J and Khan IA. (**2005**) Maca (*Lepidium meyenii*). *Encyclopedia of Dietary Supplements*, 435-443.

[83] Ochoa C. (**2001**) Maca (*Lepidium meyenii* Walp.; Brassicaceae): a nutritious root crop of the Central Andes. *Economic Botany*, **55**, 344-345.

[84] Hermann M. (**1997**) Andean roots and tubers: ahipa, arracacha, maca and yacon, International Potato Center.

[85] Dini A, Migliuolo G, Rastrelli L, Saturnino P and Schettino O. (**1994**) Chemical composition of *Lepidium meyenii*. *Food Chemistry*, **49**, 347-349.

[86] Gonzales GF, Vasquez V, Rodriguez D, Maldonado C, Mormontoy J, Portella J, Pajuelo M, Villegas L, Gasco M and Mathur P. (**2007**) Effect of two different extracts of red maca in male rats with testosterone- induced prostatic hyperplasia. *Asian Journal of Andrology*, **9**, 245-251.

[87] Esparza E, Hadzich A, Kofer W, Mithöfer A and Cosio EG. (**2015**) Bioactive maca (*Lepidium meyenii*) alkamides are a result of traditional Andean postharvest drying practices. *Phytochemistry*, **116**, 138-148.

[88]   Valerio LG and Gonzales GF. (**2005**) Toxicological aspects of the South American herbs cat's claw (*Uncaria tomentosa*) and maca (*Lepidium meyenii*). *Toxicological Reviews*, **24**, 11-35.

[89]   Zheng BL, He K, Kim CH, Rogers L, Shao Y, Huang ZY, Lu Y, Yan SJ, Qien LC and Zheng QY. (**2000**) Effect of a lipidic extract from *Lepidium meyenii* on sexual behavior in mice and rats. *Urology*, **55**, 598-602.

[90]   Dini I, Tenore GC and Dini A. (**2002**) Glucosinolates from maca (*Lepidium meyenii*). *Biochemical Systematics and Ecology*, **30**, 1087-1090.

[91]   Cui B, Zheng BL, He K and Zheng QY. (**2003**) Imidazole Alkaloids from *Lepidium meyenii*. *Journal of Natural Products*, **66**, 1101-1103.

[92]   McCollom MM, Villinski JR, McPhail KL, Craker LE and Gafner S. (**2005**) Analysis of macamides in samples of Maca (*Lepidium meyenii*) by HPLC- UV- MS/MS. *Phytochemical Analysis*, **16**, 463-469.

[93]   Ganzera M, Zhao J, Muhammad I and Khan IA. (**2002**) Chemical profiling and standardization of *Lepidium meyenii* (Maca) by reversed phase high performance liquid chromatography. *Chemical and Pharmaceutical Bulletin*, **50**, 988-991.

[94]   Lee K-J, Dabrowski K, Sandoval M and Miller MJ. (**2005**) Activity-guided fractionation of phytochemicals of maca meal, their antioxidant activities and effects on growth, feed utilization, and survival in rainbow trout (Oncorhynchus mykiss) juveniles. *Aquaculture*, **244**, 293-301.

[95]   Zha S, Zhao Q, Chen J, Wang L, Zhang G, Zhang H and Zhao B. (**2014**) Extraction, purification and antioxidant activities of the polysaccharides from maca (*Lepidium meyenii*). *Carbohydrate Polymers*, **111**, 584-587.

[96]   Cui B, Zheng BL, He K and Zheng QY. (**2005**) Imidazole alkaloids from *Lepidium meyenii* and methods of usage. Google Patents.

[97]   Fahey JW, Zalcmann AT and Talalay P. (**2001**) The chemical diversity and distribution of glucosinolates and isothiocyanates among plants. *Phytochemistry*, **56**, 5-51.

[98] Smith WA and Gupta RC. (**1999**) Determining efficacy of cancer chemopreventive agents using a cell-free system concomitant with DNA adduction. *Mutation Research/Fundamental and Molecular Mechanisms of Mutagenesis*, **425**, 143-152.

[99] Verschoyle RD, Greaves P, Cai H, Borkhardt A, Broggini M, D'Incalci M, Riccio E, Doppalapudi R, Kapetanovic IM and Steward WP. (**2006**) Preliminary safety evaluation of the putative cancer chemopreventive agent tricin, a naturally occurring flavone. *Cancer Chemotherapy and Pharmacology*, **57**, 1-6.

[100] Bai N, He K, Roller M, Lai CS, Bai L and Pan MH. (**2015**) Flavonolignans and other constituents from *Lepidium meyenii* with activities in anti-inflammation and human cancer cell lines. *Journal of Agricultural and Food Chemistry*, **63**, 2458-2463.

[101] Gomes M, Teixeira AL, Coelho A, Araújo A and Medeiros R. (**2014**) The role of inflammation in lung cancer. In *Inflammation and Cancer*, B. B. Aggarwal, B. Sung and S. C. Gupta (Eds.), Springer Basel, Basel, 1-23.

[102] Nachshon-Kedmi M, Yannai S and Fares FA. (**2004**) Induction of apoptosis in human prostate cancer cell line, PC3, by 3, 3′-diindolylmethane through the mitochondrial pathway. *British Journal of Cancer*, **91**, 1358-1363.

[103] Goey AK, Mooiman KD, Beijnen JH, Schellens JH and Meijerman I. (**2013**) Relevance of *in vitro* and clinical data for predicting CYP3A4-mediated herb–drug interactions in cancer patients. *Cancer Treatment Reviews*, **39**, 773-783.

[104] Delgoda R and Westlake AC. (**2004**) Herbal interactions involving cytochrome P450 enzymes. *Toxicological Reviews*, **23**, 239-249.

[105] Sprouse AA and van Breemen RB. (**2016**) Pharmacokinetic interactions between drugs and botanical dietary supplements. *Drug Metabolism and Disposition*, **44**, 162-171.

[106] Smith P, Bullock JM, Booker BM, Haas CE, Berenson CS and Jusko WJ. (**2004**) The influence of St. John's wort on the pharmacokinetics and protein binding of imatinib mesylate. *Pharmacotherapy: The Journal of Human Pharmacology and Drug Therapy*, **24**, 1508-1514.

[107]   Spanakis M, Vizirianakis IS, Mironidou-Tzouveleki M and Niopas I. (**2010**) *In vitro* inhibition of CYP3A4 and CYP2D6 activity by the horse chestnut constituents' aescin and aesculetin. *Frontiers in Pharmacology*

[108]   Gorman GS, Coward L, Darby A and Rasberry B. (**2013**) Effects of herbal supplements on the bioactivation of chemotherapeutic agents. *Journal of Pharmacy and Pharmacology*, **65**, 1014-1025.

[109]   Sparreboom A, Cox MC, Acharya MR and Figg WD. (**2004**) Herbal remedies in the United States: potential adverse interactions with anticancer agents. *Journal of Clinical Oncology*, **22**, 2489-2503.

[110]   Colalto C. (**2010**) Herbal interactions on absorption of drugs: Mechanisms of action and clinical risk assessment. *Pharmacological Research*, **62**, 207-227.

[111]   Lazarou J, Pomeranz BH and Corey PN. (**1998**) Incidence of adverse drug reactions in hospitalized patients: a meta-analysis of prospective studies. *JAMA*, **279**, 1200-1205.

[112]   Balimane PV, Han Y-H and Chong S. (**2006**) Current industrial practices of assessing permeability and P-glycoprotein interaction. *The AAPS Journal*, **8**, E1-E13.

[113]   Products CfPM. (**1997**) Note for guidance on the investigation of drug interactions. *London: EMEA*.

[114]   Petit C, Bujard A, Skalicka-Woźniak K, Cretton S, Houriet J, Christen P, Carrupt P-A and Wolfender J-L. (**2016**) Prediction of the passive intestinal absorption of medicinal plant extract constituents with the Parallel Artificial Membrane Permeability Assay (PAMPA). *Planta Medica*, **82**, 424-431.

[115]   Matsson P, Bergström CA, Nagahara N, Tavelin S, Norinder U and Artursson P. (**2005**) Exploring the role of different drug transport routes in permeability screening. *Journal of Medicinal Chemistry*, **48**, 604-613.

[116]   Korzekwa K, Nagar S, Tucker J, Weiskircher EA, Bhoopathy S and Hidalgo IJ. (**2012**) Models to predict unbound intracellular drug concentrations in the presence of transporters. *Drug Metabolism and Disposition*, dmd. 111.044289.

[117] Yang W, Hou J, Lu Y, Chen PC, Liao SG and Huang Y. (**2015**) [Intestinal absorption kinetics of Polygonum capitatum extract in rats]. *Zhongguo Zhong Yao Za Zhi*, **40**, 4281-4287.

[118] Kirchmair J, Goller AH, Lang D, Kunze J, Testa B, Wilson ID, Glen RC and Schneider G. (**2015**) Predicting drug metabolism: experiment and/or computation? *Natural Reviews Drug Discovery*, **14**, 387-404.

[119] Ando Y. (**2004**) Cytochrome P450 and Anticancer Drugs. In *Handbook of Anticancer Pharmacokinetics and Pharmacodynamics*, W. D. Figg and H. L. McLeod (Eds.), Humana Press, Totowa, NJ, 215-229.

[120] Yamazaki H, Nakajima M, Nakamura M, Asahi S, Shimada N, Gillam EM, Guengerich FP, Shimada T and Yokoi T. (**1999**) Enhancement of cytochrome P-450 3A4 catalytic activities by cytochrome b 5 in bacterial membranes. *Drug Metabolism and Disposition*, **27**, 999-1004.

[121] Williams JA, Hyland R, Jones BC, Smith DA, Hurst S, Goosen TC, Peterkin V, Koup JR and Ball SE. (**2004**) Drug-drug interactions for UDP-glucuronosyltransferase substrates: a pharmacokinetic explanation for typically observed low exposure (AUC_1/AUC) ratios. *Drug Metabolism and Disposition*, **32**, 1201-1208.

[122] Bashir MK, Ismail S, Lam CK, Chua JK and Hussin AH. (**2015**) The *in vitro* and *ex vivo* effect of phyllanthus niruri methanol extract on hepatic UDP-glucuronyltransferase enzyme activity in STZ-induced diabetic sprague dawley rats. *International Journal of Pharmacy and Pharmaceutical Sciences*, **7**, 105-109.

[123] Thelen K and Dressman JB. (**2009**) Cytochrome P450-mediated metabolism in the human gut wall. *J Pharm Pharmacol*, **61**, 541-558.

[124] Shimada T, Yamazaki H, Mimura M, Inui Y and Guengerich FP. (**1994**) Interindividual variations in human liver cytochrome P-450 enzymes involved in the oxidation of drugs, carcinogens and toxic chemicals: studies with liver microsomes of 30 Japanese and 30 Caucasians. *Journal of Pharmacology and Experimental Therapeutics*, **270**, 414-423.

[125] Foti RS, Rock DA, Wienkers LC and Wahlstrom JL. (**2010**) Selection of alternative CYP3A4 probe substrates for clinical drug interaction studies using *in vitro* data and *in vivo* simulation. *Drug Metabolism and Disposition*, dmd. 110.032094.

[126] Abe Y, Sasaki H, Osaki T, Kamiya K, Kawano R, Miki N and Takeuchi S. (**2012**) Rapid and accurate IC50 determination using logarithmic concentration generator. In *Chemical and Biological Microsystems Society*, Okinawa, Japan, 956-959.

[127] Wang Y, Wu S, Chen Z, Zhang H and Zhao W. (**2015**) Inhibitory effects of cytochrome P450 enzymes CYP1A2, CYP2A6, CYP2E1 and CYP3A4 by extracts and alkaloids of *Gelsemium elegans* roots. *Journal of Ethnopharmacology*, **166**, 66-73.

[128] McGinnity DF, Berry AJ, Kenny JR, Grime K and Riley RJ. (**2006**) Evaluation of time-dependent cytochrome P450 inhibition using cultured human hepatocytes. *Drug Metabolism and Disposition*, **34**, 1291-1300.

[129] Patil D, Gautam M, Gairola S, Jadhav S and Patwardhan B. (**2014**) Effect of botanical immunomodulators on human CYP3A4 inhibition: implications for concurrent use as adjuvants in cancer therapy. *Integrative Cancer Therapies*, **13**, 167-175.

[130] Zhang JG, Ho T, Callendrello AL, Clark RJ, Santone EA, Kinsman S, Xiao D, Fox LG, Einolf HJ and Stresser DM. (**2014**) Evaluation of calibration curve–based approaches to predict clinical inducers and noninducers of CYP3A4 with plated human hepatocytes. *Drug Metabolism and Disposition*, **42**, 1379-1391.

[131] Li G, Huang K, Nikolic D and Van Breemen RB. (**2015**) High-throughput cytochrome P450 cocktail inhibition assay for assessing drug-drug and drug-botanical interactions. *Drug Metabolism and Disposition*, dmd. 115.065987.

[132] Yuan R, Madani S, Wei XX, Reynolds K and Huang SM. (**2002**) Evaluation of cytochrome P450 probe substrates commonly used by the pharmaceutical industry to study *in vitro* drug interactions. *Drug Metabolism and Disposition*, **30**, 1311-1319.

[133] Yuan Y, Qiu X, Nikolić D, Chen S-N, Huang K, Li G, Pauli GF and Van Breemen RB. (**2014**) Inhibition of human cytochrome P450 enzymes by hops (*Humulus lupulus*) and hop prenylphenols. *European Journal of Pharmaceutical Sciences*, **53**, 55-61.

[134] Fowler S and Zhang H. (**2008**) In vitro evaluation of reversible and irreversible cytochrome P450 inhibition: current status on methodologies and their utility for predicting drug–drug interactions. *The AAPS Journal*, **10**, 410-424.

[135] Mulabagal V and Calderon AI. (**2012**) Liquid chromatography/mass spectrometry based fingerprinting analysis and mass profiling of *Euterpe oleracea* (açai) dietary supplement raw materials. *Food Chemistry*, **134**, 1156-1164.

[136] Minich DM, Vonk RJ and Verkade HJ. (**1997**) Intestinal absorption of essential fatty acids under physiological and essential fatty acid-deficient conditions. *Journal of Lipid Research*, **38**, 1709-1721.

[137] Ockner RK, Pittman JP and Yager JL. (**1972**) Differences in the intestinal absorption of saturated and unsaturated long chain fatty acids. *Gastroenterology*, **62**, 981-992.

[138] Calder PC. (**2016**) Fatty Acids: Metabolism. In *Encyclopedia of Food and Health*, Academic Press, Oxford, 632-644.

[139] Valentová K, Buckiová D, Křen V, Pěknicová J, Ulrichová J and Šimánek V. (**2006**) The *in vitro* biological activity of Lepidium meyenii extracts. *Cell Biology and Toxicology*, **22**, 91-99.

[140] Corning Incorporated. (**2013**) Corning® Gentest™ PAMPA Plate System Frequently Asked Questions. Corning Incorporated Life Sciences

[141] Wohnsland F and Faller B. (**2001**) High-throughput permeability pH profile and high-throughput alkane/water log P with artificial membranes. *Journal of Medicinal Chemistry*, **44**, 923-930.

[142] Franke H, Galla H-J and Beuckmann CT. (**1999**) An improved low-permeability in vitro-model of the blood–brain barrier: transport studies on retinoids, sucrose, haloperidol, caffeine and mannitol. *Brain Research*, **818**, 65-71.

[143] Bujard A, Sol M, Carrupt P-A and Martel S. (**2014**) Predicting both passive intestinal absorption and the dissociation constant toward albumin using the PAMPA technique. *European Journal of Pharmaceutical Sciences*, **63**, 36-44.

[144] Hu M and Amidon GL. (**1988**) Passive and Carrier-Mediated Intestinal Absorption Components of Captopril. *Journal of Pharmaceutical Sciences*, **77**, 1007-1011.

[145] Sterling HJ, Batchelor JD, Wemmer DE and Williams ER. (**2010**) Effects of buffer loading for electrospray ionization mass spectrometry of a noncovalent protein complex that requires high concentrations of essential salts. *Journal of the American Society for Mass Spectrometry*, **21**, 1045-1049

[146] The Nest Group Inc. (**2015**) Detergent and salt removal from polar compounds. In *International Summit on Current Trends in Mass Spectrometry*, New Orleans, USA, 1-42.

[147] Lu Y-l, He Y-q, Wang M, Zhang L, Yang L, Wang Z-t and Ji G. (**2010**) Characterization of nuciferine metabolism by P450 enzymes and uridine diphosphate glucuronosyltransferases in liver microsomes from humans and animals. *Acta Pharmacologica Sinica*, **31**, 1635-1642.

[148] Liu H, Wu Z, Ma Z and Wu B. (**2014**) Glucuronidation of macelignan by human liver microsomes and expressed UGT enzymes: identification of UGT1A1 and 2B7 as the main contributing enzymes. *Biopharmaceutics and Drug Disposition*, **35**, 513-524.

[149] Ohno S and Nakajin S. (**2009**) Determination of mRNA expression of human UDP-Glucuronosyltransferases and application for localization in various human tissues by real-time reverse transcriptase-polymerase chain reaction. *Drug Metabolism and Disposition*, **37**, 32-40..

[150] Spencer JP, Chowrimootoo G, Choudhury R, Debnam ES, Srai SK and Rice-Evans C. (**1999**) The small intestine can both absorb and glucuronidate luminal flavonoids. *FEBS Letters*, **458**, 224-230.

[151] Liska DJ. (**1998**) The detoxification enzyme systems. *Alternative Medicine Review*, **3**, 187-198

[152] Doherty MM and Pang KS. (**1997**) First-Pass Effect: Significance of the intestine for absorption and metabolism. *Drug and Chemical Toxicology*, **20**, 329-344.

[153] Takano R, Furumoto K, Shiraki K, Takata N, Hayashi Y, Aso Y and Yamashita S. (**2008**) Rate-limiting steps of oral absorption for poorly water-soluble drugs in dogs; prediction from a miniscale dissolution test and a physiologically-based computer simulation. *Pharmaceutical Research*, **25**, 2334-2344.

[154] Kay CD. (**2006**) Aspects of anthocyanin absorption, metabolism and pharmacokinetics in humans. *Nutrition Research Reviews*, **19**, 137-146

[155] Kay CD, Kroon PA and Cassidy A. (**2009**) The bioactivity of dietary anthocyanins is likely to be mediated by their degradation products. *Molecular Nutrition and Food Research*, **53**, S92-S101.

[156] Matthias A, Penman K, Matovic N, Bone K, De Voss J and Lehmann R. (**2005**) Bioavailability of Echinacea constituents: Caco-2 monolayers and pharmacokinetics of the alkylamides and caffeic acid conjugates. *Molecules*, **10**, 1242.

[157] Getahun SM and Chung F-L. (**1999**) Conversion of glucosinolates to isothiocyanates in humans after ingestion of cooked Watercress. *Cancer Epidemiology, Biomarkers and Prevention*, **8**, 447-451.

[158] Agilent Technologies. (**2013**) Powerful software solutions for drug metabolite quantitation and identification. *Bioanalysis*.

[159] Adams SE. (**2010**) Molecular similarity and xenobiotic metabolism. In *Department of Chemistry*, University of Cambridge.

[160] Yousofshahi M, Manteiga S, Wu C, Lee K and Hassoun S. (**2015**) Proximal: A method for prediction of xenobiotic metabolism. *BMC Systems Biology*, **9**, 94.

[161] Hou T, Wang J, Zhang W and Xu X. (**2007**) ADME evaluation in drug discovery. 6. Can oral bioavailability in humans be effectively predicted by simple molecular property-based rules? *Journal of Chemical Information and Modeling*, **47**, 460-463.

[162] Waring MJ. (**2009**) Defining optimum lipophilicity and molecular weight ranges for drug candidates—molecular weight dependent lower logD limits based on permeability. *Bioorganic and Medicinal Chemistry Letters*, **19**, 2844-2851.

[163] Kamiloglu S, Capanoglu E, Grootaert C and Van Camp J. (**2015**) Anthocyanin absorption and metabolism by human intestinal Caco-2 Cells--A Review. *International Journal of Molecular Sciences*, **16**, 21555-21574.

[164] Collarini EJ and Oxender DL. (**1987**) Mechanisms of transport of amino acids across membranes. *Annual Review of Nutrition*, **7**, 75-90.

[165] Germond JE, Philippossian G, Richli U, Bracco I and Arnaud MJ. (**1987**) Rapid and complete urinary elimination of [14C]-5-hydroxymethyl-2-furaldehyde administered orally or intravenously to rats. *Journal of Toxicology and Environmental Health*, **22**, 79-89.

[166] Veronica B. Godfrey L-JC, Robert J. Griffin, Edward H. Lebetkin, Leo T. Burka. (**1999**) Distribution and metabolism of (5-hydroxymethyl)furfural in male F344 rats and B6C3F1 mice after oral administration. *Journal of Toxicology and Environmental Health, Part A*, **57**, 199-210.

[167] Liu L, Guo L, Zhao C, Wu X, Wang R and Liu C. (**2015**) Characterization of the intestinal absorption of seven flavonoids from the flowers of *Trollius chinensis* using the Caco-2 cell monolayer model. *PLoS One*, **10**, e0119263.

[168] Jung CT, Wickett RR, Desai PB and Bronaugh RL. (**2003**) *In vitro* and *in vivo* percutaneous absorption of catechol. *Food and Chemical Toxicology*, **41**, 885-895.

[169] Day AJ, DuPont MS, Ridley S, Rhodes M, Rhodes MJ, Morgan MR and Williamson G. (**1998**) Deglycosylation of flavonoid and isoflavonoid glycosides by human small intestine and liver β- glucosidase activity. *FEBS Letters*, **436**, 71-75.

[170] Walle T, Otake Y, Walle UK and Wilson FA. (**2000**) Quercetin glucosides are completely hydrolyzed in ileostomy patients before absorption. *The Journal of Nutrition*, **130**, 2658-2661.

[171] Kuhnle G, Spencer JP, Schroeter H, Shenoy B, Debnam ES, Srai SKS, Rice-Evans C and Hahn U. (**2000**) Epicatechin and catechin are O-methylated and glucuronidated in the small intestine. *Biochemical and Biophysical Research Communications*, **277**, 507-512.

[172] McMAHON TF and Birnbaum LS. (**1991**) Age-related changes in disposition and metabolism of benzene in male C57BL/6N mice. *Drug Metabolism and Disposition*, **19**, 1052-1057.

[173] Keski-Hynnilä H, Andersin R, Luukkanen L, Taskinen J and Kostiainen R. (**1998**) Analysis of catechol-type glucuronides in urine samples by liquid chromatography–electrospray ionization-tandem mass spectrometry. *Journal of Chromatography A*, **794**, 75-83.

[174]   He G-Y, Cai T, Xu X-Y, Fang D-M and Wu Z-J. (**2016**) Radical ions and dehydro cations in detection of 2, 3′-bisindolylmethanes using electrospray mass spectrometry. *International Journal of Mass Spectrometry*, **410**, 63-67.

[175]   Xu G, Huang T, Miao S, Zhang J and McClure TD. (**2008**) Study of free radical fragment ions generated from ESI-CID-MS-MS using LTQ and LTQ Orbitrap mass spectrometers. *LC GC North America*, **45**, 64.

[176]   Pan Y, Zhang J, Li H, Wang YZ and Li WY. (**2016**) Characteristic fingerprinting based on macamides for discrimination of maca (*Lepidium meyenii*) by LC/MS/MS and multivariate statistical analysis. *Journal of the Science of Food and Agriculture*, **96**, 4475-4483.

[177]   Yang C-J, Wang Z-B, Mi Y-Y, Gao M-J, Lv J-N, Meng Y-H, Yang B-Y and Kuang H-X. (**2016**) UHPLC-MS/MS determination, pharmacokinetic, and bioavailability study of taxifolin in rat plasma after oral administration of its nanodispersion. *Molecules*, **21**, 494.

[178]   Rodríguez V, Sweet C, Timmermann B and Sólyom A. (**2004**) Development of an LC/MS/MS method to separate and analyze curcuminoids, their metabolites and degradation products. In *Poster presented by Aniko M. Sólyom at the 118th AOAC International Annual Meeting and Exposition*.

[179]   Fang J. (**2014**) Bioavailability of anthocyanins. *Drug Metabolism Reviews*, **46**, 508-520.

[180]   Fabre N, Rustan I, de Hoffmann E and Quetin-Leclercq J. (**2001**) Determination of flavone, flavonol, and flavanone aglycones by negative ion liquid chromatography electrospray ion trap mass spectrometry. *Journal of the American Society for Mass Spectrometry*, **12**, 707-715.

[181]   Perret C, Tabacchi R and Pezet R. (**2001**) Analysis of oligomeric and polymeric tannins of grape berries by liquid chromatography/electrospray ionization multiple-stage tandem mass spectrometry. *European Journal of Mass Spectrometry*, **7**, 419-426.

[182]   Wiczkowski W, Szawara-Nowak D and Romaszko J. (**2016**) The impact of red cabbage fermentation on bioavailability of anthocyanins and antioxidant capacity of human plasma. *Food Chemistry*, **190**, 730-740.

[183]   Vera de Rosso V, Hillebrand S, Cuevas Montilla E, Bobbio FO, Winterhalter P and Mercadante AZ. (**2008**) Determination of anthocyanins from acerola (*Malpighia*

emarginata DC.) and açaí *(Euterpe oleracea* Mart.) by HPLC–PDA–MS/MS. *Journal of Food Composition and Analysis*, **21**, 291-299.

[184] washina T and Matsumoto S. (**2013**) Flavonoid glycosides from the Fern, Schizaea (Schizaeaceae) in South Pacific region, and their distribution pattern. *Bulletin of the National Museum of Nature and Science, Ser. B, Botany*, **39**, 195-201.

[185] Ibrahim RM, El-Halawany AM, Saleh DO, El Naggar EMB, El-Shabrawy AE-RO and El-Hawary SS. (**2015**) HPLC-DAD-MS/MS profiling of phenolics from Securigera securidaca flowers and its anti-hyperglycemic and anti-hyperlipidemic activities. *Revista Brasileira de Farmacognosia*, **25**, 134-141.

[186] Antonio L, Grillasca J-P, Taskinen J, Elovaara E, Burchell B, Piet M-H, Ethell B, Ouzzine M, Fournel-Gigleux S and Magdalou J. (**2002**) Characterization of catechol glucuronidation in rat liver. *Drug Metabolism and Disposition*, **30**, 199-207.

[187] Zhang Y, Tie X, Bao B, Wu X and Zhang Y. (**2007**) Metabolism of flavone C-glucosides and p-coumaric acid from antioxidant of bamboo leaves (AOB) in rats. *British Journal of Nutrition*, **97**, 484-494.

[188] Wu L, Liu J, Han W, Zhou X, Yu X, Wei Q, Liu S and Tang L. (**2015**) Time-dependent metabolism of Luteolin by human UDP-glucuronosyltransferases and its intestinal first-pass glucuronidation in mice. *Journal of Agricultural and Food Chemistry*, **63**, 8722-8733.

[189] Day AJ, Bao Y, Morgan MR and Williamson G. (**2000**) Conjugation position of quercetin glucuronides and effect on biological activity. *Free Radical Biology and Medicine*, **29**, 1234-1243.

[190] Lee J, Ebeler SE, Zweigenbaum JA and Mitchell AE. (**2012**) UHPLC-(ESI) QTOF MS/MS profiling of quercetin metabolites in human plasma postconsumption of applesauce enriched with apple peel and onion. *Journal of Agricultural and Food Chemistry*, **60**, 8510-8520.

[191] Olthof MR, Hollman PC, Buijsman MN, van Amelsvoort JM and Katan MB. (**2003**) Chlorogenic acid, quercetin-3-rutinoside and black tea phenols are extensively metabolized in humans. *The Journal of Nutrition*, **133**, 1806-1814.

[192] Verma PRP, Singh SK and Viswanathan S. (**2015**) LC- ESI- MS/MS analysis of quercetin in rat plasma after oral administration of biodegradable nanoparticles. *Biomedical Chromatography*, **29**, 1731-1736.

[193] Chapman DE, Moore TJ, Michener S and Powis G. (**1990**) Metabolism and covalent binding of [14C] toluene by human and rat liver microsomal fractions and liver slices. *Drug Metabolism and Disposition*, **18**, 929-936.

[194] Yang S, Savvides P, Liu L, Gerson SL and Xu Y. (**2012**) Development and validation of an LC–MS/MS method for pharmacokinetic study of methoxyamine in phase I clinical trial. *Journal of Chromatography B*, **901**, 25-33.

[195] Penner N, Ramanathan R, Zgoda-Pols J and Chowdhury S. (**2010**) Quantitative determination of hippuric and benzoic acids in urine by LC–MS/MS using surrogate standards. *Journal of Pharmaceutical and Biomedical Analysis*, **52**, 534-543.

[196] Bridges J, French M, Smith R and Williams R. (**1970**) The fate of benzoic acid in various species. *Biochemical Journal*, **118**, 47-51.

[197] Martinez Barbosa ME, Cammas S, Appel M and Ponchel G. (**2004**) Investigation of the degradation mechanisms of poly (malic acid) esters in vitro and their related cytotoxicities on J774 macrophages. *Biomacromolecules*, **5**, 137-143.

[198] Ng L-K, Lafontaine P and Vanier M. (**2004**) Characterization of cigarette tobacco by direct Electrospray Ionization−Ion Trap mass spectrometry (ESI-ITMS) analysis of the aqueous extract a novel and simple approach. *Journal of Agricultural and Food Chemistry*, **52**, 7251-7257.

[199] Šalić A, Pindrić K and Zelić B. (**2013**) Bioproduction of food additives hexanal and hexanoic acid in a microreactor. *Applied Biochemistry and Biotechnology*, **171**, 2273-2284.

[200] Eggink M, Wijtmans M, Kretschmer A, Kool J, Lingeman H, de Esch IJP, Niessen WMA and Irth H. (**2010**) Targeted LC–MS derivatization for aldehydes and carboxylic acids with a new derivatization agent 4-APEBA. *Analytical and Bioanalytical Chemistry*, **397**, 665-675.

[201] Zhao M, Xu J, Qian D, Guo J, Jiang S, Shang E-x, Duan J-a and Du L. (**2014**) Characterization of the metabolism of 5-hydroxymethylfurfural by human intestinal microflora using ultra-high performance liquid chromatography-quadrupole time-of-flight mass spectrometry. *Analytical Methods*, **6**, 3826-3833.

[202] Speltini A, Sturini M, Dondi D, Annovazzi E, Maraschi F, Caratto V, Profumo A and Buttafava A. (**2014**) Sunlight-promoted photocatalytic hydrogen gas evolution from water-suspended cellulose: a systematic study. *Photochemical & Photobiological Sciences*, **13**, 1410-1419.

[203] Mutlib AE, Dickenson P, Chen S-Y, Espina RJ, Daniels JS and Gan L-S. (**2002**) Bioactivation of benzylamine to reactive intermediates in rodents: formation of glutathione, glutamate, and peptide conjugates. *Chemical Research in Toxicology*, **15**, 1190-1207.

[204] Kerns EH, Volk KJ, Hill SE and Lee MS. (**1995**) Profiling new taxanes using LC/MS and LC/MS/MS substructural analysis techniques. *Rapid Communications in Mass Spectrometry*, **9**, 1539-1545.

[205] Pei K, Ou J, Huang J and Ou S. (**2016**) *p-* Coumaric acid and its conjugates: dietary sources, pharmacokinetic properties and biological activities. *Journal of the Science of Food and Agriculture*.

[206] Li N, Liu C, Mi S, Wang N, Zheng X, Li Y, Huang X, He S, Chen H and Xu X. (**2012**) Simultaneous determination of oleanolic acid, *p*-coumaric acid, ferulic acid, kaemperol and quercetin in rat plasma by LC–MS-MS and application to a pharmacokinetic study of Oldenlandia diffusa extract in rats. *Journal of Chromatographic Science*, **50**, 885-892.

[207] Food and Drug Administration. (**2012**) Guidance for industry: drug interaction studies-study design, data analysis, implications for dosing, and labeling recommendations. *Center for Drug Evaluation and Research (CDER), Rockville*, 1-75

[208] Wu H, Kelley CJ, Pino-Figueroa A, Vu HD and Maher TJ. (**2013**) Macamides and their synthetic analogs: Evaluation of in vitro FAAH inhibition. *Bioorganic and Medicinal Chemistry*, **21**, 5188-5197.

[209] dos Santos DS, Piovesan LA, D'Oca CRM, Hack CRL, Treptow TGM, Rodrigues MO, Vendramini-Costa DB, Ruiz ALTG, de Carvalho JE and D'Oca MGM. (**2015**) Antiproliferative activity of synthetic fatty acid amides from renewable resources. *Bioorganic and Medicinal Chemistry*, **23**, 340-347.

[210] Srovnalova A, Svecarova M, Kopecna Zapletalova M, Anzenbacher P, Bachleda P, Anzenbacherova E and Dvorak Z. (**2014**) Effects of anthocyanidins and anthocyanins on the expression and catalytic activities of CYP2A6, CYP2B6, CYP2C9, and CYP3A4 in primary human hepatocytes and human liver microsomes. *Journal of Agricultural and Food Chemistry*, **62**, 789-797.

[211] Dreiseitel A, Schreier P, Oehme A, Locher S, Hajak G and Sand PG. (**2008**) Anthocyanins and their metabolites are weak inhibitors of cytochrome P450 3A4. *Molecular Nutrition and Food Research*, **52**, 1428-1433.

[212] Vitaglione P, Donnarumma G, Napolitano A, Galvano F, Gallo A, Scalfi L and Fogliano V. (**2007**) Protocatechuic acid is the major human metabolite of cyanidin-glucosides. *The Journal of Nutrition*, **137**, 2043-2048.

[213] O'Leary KA, Day AJ, Needs PW, Mellon FA, O'Brien NM and Williamson G. (**2003**) Metabolism of quercetin-7- and quercetin-3-glucuronides by an in vitro hepatic model: the role of human beta-glucuronidase, sulfotransferase, catechol-O-methyltransferase and multi-resistant protein 2 (MRP2) in flavonoid metabolism. *Biochemical Pharmacology*, **65**, 479-491.

[214] Argikar UA. (**2012**) Unusual glucuronides. *Drug Metabolism and Disposition*, **40**, 1239-1251.

[215] MQG de Faria C, C Nazare A, S Petronio M, C Paracatu L, L Zeraik M, O Regasini L, HS Silva D, M da Fonseca L and F Ximenes V. (**2012**) Protocatechuic acid alkyl esters: hydrophobicity as a determinant factor for inhibition of NADPH oxidase. *Current Medicinal Chemistry*, **19**, 4885-4893.

[216] Schweigert N, Zehnder AJ and Eggen RI. (**2001**) Chemical properties of catechols and their molecular modes of toxic action in cells, from microorganisms to mammals. *Environmental Microbiology*, **3**, 81-91.

[217] Dehal SS and Kupfer D. (**1999**) Cytochrome P-450 3A and 2D6 catalyze orthohydroxylation of 4-hydroxytamoxifen and 3-hydroxytamoxifen (droloxifene) yielding tamoxifen catechol: involvement of catechols in covalent binding to hepatic proteins. *Drug Metabolism and Disposition*, **27**, 681-688.

[218] Stupans I, Stretch G and Hayball P. (**2000**) Olive oil phenols inhibit human hepatic microsomal activity. *The Journal of Nutrition*, **130**, 2367-2370.

[219] Stupans I, Tan HW, Kirlich A, Tuck K, Hayball P and Murray M. (**2002**) Inhibition of CYP3A‐ mediated oxidation in human hepatic microsomes by the dietary derived complex phenol, gallic acid. *Journal of Pharmacy and Pharmacology*, **54**, 269-275.

[220] Razis AFA, Bagatta M, De Nicola GR, Iori R and Ioannides C. (**2010**) Intact glucosinolates modulate hepatic cytochrome P450 and phase II conjugation activities and may contribute directly to the chemopreventive activity of cruciferous vegetables. *Toxicology*, **277**, 74-85.

[221] Mahéo K, Morel F, Langouët S, Kramer H, Le Ferrec E, Ketterer B and Guillouzo A. (**1997**) Inhibition of cytochromes P-450 and induction of glutathione S-transferases by sulforaphane in primary human and rat hepatocytes. *Cancer Research*, **57**, 3649-3652.

[222] Konsue N and Ioannides C. (**2010**) Modulation of carcinogen-metabolising cytochromes P450 in human liver by the chemopreventive phytochemical phenethyl isothiocyanate, a constituent of cruciferous vegetables. *Toxicology*, **268**, 184-190.

[223] Muthiah YD, Ong CE, Sulaiman SA, Tan SC and Ismail R. (**2012**) *In‐ vitro* inhibitory effect of Tualang honey on cytochrome P450 2C8 activity. *Journal of Pharmacy and Pharmacology*, **64**, 1761-1769.

[224] Ulbricht RJ, Northup SJ and Thomas JA. (**1984**) A review of 5-hydroxymethylfurfural (HMF) in parenteral solutions. *Fundamental and Applied Toxicology*, **4**, 843-853.

[225] Capuano E and Fogliano V. (**2011**) Acrylamide and 5-hydroxymethylfurfural (HMF): A review on metabolism, toxicity, occurrence in food and mitigation strategies. *LWT-Food Science and Technology*, **44**, 793-810.

[226] Quintieri L, Palatini P, Nassi A, Ruzza P and Floreani M. (**2008**) Flavonoids diosmetin and luteolin inhibit midazolam metabolism by human liver microsomes and recombinant CYP 3A4 and CYP3A5 enzymes. *Biochemical Pharmacology*, **75**, 1426-1437.

[227] Katz A. (**2010**) Chapter 11 - Alternative Medicine for Prostate Cancer: Diet, Vitamins, Minerals, and Supplements A2 - Su, Li-Ming. In *Early Diagnosis and Treatment of Cancer Series: Prostate Cancer*, Content Repository Only!, Philadelphia, 207-228.

[228] Wang L-S and Stoner GD. (**2008**) Anthocyanins and their role in cancer prevention. *Cancer Letters*, **269**, 281-290.

[229] Thomasset S, Teller N, Cai H, Marko D, Berry DP, Steward WP and Gescher AJ. (**2009**) Do anthocyanins and anthocyanidins, cancer chemopreventive pigments in the diet, merit development as potential drugs? *Cancer Chemotherapy and Pharmacology*, **64**, 201-211.

[230] Valentová K, Stejskal D, Bartek J, Dvořáčková S, Křen V, Ulrichová J and Šimánek V. (**2008**) Maca (*Lepidium meyenii*) and yacon (*Smallanthus sonchifolius*) in combination with silymarin as food supplements: *In vivo* safety assessment. *Food and Chemical Toxicology*, **46**, 1006-1013.

[231] Verschoyle RD, Greaves P, Cai H, Borkhardt A, Broggini M, D'Incalci M, Riccio E, Doppalapudi R, Kapetanovic IM, Steward WP and Gescher AJ. (**2006**) Preliminary safety evaluation of the putative cancer chemopreventive agent tricin, a naturally occurring flavone. *Cancer Chemotherapy and Pharmacology*, **57**, 1-6.

[232] Wienkers LC and Heath TG. (**2005**) Predicting *in vivo* drug interactions from *in vitro* drug discovery data. *Nature Reviews Drug discovery*, **4**, 825-833.

[233] Konishi Y, Hitomi Y and Yoshioka E. (**2004**) Intestinal absorption of *p*-coumaric and gallic acids in rats after oral administration. *Journal of Agricultural and Food Chemistry*, **52**, 2527-2532.

[234] Ferruzzi MG, Lobo JK, Janle EM, Cooper B, Simon JE, Wu Q-L, Welch C, Ho L, Weaver C and Pasinetti GM. (**2009**) Bioavailability of gallic acid and catechins from grape seed polyphenol extract is improved by repeated dosing in rats: implications for treatment in Alzheimer's disease. *Journal of Alzheimer's Disease*, **18**, 113-124.

[235] Dutton GF. (**1980**) *Glucuronidation of drugs and other compounds*, CRC Press, Boca Raton, Fla.

[236] Langguth HS and Benet LZ. (**1992**) Acyl glucuronides revisited: Is the glucuronidation proces a toxification as well as a detoxification mechanism? *Drug Metabolism Reviews*, **24**, 5-47.

[237] Olson JA, Moon RC, Anders M, Fenselau C and Shane B. (**1992**) Enhancement of biological activity by conjugation reactions. *The Journal of Nutrition*, **122**, 615-624.

[238] Bailey MJ, Worrall S, de Jersey J and Dickinson RG. (**1998**) Zomepirac acyl glucuronide covalently modifies tubulin in vitro and in vivo and inhibits its assembly in an in vitro system. *Chemico-biological Interactions*, **115**, 153-166.

[239] Finch A and Pillans P. (**2014**) P-glycoprotein and its role in drug-drug interactions. *Australian Prescriber*, **37**, 137-139.

[240] Pan X, Mei H, Qu S, Huang S, Sun J, Yang L and Chen H. (**2016**) Prediction and characterization of P-glycoprotein substrates potentially bound to different sites by emerging chemical pattern and hierarchical cluster analysis. *International Journal of Pharmaceutics*, **502**, 61-69.

[241] Gatlik-Landwojtowicz E, Äänismaa P and Seelig A. (**2006**) Quantification and characterization of P-glycoprotein−substrate interactions. *Biochemistry*, **45**, 3020-3032.

[242] Hollman PC. (**2004**) Absorption, bioavailability, and metabolism of flavonoids. *Pharmaceutical Biology*, **42**, 74-83.

[243] Esselen M, Boettler U, Teller N, Bächler S, Hutter M, Rüfer CE, Skrbek S and Marko D. (**2011**) Anthocyanin-rich blackberry extract suppresses the DNA-damaging properties of Topoisomerase I and II poisons in colon carcinoma cells. *Journal of Agricultural and Food Chemistry*, **59**, 6966-6973.

[244] Teller N, Thiele W, Marczylo TH, Gescher AJ, Boettler U, Sleeman J and Marko D. (**2009**) Suppression of the kinase activity of receptor tyrosine kinases by anthocyanin-rich mixtures extracted from bilberries and grapes. *Journal of Agricultural and Food Chemistry*, **57**, 3094-3101.

[245] Aichinger G, Pahlke G, Nagel L, Berger W and Marko D. (**2016**) Bilberry extract, its major polyphenolic compounds, and the soy isoflavone genistein antagonize the cytostatic drug erlotinib in human epithelial cells. *Food and Function*, **7**, 3628-3636.

[246] Ling J, Johnson KA, Miao Z, Rakhit A, Pantze MP, Hamilton M, Lum BL and Prakash C. (**2006**) Metabolism and excretion of erlotinib, a small molecule inhibitor of epidermal growth factor receptor tyrosine kinase, in healthy male volunteers. *Drug Metabolism and Disposition*, **34**, 420-426.